SPREADING SEQUENCE DESIGN FOR RELAY NETWORKS UNDER MULTIPATH FADING

A Dissertation by

Jie Yang

Master of Science, Jilin University, China, 2005

Bachelor of Science, Jilin University, China, 2002

Submitted to the Department of Electrical Engineering and Computer Science
and the faculty of the Graduate School of
Wichita State University
in partial fulfillment of
the requirements for the degree of
Doctor of Philosophy

May 2014

SPREADING SEQUENCE DESIGN FOR RELAY NETWORKS UNDER MULTIPATH FADING

The following faculty members have examined the final copy of this dissertation for form and content, and recommend that it be accepted in partial fulfillment of the requirement for the degree of Doctor of Philosophy with a major in Electrical Engineering.

Hyuck M. Kwon, Committee Chair

John Watkins, Committee Member

Edwin Sawan, Committee Member

Xiaomi Hu, Committee Member

Visvakumar Aravinthan, Committee Member

Accepted for the College of Engineering

Royce Bowden, Dean

Accepted for the Graduate School

Abu S. M. Masud, Interim Dean

DEDICATION

To my parents for their love, support, and encouragement

ACKNOWLEDGEMENTS

I would like to express my deepest gratitude to my advisor, Dr. Hyuck M. Kwon, for his academic guidance, caring, and patience, and for providing me with an excellent atmosphere for doing research.

I appreciate Dr. John Watkins and Dr. M. Edwin Sawan for their valuable support and encouragement over the past several years. I would like to thank Dr. Xiaomi Hu for his guidance and help in my Ph.D. study, and Dr. Visvakumar Aravinthan for serving on my defense committee. I also thank my fellow graduate students for their support, feedback, and friendship.

I also thank my parents who have always supported and encouraged me with their best wishes.

ABSTRACT

Multipath frequency-selective fading can degrade the performance of a wireless communication system significantly as the data rate increases, e.g., when the data rate is as high as those of systems beyond long-term evolution (LTE)-Advanced. An effective method to combat multipath fading is a code division multiple access (CDMA) scheme. The objective of this dissertation is to present an effective method in designing nonbinary, secure, and optimum spreading and despreading pseudo noise (PN) sequences for CDMA multi-relay networks under frequency-selective fading by employing a maximum signal-to-interference-plus-noise ratio (SINR) criterion. This dissertation assumes that channel state information (CSI) is known at a central station such as a cloud radio access network (CRAN), which computes the optimum PN sequences and forwards them to both sources and destinations. This dissertation considers both partially and fully connected relay networks consisting of multiple sources, multiple relays, and multiple destinations. Direct links from sources to destinations are available in fully connected relay networks, whereas they are not available in partially connected relay networks. This dissertation also finds the optimum PN spreading and despreading sequences jointly and iteratively using the proposed novel method for multiple sources and destinations. Furthermore, it examines the sensitivity of the proposed schemes to imperfect CSI and wideband jamming. Simulation results verify that the proposed method can effectively improve system performance and can converge much faster in finding optimum PN sequences jointly for multiple sources and destinations than existing schemes under the same environment.

TABLE OF CONTENTS

LIST OF FIGURES

LIST OF FIGURES (continued)

LIST OF ABBREVIATIONS

AF	Amplify-and-Forward
AWGN	Additive White Gaussian Noises
BER	Bit Error Rate
BPSK	Binary Phase Shift Keying
BS	Base Station
CDMA	Code Division Multiple Access
CRAN	Cloud Radio Access Network
CSI	Channel State Information
CU	Channel Uncertainty
DS-CDMA	Code Division Multiple Access
FC	Fully Connected
i.i.d.	Independent and Identically Distributed
MAI	Multiple-Access Interference
MIMO	Multiple-Input Multiple-Output
OFDM	Orthogonal Frequency Division Multiplexing
PN	Pseudo Noise
PC	Partially Connected
SINR	Signal-to-Interference-plus-Noise Ratio
SNR	Signal-to-Noise Ratio
SVD	Singular Value Decomposition

LIST OF SYMBOLS

$\triangleq$	Definition
$\mathbf{A}$	Matrix (Uppercase Boldface)
$\mathbf{a}$	Vector (Lowercase Boldface)
a	Scalar (Italic Character)
$\mathbf{A}^{-1}$	Inverse of **A**
$\mathbf{A}^{*}$	Complex Conjugate of **A**
$\mathbf{A}^{\dagger}$	Optimum **A**
$\mathbf{A}^{H}$	Hermitian of **A**
$\mathbf{A}^{T}$	Transpose of **A**
$\mathbf{I}_N$	$N \times N$ Identity Matrix
$\mathbf{0}$	Either Matrix or Vector Consisting of all Zero Entries with Appropriate Dimensions
$\|a\|$	Absolute Value of a
$\|\mathbf{a}\|$	2-Norm of **a**
$E[\,\cdot\,]$	Expectation Operator

CHAPTER 1

INTRODUCTION

Cooperative communication, which allows resource sharing among multiple users, is one of the fastest growing areas of research, and has been considered and analyzed in the literature because the performance of a wireless network can be greatly improved by exploiting cooperation among different users. Relay coding strategies can be classified into three categories: amplify-and-forward (AF), decode-and-forward (DF), and compress-and-forward (CF). In AF relay systems, relays amplify the received signal without decoding it [1–11]. In DF relay systems, the signal is fully decoded and then re-encoded at the relays prior to retransmission [12–16]. In CF relay systems, relays compress the received signal, then encode a compressed version and send it to the destination [17, 18]. This dissertation considers AF relay networks.

Multipath fading is a feature that must be taken into account when designing a wireless communication system, whereby the signal will reach the destination not only via the direct path but also via reflections from objects such as ground, hills, buildings, etc. Frequency-selective fading occurs when multipath fading affects different frequencies across the channel bandwidth to different degrees, which means that the phase and amplitude of the signal varies across the channel. This occurs when data symbol intervals become smaller than multipath delay spread intervals. For example, the data symbol interval of the recently developed long-term evolution (LTE) wireless communication systems or beyond are typically smaller than the multipath delay spread intervals. In this case, simply maintaining the overall amplitude of the received signal will not overcome the effects of selective fading. Various researchers have worked on overcoming the effect of frequency-selective fading [19–22].

Some digital signal formats, e.g., orthogonal frequency division multiplexing (OFDM) are able to spread the data of a high rate over a wideband channel consisting of a large number of narrowband subcarriers. When only a portion of the data is lost by any nulls of a few narrowband subcarriers, that portion can be reconstituted using forward error correction techniques, thus mitigating the effects of selective multipath fading. This is why OFDM has been researched extensively and used in existing systems such as 4G LTE and IEEE 802.11 WiFi wireless communication systems [23–28].

However, another effective method to combat multipath fading is a direct sequence-code division multiple access (DS-CDMA) scheme, which has not been investigated much for relay network communication systems. Extensions of new network architectures such as relay and heterogeneous scenarios to DS-CDMA are still highly relevant, since upgrades to legacy 3G cellular systems such as wideband code division multipath access (WCDMA) are continually in progress and under study in 3GPP [29, 30]. In addition, security can be enhanced by employing a CDMA system if the spreading and despreading PN sequences are not available to a jammer but to the sources and destinations. The above provides the motivation to study relay optimization methods for DS-CDMA systems.

To combat the deleterious effects of multiple-access interference (MAI), the traditional approach in the CDMA scheme has been to employ fixed orthogonal user sequences or signatures with low cross-correlation properties [31, 32]. However, the orthogonality or desired cross-correlations of transmitted sequences can usually be destroyed when received at the base station (BS) or the destination due to multipath fading, and inter-symbol and multi-access interference. One approach to circumvent these problems is to dynamically allocate user sequences in an adaptive manner, either in the form of an iterative search [33] or a dynamic sequence allocation on a symbol-by-symbol basis [34]. Another approach is to construct optimal transmitter user sequences based on any available channel state information (CSI) that may be available via the reverse link to maximize a performance measure of choice [35–37]. The design of the pre-coder based on full channel knowledge has been investigated for frequency-selective fading channels using various criteria such as minimum pairwise-error probability (PEP), minimum mean square error (MMSE), etc. [38–41]. Spread-spectrum relay channels with deterministic (fixed) or random spreading sequences have been examined [42, 43]. In a distributed relay network, the time synchronization among the different nodes is important. Assuming PN code synchronization, this dissertation studies the PN sequence designing problem for multiple sources and multiple destinations in AF multi-relay networks.

The objective of this dissertation is to propose a unique, simple, and effective method in finding optimum nonbinary adaptive PN spreading and despreading sequences for relay network communication systems under multipath fading. For this purpose, the signal-to-interference-plus-noise ratio (SINR) criterion and CSI are employed. As a system model, linear relaying schemes with an amplify-and-forward (AF) protocol are analyzed. The relay operates in a half-duplex mode, i.e., it does not transmit and receive simultaneously on the same frequency, and it is assumed that all channels undergo frequency-selective fading.

In this research, two types of network connectivity are considered:

- Partially connected (PC), where no direct links between the sources and the destinations are available.
- Fully connected (FC), where direct links between the sources and the destinations are available.

This dissertation conjectures and assumes that the conventional double-dwell PN code acquisition and early-late PN code tracking [44] are also effective for the nonbinary complex PN codes. This will be studied in the future.

The main contributions of this dissertation are summarized as follows:

- This dissertation finds optimum PN sequences by employing the Cholesky decomposition and singular value decomposition (SVD) [45]. The proposed method is unique, simple, and efficient, compared to existing methods. In addition, it is applicable to a general relay system model with multiple sources, relays, and destinations.
- DS-CDMA systems with the proposed optimized relaying adaptive PN sequences show much better performance than those with non-adaptive PN sequences.
- The proposed optimal PN sequences employ CSI, which is available only to the desired destinations or the sources. Hence, the proposed PN sequences are not available to a jammer, but they are available to the sources or destinations. In addition, the PN sequences keep changing from one frame to another when the channel is quasi-static. Therefore, the proposed DS-CDMA relay network is secure, compared to existing systems with fixed-PN sequences.
- The proposed method converges much faster in jointly and iteratively finding optimum PN sequences for multiple source-destination pairs than existing schemes [36] under the same environment.

A disadvantage of the proposed method is that it requires CSI to compute the optimal PN sequences at either the destination for the uplink or the source for the downlink. Therefore, the impact of imperfect CSI and wideband jamming on system performance is also evaluated.

The remainder of this dissertation is organized into four chapters. Chapter 2 describes and analyzes the partially connected relay network and proposes the optimal PN sequence design. Chapter 3 studies the case of the fully connected relay network. Chapter 4 studies the multihop relay network. Chapter 5 concludes the dissertation.

The following notation is used through this dissertation: Matrices, vectors, and scalars are denoted, respectively, by uppercase boldface, lowercase boldface, and italic characters (e.g., $\boldsymbol{A}$, $\boldsymbol{a}$, and a). The inverse or pseudo-inverse is denoted by $\boldsymbol{A}^{-1}$. The transpose and Hermitian of $\boldsymbol{A}$ are denoted, respectively, by $\boldsymbol{A}^{\mathrm{T}}$ and $\boldsymbol{A}^{\mathrm{H}}$. Notation $\boldsymbol{a}^{\dagger}$ represents the optimal sequence vector. Notations $|a|$ and $||\boldsymbol{a}||$ denote the absolute or magnitude values of a for any scalar and 2-norm of $\boldsymbol{a}$. The expectation operator is denoted by $E[\cdot]$.

CHAPTER 2

PARTIALLY CONNECTED RELAY NETWORK

2.1 PC Network with One Source, One Relay, and One Destination

When the source and the destination are far away, the direct link may be too weak. If relays are located between sources and destinations, then they can improve the overall communications link performance. In this case, the direct link can be neglected.

Definition 1 (Partially Connected): A relay network is called a partially connected relay network when the direct link from the source to the destination is not too weak and hence negligible, as shown in Figure 2.1. This chapter focuses on the PC relay. First, consider the simplest three-terminal network with one source, one relay, and one destination, each equipped with a single antenna, as shown in Figure 2.2. The source is denoted as S, the relay as R, and the destination as D. The symbol to be transmitted from the source is x, $\boldsymbol{s}$ is the $(N \times 1)$ spreading sequence vector, and $\boldsymbol{c}$ is the $(N \times 1)$ despreading sequence vector at the destination. Both $\boldsymbol{s}$ and $\boldsymbol{c}$ have the unit norm throughout this dissertation.

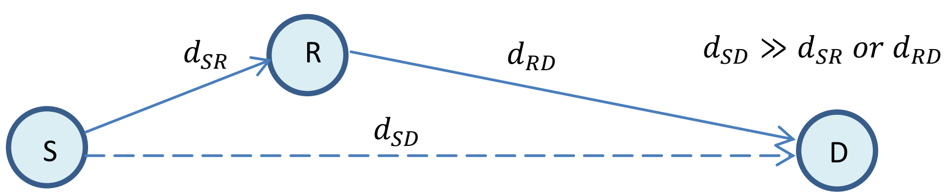

Figure 2.1. Partially connected relay network.

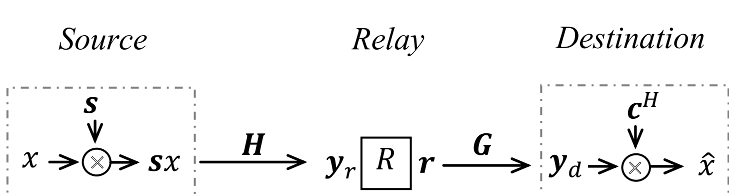

Figure 2.2. PC relay network with one source, one relay, and one destination.

Assume that the source employs a length N spreading sequence $\boldsymbol{s} = [s_1, s_2, \cdots, s_N]^T$ to transmit its information symbol x, with power $E\{|x|^2\} = P_s$. The channel between the source and the relay is a frequency-selective fading channel with L taps: $\boldsymbol{h} = [h_1, h_2, \cdots, h_L]^T$ with a complex channel coefficient h_l per path, $l = 1, \cdots L$. If $L \ll N$, then inter-symbol interference is negligible [36]. The output of the chip-matched filter during the current data symbol interval at the relay is

$$y_{r,t} = \sum_{l=1}^{L} x s_t h_j + n_{r,t}, \quad 0 \leq t \leq N-1 \tag{2.1}$$

where $n_{r,t}$ is a zero-mean complex additive Gaussian noise with variance σ_n^2.

The received signal at the relay can be written in an $N \times 1$ vector form as

$$\boldsymbol{y}_r = \boldsymbol{Hs}x + \boldsymbol{n}_r \tag{2.2}$$

where $\boldsymbol{n}_r$ is the zero-mean complex additive Gaussian noise vector with covariance matrix $\boldsymbol{Z}_r = E\{\boldsymbol{n}_r \boldsymbol{n}_r^H\} = \sigma_{nr}^2 \boldsymbol{I}$.

The multipath channel can be represented as an $N \times N$ matrix as in the work of Peiris et al. [46]:

$$H = \begin{bmatrix} h_1 & 0 & 0 & \cdots & 0 \\ h_2 & h_1 & 0 & \cdots & \vdots \\ \vdots & h_2 & h_1 & \cdots & \vdots \\ h_L & \vdots & h_2 & \cdots & \vdots \\ \vdots & h_L & \vdots & \ddots & 0 \\ 0 & \vdots & \vdots & \cdots & h_1 \end{bmatrix}. \tag{2.3}$$

Under the amplify-and-forward protocol, the relay sends $\boldsymbol{r} = \alpha \boldsymbol{y}_r$ to the destination with

$$\alpha = \sqrt{\frac{P_R}{E\{\|\boldsymbol{y}_r\|^2\}}} \tag{2.4}$$

where α is a scaling factor that preserves power constraint P_R at the relay.

The received signal at the destination through the relay-destination link is

$$\boldsymbol{y}_d = \boldsymbol{Gr} + \boldsymbol{n}_d = \alpha \boldsymbol{GHs}x + \tilde{\boldsymbol{n}}_d \tag{2.5}$$

where $\tilde{\boldsymbol{n}}_d \triangleq \alpha \boldsymbol{G}\boldsymbol{n}_r + \boldsymbol{n}_d$ is the cumulative noise vector with covariance matrix $\boldsymbol{K} = \alpha^2 \boldsymbol{G}\boldsymbol{Z}_r\boldsymbol{G}^H + \boldsymbol{Z}_d$ with $\boldsymbol{Z}_d = E\{\boldsymbol{n}_d\boldsymbol{n}_d^H\}$, and $\boldsymbol{G}$ represents the frequency-selective channel matrix between relay and destination.

By defining the destination receive filter (despreading sequence) as $\boldsymbol{c}$, then the destination generates its despread symbol as

$$\hat{x} = \boldsymbol{c}^H \boldsymbol{y}_d = \alpha \boldsymbol{c}^H \boldsymbol{G}\boldsymbol{H}\boldsymbol{s}x + \boldsymbol{c}^H \tilde{\boldsymbol{n}}_d \tag{2.6}$$

Lemma 1: Define $\boldsymbol{A}$ as the Cholesky decomposition matrix of Hermitian matrix $\boldsymbol{K}$ as $\boldsymbol{K} = \boldsymbol{A}\boldsymbol{A}^H$; then the SINR maximizing sequences are $\boldsymbol{s}^\dagger = \boldsymbol{v}_{max}$ and $\boldsymbol{c}^\dagger = (\boldsymbol{A}^H)^{-1}\boldsymbol{u}_{max}$, where $\boldsymbol{v}_{max}$ and $\boldsymbol{u}_{max}$ are the right and left singular vectors, respectively, corresponding to the maximum singular value λ_{max} of matrix $\boldsymbol{A}^{-1}\boldsymbol{G}\boldsymbol{H}$. The corresponding maximum SINR can be written as

$$\max_{\boldsymbol{s},\boldsymbol{c}} \gamma = \alpha^2 P_s |\lambda_{max}|^2.$$

Proof of Lemma 1: The SINR is

$$\gamma = \frac{E\left[\left|\alpha \boldsymbol{c}^H \boldsymbol{G}\boldsymbol{H}\boldsymbol{s}x\right|^2\right]}{E\left[\left|\boldsymbol{c}^H \tilde{\boldsymbol{n}}_d\right|^2\right]} \tag{2.7}$$

$$= \frac{\alpha^2 P_s \left|\boldsymbol{c}^H \boldsymbol{G}\boldsymbol{H}\boldsymbol{s}\right|^2}{\boldsymbol{c}^H \boldsymbol{K}\boldsymbol{c}} \tag{2.8}$$

$$= \frac{\alpha^2 P_s \left|\boldsymbol{c}^H \boldsymbol{A}\boldsymbol{A}^{-1}\boldsymbol{G}\boldsymbol{H}\boldsymbol{s}\right|^2}{\boldsymbol{c}^H \boldsymbol{A}\boldsymbol{A}^H \boldsymbol{c}} \tag{2.9}$$

$$= \frac{\alpha^2 P_s \left|\tilde{\boldsymbol{c}}^H (\boldsymbol{A}^{-1}\boldsymbol{G}\boldsymbol{H})\boldsymbol{s}\right|^2}{\tilde{\boldsymbol{c}}^H \tilde{\boldsymbol{c}}} \tag{2.10}$$

$$= \frac{\alpha^2 P_s \left|\tilde{\boldsymbol{c}}^H (\boldsymbol{U}\Sigma\boldsymbol{V}^{\boldsymbol{H}})\boldsymbol{s}\right|^2}{|\tilde{\boldsymbol{c}}|^2} \tag{2.11}$$

where $\tilde{\boldsymbol{c}} \triangleq \boldsymbol{A}^H\boldsymbol{c}$, Cholesky decomposition is applied to the Hermitian matrix $\boldsymbol{K}$ in equation (2.8) such that $\boldsymbol{K} = \boldsymbol{A}\boldsymbol{A}^H$, and singular-value decomposition is applied to matrix $\boldsymbol{A}^{-1}\boldsymbol{G}\boldsymbol{H}$ in equation (2.10). If sequences are designed as $\boldsymbol{s}^\dagger = \boldsymbol{v}_{max}$ and $\boldsymbol{c}^\dagger = (\boldsymbol{A}^H)^{-1}\boldsymbol{u}_{max}$, then the SINR is maximized, which is $\alpha^2 P_s|\lambda_{max}|^2$. ■

2.2 Uplink PC Relay Network

2.2.1 PC Network with Two Sources, One Relay, and One Destination

An uplink relay network with two sources, one relay, and one destination is shown in Figure 2.3. Source one is denoted as S_1, source two as S_2, the relay as R, and the destination as D. Sources 1 and 2 transmit symbols x_1 and x_2, and employ spreading sequences $\boldsymbol{s}_1$ and $\boldsymbol{s}_2$, respectively. The multipath channel from S_1 to R is denoted by $\boldsymbol{H}_1$, from S_2 to R by $\boldsymbol{H}_2$, and from R to D by $\boldsymbol{G}$. The destination processes the received signal with two sets of despreading sequences, $\boldsymbol{c}_1$ for symbols from S_1 (upper branch) and $\boldsymbol{c}_2$ for symbols from S_2 (lower branch).

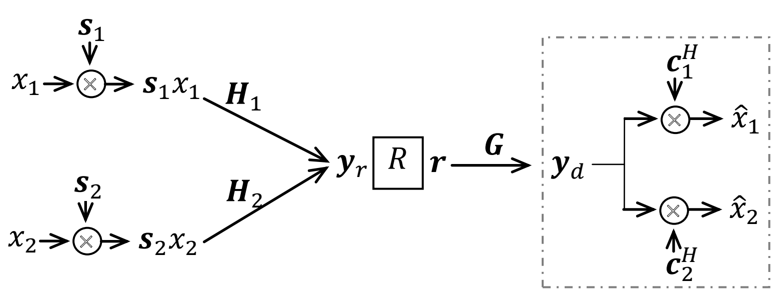

Figure 2.3. Uplink PC relay network with two sources, one relay, and one destination.

The received signal at the relay can be written as

$$\boldsymbol{y}_r = \boldsymbol{H}_1\boldsymbol{s}_1x_1 + \boldsymbol{H}_2\boldsymbol{s}_2x_2 + \boldsymbol{n}_r. \quad (2.12)$$

Then the AF relay forwards signal $\boldsymbol{r} = \alpha\boldsymbol{y}_r$ to the destination. So the received signal at the destination can be written as

$$\boldsymbol{y}_d = \alpha\boldsymbol{G}\boldsymbol{H}_1\boldsymbol{s}_1x_1 + \alpha\boldsymbol{G}\boldsymbol{H}_2\boldsymbol{s}_2x_2 + \tilde{\boldsymbol{n}}_d \quad (2.13)$$

where $\tilde{\boldsymbol{n}}_d \triangleq \alpha\boldsymbol{G}\boldsymbol{n}_r + \boldsymbol{n}_d$.

Then the destination despreads the received signal for S_1 and S_2, respectively, as

$$\hat{x}_1 = \boldsymbol{c}_1^H \boldsymbol{y}_d = \alpha \boldsymbol{c}_1^H \boldsymbol{G}\boldsymbol{H}_1 \boldsymbol{s}_1 x_1 + \alpha \boldsymbol{c}_1^H \boldsymbol{G}\boldsymbol{H}_2 \boldsymbol{s}_2 x_2 + \boldsymbol{c}_1^H \tilde{\boldsymbol{n}}_d \tag{2.14}$$

$$\hat{x}_2 = \boldsymbol{c}_2^H \boldsymbol{y}_d = \alpha \boldsymbol{c}_2^H \boldsymbol{G}\boldsymbol{H}_1 \boldsymbol{s}_1 x_1 + \alpha \boldsymbol{c}_2^H \boldsymbol{G}\boldsymbol{H}_2 \boldsymbol{s}_2 x_2 + \boldsymbol{c}_2^H \tilde{\boldsymbol{n}}_d. \tag{2.15}$$

Define $\boldsymbol{Q}_{PU1} \triangleq \alpha^2 P_s \boldsymbol{G}\boldsymbol{H}_2 \boldsymbol{s}_2 \boldsymbol{s}_2^H \boldsymbol{H}_2^H \boldsymbol{G}^H + \boldsymbol{K}$ as the covariance matrix of the interference plus noise $\alpha \boldsymbol{c}_1^H \boldsymbol{G}\boldsymbol{H}_2 \boldsymbol{s}_2 x_2 + \boldsymbol{c}_1^H \tilde{\boldsymbol{n}}_d$ for source 1. Here, the subscript *PU1* denotes, respectively, the partially connected relay, uplink, and source 1 detection. Apply Cholesky decomposition to matrix $\boldsymbol{Q}_{PU1}$ as $\boldsymbol{Q}_{PU1} = \boldsymbol{A}_{PU1}\boldsymbol{A}_{PU1}^H$. Note that $\boldsymbol{Q}_{PU1}$is a function of $\boldsymbol{s}_2$. Then the spreading and despreading sequences that maximize the SINR for the upper branch source 1 can be found as $\boldsymbol{s}_1^\dagger = \boldsymbol{v}_{PU1,max}$ and $\boldsymbol{c}_1^\dagger = (\boldsymbol{A}_{PU1}^H)^{-1}\boldsymbol{u}_{PU1,max}$, where $\boldsymbol{v}_{PU1,max}$ and $\boldsymbol{u}_{PU1,max}$ are the right and left singular vectors, respectively, corresponding to the maximum singular value $\lambda_{1,max}$ of matrix $\boldsymbol{A}_{PU1}^{-1}\boldsymbol{G}\boldsymbol{H}_1$. Then the maximum SINR for the uplink relay network can be written as

$$\max_{\boldsymbol{s}_1,\boldsymbol{c}_1} \gamma_1 = \alpha^2 P_s \left|\lambda_{PU1,max}\right|^2. \tag{2.16}$$

Define $\boldsymbol{Q}_{PU2} \triangleq \alpha^2 P_s \boldsymbol{G}\boldsymbol{H}_1 \boldsymbol{s}_1 \boldsymbol{s}_1^H \boldsymbol{H}_1^H \boldsymbol{G}^H + \boldsymbol{K}$ as the covariance matrix of the interference plus noise $\alpha \boldsymbol{c}_2^H \boldsymbol{G}\boldsymbol{H}_1 \boldsymbol{s}_1 x_1 + \boldsymbol{c}_2^H \tilde{\boldsymbol{n}}_d$. Apply Cholesky decomposition to matrix $\boldsymbol{Q}_2$ as $\boldsymbol{Q}_{PU2} = \boldsymbol{A}_{PU2}\boldsymbol{A}_{PU2}^H$. Then the sequences that maximizing the SINR for the lower branch can be found as $\boldsymbol{s}_2^\dagger = \boldsymbol{v}_{PU2,max}$, and $\boldsymbol{c}_2^\dagger = (\boldsymbol{A}_{PU2}^H)^{-1}\boldsymbol{u}_{PU2,max}$, where $\boldsymbol{v}_{PU2,max}$ and $\boldsymbol{u}_{PU2,max}$ are the right and left singular vectors, respectively, corresponding to the maximum singular value $\lambda_{PU2,max}$ of matrix $\boldsymbol{A}_{PU2}^{-1}\boldsymbol{G}\boldsymbol{H}_2$. Then the maximum SINR for the uplink relay network can be written as

$$\max_{\boldsymbol{s}_2,\boldsymbol{c}_2} \gamma_{PU2} = \alpha^2 P_s \left|\lambda_{PU2,max}\right|^2. \tag{2.17}$$

The joint iterative algorithm to find both the spreading sequences $\boldsymbol{s}_1$and $\boldsymbol{s}_2$ for users 1 and 2 is stated in the following steps:

Step 1. Set an initial vector $\boldsymbol{s}_2$ with $\|\boldsymbol{s}_2\| = 1$, e.g., $\boldsymbol{s}_2 = (1,\ 1,\ \cdots,\ 1)^T/\sqrt{N}$.

Step 2. Obtain $\boldsymbol{s}_1$ using $\boldsymbol{s}_2$ as follows:

2a. Calculate $\boldsymbol{Q}_{PU1} \triangleq \alpha^2 P_s \boldsymbol{G}\boldsymbol{H}_2\boldsymbol{s}_2\boldsymbol{s}_2^H\boldsymbol{H}_2^H\boldsymbol{G}^H + \boldsymbol{K}$.

2b. Obtain $\boldsymbol{A}_{PU1}$ by Cholesky decomposition: $\boldsymbol{Q}_{PU1} = \boldsymbol{A}_{PU1}\boldsymbol{A}_{PU1}^H$.

2c. Apply the SVD to $\boldsymbol{A}_{PU1}^{-1}\boldsymbol{G}\boldsymbol{H}_1$ as $\boldsymbol{A}_{PU1}^{-1}\boldsymbol{G}\boldsymbol{H}_1 = \boldsymbol{U}_{PU1}\sum_{PU1}\boldsymbol{V}_{PU1}^H$. Then determine $\boldsymbol{s}_1$ as the right singular vector $\boldsymbol{v}_{PU1,max}$ corresponding to the maximum singular value $\lambda_{PU1,max}$ of $\boldsymbol{A}_{PU1}^{-1}\boldsymbol{G}\boldsymbol{H}_1$. When the singular values in matrix $\sum_{PU1}$ are in decreasing order, then $\boldsymbol{s}_1$ is the first column of matrix $\boldsymbol{V}_{PU1}$.

Step 3. Compute $\boldsymbol{s}_2$ using $\boldsymbol{s}_1$ as follows:

3a. Calculate $\boldsymbol{Q}_{PU2} \triangleq \alpha^2 P_s \boldsymbol{G}\boldsymbol{H}_1\boldsymbol{s}_1\boldsymbol{s}_1^H\boldsymbol{H}_1^H\boldsymbol{G}^H + \boldsymbol{K}$.

3b. Obtain $\boldsymbol{A}_{PU2}$ by Cholesky decomposition: $\boldsymbol{Q}_{PU2} = \boldsymbol{A}_{PU2}\boldsymbol{A}_{PU2}^H$.

3c. Apply the SVD to $\boldsymbol{A}_{PU2}^{-1}\boldsymbol{G}\boldsymbol{H}_2$ as $\boldsymbol{A}_{PU2}^{-1}\boldsymbol{G}\boldsymbol{H}_2 = \boldsymbol{U}_{PU2}\sum_{PU2}\boldsymbol{V}_{PU2}^H$. Then determine $\boldsymbol{s}_2$ as the right singular vector $\boldsymbol{v}_{PU2,max}$ corresponding to the maximum singular value $\lambda_{PU2,max}$ of $\boldsymbol{A}_{PU2}^{-1}\boldsymbol{G}\boldsymbol{H}_2$. When the singular values in matrix $\sum_{PU2}$ are in decreasing order, then $\boldsymbol{s}_2$ is the first column of matrix $\boldsymbol{V}_{PU2}$.

Step 4. Repeat Steps 2 and 3 until $\lambda_{PU1,max}$ and $\lambda_{PU2,max}$ converge as $\left|\lambda_{PU1,max}{}^{(m)} - \lambda_{PU1,max}{}^{(m-1)}\right| < \varepsilon$ and $\left|\lambda_{PU2,max}{}^{(m)} - \lambda_{PU2,max}{}^{(m-1)}\right| < \varepsilon$.

Then $\boldsymbol{c}_1$ is the left singular vector $\boldsymbol{u}_{PU1,max}$ corresponding to the maximum singular value $\lambda_{PU1,max}$ of $\boldsymbol{A}_{PU1}^{-1}\boldsymbol{G}\boldsymbol{H}_1$, and $\boldsymbol{c}_2$ is the left singular vector $\boldsymbol{u}_{PU2,max}$ corresponding to the maximum singular value $\lambda_{PU2,max}$ of $\boldsymbol{A}_{PU2}^{-1}\boldsymbol{G}\boldsymbol{H}_2$. The proposed algorithm described in this example can be easily extended for more than two users.

Remark 1: The complexity of the proposed algorithm per iteration is $O(N^2)$ for the global optimum case, whereas the complexity of the algorithm in the work of Rajappan and Honig [36] is $O(N^2)$ per iteration for the local optimum case.

2.2.2 PC Network with M Sources, K Relay, and One Destination

Figure 2.4 shows a PC relay network with M number of sources, K number of relays, and one destination, which detects symbols transmitted by M sources simultaneously. Here, the sources, relays, and destination can represent the mobiles, relays, and base station, respectively, in an uplink of a cellular system. $\boldsymbol{H}_{ij}$ is defined as the channel matrix from source i to relay j, and $\boldsymbol{G}_j$ as the channel matrix from relay j to destination, where i denotes the source index $(i = 1, \cdots, M)$, and j is the relay index $(j = 1, \cdots, K)$. Note that even if a single antenna is employed at each transmitter, an $N \times N$ matrix is needed to describe the channel from a transmitter to a receiver due to the time-spreading of N chips per symbol.

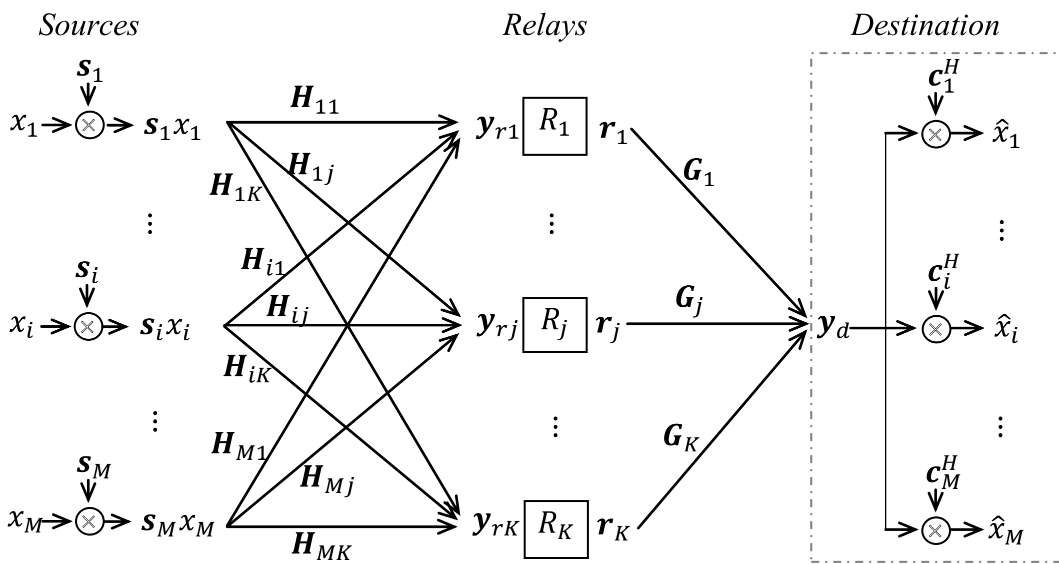

Figure 2.4. Uplink PC relay network with M sources, K relays, and one destination.

Assume that source S_i employs a length-N spreading sequence $\boldsymbol{s}_i = [s_{i1}, s_{i2}, \cdots, s_{iN}]^T$ to transmit its information symbol x_i, with power $E\{|x_i|^2\} = P_s$. The received signal at relay R_j from the M sources is

$$\boldsymbol{y}_{rj} = \sum_{i=1}^{M} \boldsymbol{H}_{i,j} \boldsymbol{s}_i x_i + \boldsymbol{n}_{rj} \tag{2.18}$$

where $\boldsymbol{H}_{i,j}$ is the $N \times N$ channel matrix from source S_i to relay R_j.

Here, $\boldsymbol{n}_{rj}$ is a zero-mean complex additive white Gaussian noise (AWGN) vector with covariance matrix $\boldsymbol{Z}_{rj} = E\{\boldsymbol{n}_{rj}\boldsymbol{n}_{rj}^H\} = \sigma_{nrj}^2 \boldsymbol{I}_N$. Using the AF protocol, relay j sends $\boldsymbol{r}_j = \alpha_j \boldsymbol{y}_{rj}$ to the destination, where $\alpha_j = \sqrt{\frac{P_R}{E\{\|\boldsymbol{y}_{rj}\|^2\}}}$ is the scaling factor that preserves power constraint P_R at the relay. The received signal at the destination from the K relays is

$$\boldsymbol{y}_d = \sum_{j=1}^{K} \boldsymbol{G}_j \boldsymbol{r}_j + \boldsymbol{n}_d \qquad (2.19)$$

$$= \sum_{k=1}^{M} \sum_{j=1}^{K} (\alpha_j \boldsymbol{G}_j \boldsymbol{H}_{k,j} \boldsymbol{s}_k x_k) + \sum_{j=1}^{K} \alpha_j \boldsymbol{G}_j \boldsymbol{n}_{rj} + \boldsymbol{n}_d \qquad (2.20)$$

$$= \sum_{k=1}^{M} (\boldsymbol{T}_{PUk} \boldsymbol{s}_k x_k) + \widetilde{\boldsymbol{n}}_d \qquad 2.21)$$

where $\boldsymbol{T}_{PUk} \triangleq \sum_{j=1}^{K}(\alpha_j \boldsymbol{G}_j \boldsymbol{H}_{k,j})$, and $\widetilde{\boldsymbol{n}}_d \triangleq \sum_{j=1}^{K} \alpha_j \boldsymbol{G}_j \boldsymbol{n}_{rj} + \boldsymbol{n}_d$. The covariance matrix of $\widetilde{\boldsymbol{n}}_d$ is denoted by $\boldsymbol{K} = \sum_{j=1}^{K} \alpha_j^2 \boldsymbol{G}_j \boldsymbol{Z}_{rj} \boldsymbol{G}_j^H + \boldsymbol{Z}_d$, with the relay noise covariance matrix $\boldsymbol{Z}_{rj} \triangleq E\{\boldsymbol{n}_{rj}\boldsymbol{n}_{rj}^H\}$ and the destination noise covariance matrix $\boldsymbol{Z}_d \triangleq E\{\boldsymbol{n}_d \boldsymbol{n}_d^H\}$. Then the destination despreads the received signal for source i by despreading sequence $\boldsymbol{c}_i$ as

$$\hat{x}_i = \boldsymbol{c}_i^H \boldsymbol{y}_d \qquad (2.22)$$

$$= \boldsymbol{c}_i^H \left(\sum_{k=1}^{M} (\boldsymbol{T}_{PUk} \boldsymbol{s}_k x_k) + \widetilde{\boldsymbol{n}}_d\right) \qquad (2.23)$$

$$= \boldsymbol{c}_i^H \boldsymbol{T}_{PUi} \boldsymbol{s}_i x_i + \boldsymbol{c}_i^H \left(\sum_{\substack{k=1 \\ k \neq i}}^{M} (\boldsymbol{T}_{PUk} \boldsymbol{s}_k x_k) + \widetilde{\boldsymbol{n}}_d\right) \qquad (2.24)$$

Theorem 1: Define $\boldsymbol{Q}_{PUi} \triangleq \sum_{\substack{k=1 \\ k \neq i}}^{M} (P_s \boldsymbol{T}_{PUk} \boldsymbol{s}_k \boldsymbol{s}_k^H \boldsymbol{T}_{PUk}^H) + \boldsymbol{K}$ as the covariance matrix of the interference plus noise components in equation (2.24), excluding the desired signal. Apply Cholesky decomposition to matrix $\boldsymbol{Q}_{PUi}$ as $\boldsymbol{Q}_{PUi} = \boldsymbol{A}_{PUi} \boldsymbol{A}_{PUi}^H$. Then the optimal spreading and despreading sequences that maximize $SINR_i$ can be found as $\boldsymbol{s}_i^\dagger = \boldsymbol{v}_{PUi,max}$ and $\boldsymbol{c}_i^\dagger = (\boldsymbol{A}_i^H)^{-1} \boldsymbol{u}_{PUi,max}$, respectively, where $\boldsymbol{v}_{PUi,max}$ and $\boldsymbol{u}_{PUi,max}$ are the right and left singular vectors, respectively, corresponding to the maximum singular value $\lambda_{PUi,max}$ of matrix $\boldsymbol{A}_{PUi}^{-1} \boldsymbol{T}_{PUi}$. The maximum SINR can be written as

$$\max_{s_i, c_i} \gamma_{PUi} = P_s \left| \lambda_{PUi,max} \right|^2. \quad (2.25)$$

Proof of Theorem 1: The SINR γ_{PUi} for the i^{th} user is defined to be the ratio of the desired signal component power to the interference-plus-noise power in equation (2.24) after despreading.

$$\gamma_{PUi} = \frac{E\left[\left|\boldsymbol{c}_i^H \boldsymbol{T}_{PUi} \boldsymbol{s}_i x_i\right|^2\right]}{E\left[\left|\boldsymbol{c}_i^H \left(\sum_{\substack{k=1 \\ k \neq i}}^{M} \boldsymbol{T}_{PUk} \boldsymbol{s}_k x_k + \widetilde{\boldsymbol{n}}_d\right)\right|^2\right]} \quad (2.26)$$

$$= \frac{P_s \left|\boldsymbol{c}_i^H \boldsymbol{T}_{PUi} \boldsymbol{s}_i\right|^2}{\boldsymbol{c}_i^H \left(\sum_{\substack{k=1 \\ k \neq i}}^{M} P_S \boldsymbol{T}_{PUk} \boldsymbol{s}_k {\boldsymbol{s}_k}^H {\boldsymbol{T}_{PUk}}^H + \boldsymbol{K}\right) \boldsymbol{c}_i} \quad (2.27)$$

Note that $\boldsymbol{Q}_{PUi}$ is a Hermitian matrix, so Cholesky decomposition can be applied as $\boldsymbol{Q}_{PUi} = \boldsymbol{A}_{PUi} \boldsymbol{A}_{PUi}^H$. Hence,

$$\gamma_{PUi} = \frac{P_s \left|\boldsymbol{c}_i^H \boldsymbol{T}_{PUi} \boldsymbol{s}_i\right|^2}{\boldsymbol{c}_i^H \boldsymbol{Q}_{PUi} \boldsymbol{c}_i} \quad (2.28)$$

$$= \frac{P_s \left|\boldsymbol{c}_i^H \boldsymbol{A}_{PUi} \boldsymbol{A}_{PUi}^{-1} \boldsymbol{T}_{PUi} \boldsymbol{s}_i\right|^2}{\boldsymbol{c}_i^H \boldsymbol{A}_{PUi} \boldsymbol{A}_{PUi}^H \boldsymbol{c}_i} \quad (2.29)$$

$$= \frac{P_s \left|\tilde{\boldsymbol{c}}_i^H \left(\boldsymbol{A}_{PUi}^{-1} \boldsymbol{T}_{PUi}\right) \boldsymbol{s}_i\right|^2}{\tilde{\boldsymbol{c}}_i^H \tilde{\boldsymbol{c}}_i} \quad (2.30)$$

$$= \frac{P_s \left|\tilde{\boldsymbol{c}}_i^H \left(\boldsymbol{U}_{PUi} \Sigma_{PUi} \boldsymbol{V}_{PUi}^H\right) \boldsymbol{s}_i\right|^2}{\|\tilde{\boldsymbol{c}}_i\|^2} \quad (2.31)$$

where $\tilde{\boldsymbol{c}}_i \triangleq \boldsymbol{A}_{PUi}^H \boldsymbol{c}_i$. Note also that in the numerator of equation (2.29), $\boldsymbol{A}_{PUi} \boldsymbol{A}_{PUi}^{-1}$ is intentionally inserted for successful analysis. Hence, if the sequences are designed as $\boldsymbol{s}_i^{\dagger} = \boldsymbol{v}_{PUi,max}$ and $\tilde{\boldsymbol{c}}_i = \boldsymbol{u}_{PUi,max}$, i.e.,$\boldsymbol{c}_i^{\dagger} = (\boldsymbol{A}_{PUi}^H)^{-1} \boldsymbol{u}_{PUi,max}$, then γ_i is maximized, which is $P_s \left|\lambda_{PUi,max}\right|^2$. ■

Note that if a successive inference cancellation (SIC) is employed, then equation (2.26) should be modified, thus reducing the interference and improving the performance significantly.

But this dissertation does not consider SIC because the intention here is to observe the effectiveness of the proposed algorithm. In the future, the proposed algorithm will be studied to include an SIC scheme.

Remark 2: The Rayleigh quotient, generalized Rayleigh quotient, or also called the generalized (Hermitian) eigenvalue problem, are well known [47–49] and used frequently in the literature, e.g., [50, 51]. In general, the objective function of the generalized Rayleigh quotient can be written as

$$\max_x \frac{x^H A x}{x^H B x} \tag{2.32}$$

where *A* and *B* are nonnegative definite matrices. This generalized Rayleigh quotient in equation (2.32) has been converted into the Rayleigh quotient in the literature using Choleskey factorization as

$$\max_{\tilde{x}} \frac{\tilde{x}^H D \tilde{x}}{\tilde{x}^H \tilde{x}}. \tag{2.33}$$

The optimum vector $\tilde{x}^{\dagger}$, which maximizes the Rayleigh quotient in equation (2.33), can be found as the eigenvector corresponding to the largest eigenvalue of *D*. Note that the objective function in equation (2.28) is different from the conventional ones in equations (2.32) and (2.33) because the objective function is of the type

$$\max_x \frac{\left|x^H A y\right|^2}{x^H B x}. \tag{2.34}$$

The maximization in equations (2.26) or (2.28) should be done with respect to two vectors—x (i.e., the spreading PN sequence vector $\boldsymbol{s}_i$) and y (i.e., the despreading PN sequence vector $\boldsymbol{c}_i$)—instead of one vector x used for the generalized Rayleigh quotient in equation (2.32). So the proposed objective function in equations (2.26) or (2.28) cannot be solved directly by applying the known generalized Rayleigh quotient method. Therefore, this dissertation uniquely solves the problem by inserting $\boldsymbol{A}_{PUi}\boldsymbol{A}_{PUi}^{-1}$ into equation (2.28). In addition, note that the conventional generalized Rayleigh quotient method applies the eigenvalue decomposition (EVD) in equation (2.33), but the proposed method applies the singular value decomposition (SVD) in equation (2.31).

The spreading sequence $\boldsymbol{s}_i$ $(i = 1, \cdots, M)$ needs to be generated jointly and iteratively by collaborating with other users' sequences. In other words, other users' spreading sequences are needed to find user i's spreading sequences iteratively $(i = 1, \cdots, M)$. Iteration stops when the maximum singular value of matrix $\boldsymbol{A}_{PUi}^{-1}\boldsymbol{T}_{PUi}$ converges, which means $\left|\lambda_{PUi,max}{}^{(m)} - \lambda_{PUi,max}{}^{(m-1)}\right| < \varepsilon$, where m is the iteration index, and ε is a sufficiently small number. Once $\boldsymbol{s}_i$ is determined through the iteration, $\boldsymbol{c}_i$ is calculated with no iteration.

2.3 Downlink PC Relay Network

2.3.1 PC Network with One Source, Two Relay, and Two Destinations

Figure 2.5 shows a downlink PC relay network with a base station of two sources, two relays, and two destinations. During phase one, the source transmits the combined message $(\boldsymbol{s}_1 x_1 + \boldsymbol{s}_2 x_2)$ to the relays. During phase two, the relays amplify and forward the signals to the destinations. Let $\boldsymbol{s}_1$ and $\boldsymbol{s}_2$ be the spreading sequences intending for destinations D_1 and D_2, respectively. And let $\boldsymbol{c}_1$ and $\boldsymbol{c}_2$ denote the despreading sequences employed at destinations D_1 and D_2, respectively. If there are no multipath delays and no fading in the channel, then the spreading sequence $\boldsymbol{s}_i$ should be equal to the despreading sequence $\boldsymbol{c}_i$ for user i. In general, this is not the case in practice, e.g., a relay network under a fading environment. Hence, the optimal spreading and despreading sequences can be different for a relay network and should be carefully designed.

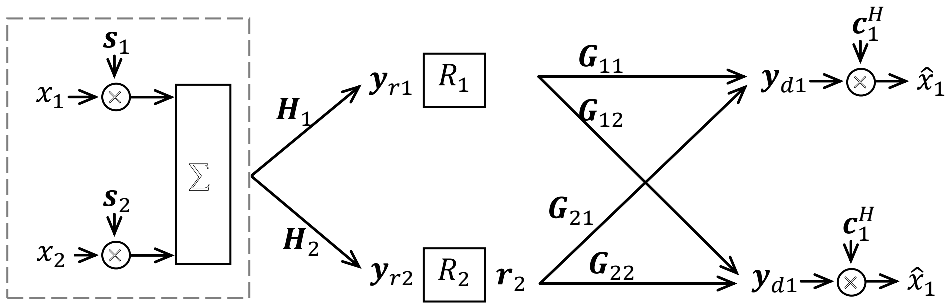

Figure 2.5. Downlink PC network with one combined source, two relays, and two destinations.

The received signal at relayR_1can be written as

$$\boldsymbol{y}_{r1} = \boldsymbol{H}_1(\boldsymbol{s}_1 x_1 + \boldsymbol{s}_2 x_2) + \boldsymbol{n}_{r1}. \tag{2.35}$$

The received signal at relayR_2can be written as

$$\boldsymbol{y}_{r2} = \boldsymbol{H}_2(\boldsymbol{s}_1 x_1 + \boldsymbol{s}_2 x_2) + \boldsymbol{n}_{r2} \tag{2.36}$$

where $\boldsymbol{n}_{r1}$ and $\boldsymbol{n}_{r2}$ are the zero-mean complex additive Gaussian noise vectors at relay one and relay two, respectively. Each has the covariance matrix $\boldsymbol{Z}_{r1} = E\{\boldsymbol{n}_{r1}\boldsymbol{n}_{r1}^H\} = \sigma_{nr1}^2 \boldsymbol{I}_N$ and $\boldsymbol{Z}_{r2} = E\{\boldsymbol{n}_{r2}\boldsymbol{n}_{r2}^H\} = \sigma_{nr2}^2 \boldsymbol{I}_N$, and it is assumed that $\sigma_{nr1}^2 = \sigma_{nr2}^2$.

The j-th AF relay sends $\mathbf{r}_j = \alpha_j \mathbf{y}_{\mathrm{rj}}$ to the destination ($j = 1, 2$), where $\alpha_j = \sqrt{\frac{P_R}{E\{\|\boldsymbol{y}_{rj}\|^2\}}}$ is the scaling factor that preserves power constraint P_R at relay R_j.

The received signals at the destinations can be written as

$$\boldsymbol{y}_{d1} = \boldsymbol{G}_{11}\boldsymbol{r}_1 + \boldsymbol{G}_{21}\boldsymbol{r}_2 + \boldsymbol{n}_{d1} \tag{2.37}$$

$$\boldsymbol{y}_{d2} = \boldsymbol{G}_{12}\boldsymbol{r}_1 + \boldsymbol{G}_{22}\boldsymbol{r}_2 + \boldsymbol{n}_{d2}. \tag{2.38}$$

Denote

$$\boldsymbol{T}_{PD1} \triangleq \alpha_1 \boldsymbol{G}_{11}\boldsymbol{H}_1 + \alpha_2 \boldsymbol{G}_{21}\boldsymbol{H}_2 \tag{2.39}$$

$$\boldsymbol{T}_{PD2} \triangleq \alpha_1 \boldsymbol{G}_{12}\boldsymbol{H}_1 + \alpha_2 \boldsymbol{G}_{22}\boldsymbol{H}_2 \tag{2.40}$$

$$\widetilde{\boldsymbol{n}}_{d1} \triangleq \alpha_1 \boldsymbol{G}_{11}\boldsymbol{n}_{r1} + \alpha_2 \boldsymbol{G}_{21}\boldsymbol{n}_{r2} + \boldsymbol{n}_{d1} \tag{2.41}$$

$$\widetilde{\boldsymbol{n}}_{d2} \triangleq \alpha_1 \boldsymbol{G}_{12}\boldsymbol{n}_{r1} + \alpha_2 \boldsymbol{G}_{22}\boldsymbol{n}_{r2} + \boldsymbol{n}_{d2}. \tag{2.42}$$

Then the received signals can be rewritten as

$$\boldsymbol{y}_{d1} = \boldsymbol{T}_{PD1}(\boldsymbol{s}_1 x_1 + \boldsymbol{s}_2 x_2) + \widetilde{\boldsymbol{n}}_{d1} \tag{2.43}$$

$$\boldsymbol{y}_{d2} = \boldsymbol{T}_{PD2}(\boldsymbol{s}_1 x_1 + \boldsymbol{s}_2 x_2) + \widetilde{\boldsymbol{n}}_{d2} \tag{2.44}$$

Let $\boldsymbol{K}_1$ and $\boldsymbol{K}_2$ denote the covariance matrices of the noise vectors $\widetilde{\boldsymbol{n}}_{d1}$ and $\widetilde{\boldsymbol{n}}_{d2}$, respectively, as

$$\boldsymbol{K}_1 = \mathrm{E}\{\widetilde{\boldsymbol{n}}_{d1}\widetilde{\boldsymbol{n}}_{d1}^H\} \tag{2.45}$$

$$\boldsymbol{K}_2 = \mathrm{E}\{\widetilde{\boldsymbol{n}}_{d2}\widetilde{\boldsymbol{n}}_{d2}^H\}. \tag{2.46}$$

The destinations despread the received signals as

$$\hat{x}_1 = \boldsymbol{c}_1^H \boldsymbol{T}_{PD1}\boldsymbol{s}_1 x_1 + \boldsymbol{c}_1^H \boldsymbol{T}_{PD1}\boldsymbol{s}_2 x_2 + \boldsymbol{c}_1^H \widetilde{\boldsymbol{n}}_{d1} \tag{2.47}$$

$$\hat{x}_2 = \boldsymbol{c}_2^H \boldsymbol{T}_{PD2}\boldsymbol{s}_1 x_1 + \boldsymbol{c}_2^H \boldsymbol{T}_{PD2}\boldsymbol{s}_2 x_2 + \boldsymbol{c}_2^H \widetilde{\boldsymbol{n}}_{d2}. \tag{2.48}$$

Let $\boldsymbol{Q}_{PD1}$ and $\boldsymbol{Q}_{PD2}$ denote the covariance matrices of the interference-plus-noise vectors as

$$\boldsymbol{Q}_{PD1} \triangleq P_s \boldsymbol{T}_{PD1}\boldsymbol{s}_2\boldsymbol{s}_2^H \boldsymbol{T}_{PD1}^H + \boldsymbol{K}_1 \tag{2.49}$$

$$\boldsymbol{Q}_{PD2} \triangleq P_s \boldsymbol{T}_{PD2}\boldsymbol{s}_1\boldsymbol{s}_1^H \boldsymbol{T}_{PD2}^H + \boldsymbol{K}_2. \tag{2.50}$$

Also, define $\boldsymbol{A}_{PD1}$ as the Cholesky decomposition matrix of covariance matrix $\boldsymbol{Q}_{PD1}$, and $\boldsymbol{A}_{PD2}$ as the Cholesky decomposition matrix of covariance matrix $\boldsymbol{Q}_{PD2}$. Let $\boldsymbol{v}_{PD1,max}$ and $\boldsymbol{u}_{PD1,max}$ denote the right and left singular vectors, respectively, corresponding to the maximum singular value $\lambda_{PD1,max}$ of matrix $\boldsymbol{A}_{PD1}^{-1}\boldsymbol{T}_{PD1}$; and $\boldsymbol{v}_{PD2,max}$ and $\boldsymbol{u}_{PD2,max}$ as the right and left singular vectors, respectively, corresponding to the maximum singular value $\lambda_{PD2,max}$ of matrix $\boldsymbol{A}_{PD2}^{-1}\boldsymbol{T}_{PD2}$.

Then the sequences that maximize the SINR at destination D_1 are $\boldsymbol{s}_1^\dagger = \boldsymbol{v}_{PD1,max}$ and $\boldsymbol{c}_1^\dagger = (\boldsymbol{A}_{PD1}^H)^{-1}\boldsymbol{u}_{PD1,max}$, and the corresponding sequences that maximize the SINR at destination D_2 are $\boldsymbol{s}_2^\dagger = \boldsymbol{v}_{PD2,max}$ and $\boldsymbol{c}_2^\dagger = (\boldsymbol{A}_{PD2}^H)^{-1}\boldsymbol{u}_{PD2,max}$. And the corresponding maximum SINR can be written as

$$\max_{\boldsymbol{s}_1,\boldsymbol{c}_1} \gamma_{PD1} = P_s\left|\lambda_{PD1,max}\right|^2 \tag{2.51}$$

$$\max_{\boldsymbol{s}_2,\boldsymbol{c}_2} \gamma_{PD2} = P_s\left|\lambda_{PD2,max}\right|^2. \tag{2.52}$$

2.3.2 PC Network with One Source, K Relays, and M Destinations

A downlink relay network with one combined source, K number of relays, and M number of destinations is shown in Figure 2.6. $\boldsymbol{H}_j$ is define as the channel matrix from the source to relay R_j, $\boldsymbol{G}_{ji}$ as the channel matrix from relay R_j to destination D_i, where i is the destination index $(i = 1, \cdots, M)$, and j as the relay index $(j = 1, \cdots, K)$. Figure 2.6 can represent a downlink network consisting of multiple mobiles, multiple relays, and a base station. Here, a base station transmits M number of spread source signals together. Since a BS downlink signal is typically much stronger than an uplink signal, only a single-layer relay system is considered adequate for cell coverage, although the analysis can be extended to a multihop downlink relay network.

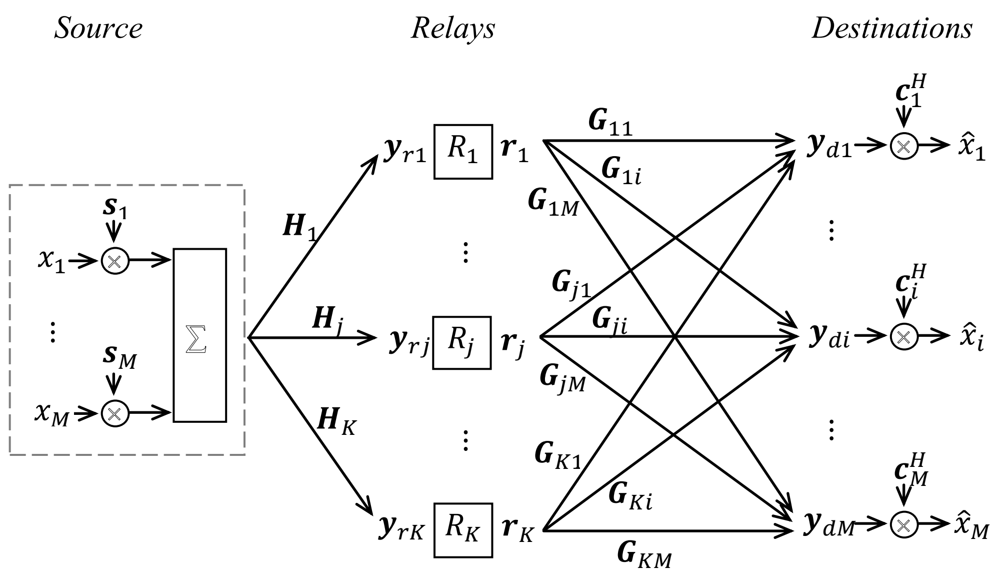

Figure 2.6. Downlink PC network with one combined source, *K* relays, and *M* destinations.

The received signal at relay R_j is

$$\boldsymbol{y}_{rj} = \boldsymbol{H}_j \sum_{i=1}^{M} \boldsymbol{s}_i x_i + \boldsymbol{n}_{rj} \tag{2.53}$$

where $\boldsymbol{n}_{rj}$ is the *N*-dimensional zero-mean complex additive Gaussian noise time sample vector sampled at every chip at relay R_j with covariance matrix $\boldsymbol{Z}_{rj} = E\{\boldsymbol{n}_{rj}\boldsymbol{n}_{rj}^H\} = \sigma_{nrj}^2 \boldsymbol{I}_N$. Relay R_j forwards $\boldsymbol{r}_j = \alpha_j \boldsymbol{y}_{rj}$ to the destination, where α_j is the scaling factor that preserves power constraint P_R at relay R_j, $\alpha_j = \sqrt{\frac{P_R}{E\{\|\boldsymbol{y}_{rj}\|^2\}}}$.

The received signals at destination D_i can be written as

$$\boldsymbol{y}_{di} = \sum_{j=1}^{K} \boldsymbol{G}_{ji} \boldsymbol{r}_j + \boldsymbol{n}_{di} \tag{2.54}$$

$$= \left(\sum_{j=1}^{K} \alpha_j \boldsymbol{G}_{ji} \boldsymbol{H}_j\right)\left(\sum_{k=1}^{M} \boldsymbol{s}_k x_k\right) + \sum_{j=1}^{k} \alpha_j \boldsymbol{G}_{ji} \boldsymbol{n}_{rj} + \boldsymbol{n}_{di}. \tag{2.55}$$

Denote

$$\boldsymbol{T}_{PDi} \triangleq \sum_{j=1}^{K} \alpha_j \boldsymbol{G}_{ji} \boldsymbol{H}_j \text{ and} \tag{2.56}$$

$$\widetilde{\boldsymbol{n}}_{di} \triangleq \sum_{j=1}^{k} \alpha_j \boldsymbol{G}_{ji} \boldsymbol{n}_{rj} + \boldsymbol{n}_{di}. \tag{2.57}$$

Then the received signal at destination D_i can be rewritten as

$$\boldsymbol{y}_{di} = \boldsymbol{T}_{PDi} \sum_{k=1}^{M} \boldsymbol{s}_k x_k + \widetilde{\boldsymbol{n}}_{di}. \tag{2.58}$$

And the covariance matrix of the overall noise vector can be written as

$$\boldsymbol{K}_i = \mathrm{E}\{\widetilde{\boldsymbol{n}}_{di} \widetilde{\boldsymbol{n}}_{di}{}^H\} \tag{2.59}$$

$$= \sum_{j=1}^{K} \alpha_j{}^2 \boldsymbol{G}_{ji} \mathbf{Z}_{\mathrm{rj}} \boldsymbol{G}_{ji}{}^H + \boldsymbol{Z}_{di}. \tag{2.60}$$

The destination despreads the received signal for source i as

$$\hat{x}_i = \boldsymbol{c}_i{}^H \boldsymbol{y}_{di} \tag{2.61}$$

$$= \boldsymbol{c}_i{}^H \boldsymbol{T}_{PDi} \sum_{k=1}^{M} \boldsymbol{s}_k x_k + \boldsymbol{c}_i{}^H \widetilde{\boldsymbol{n}}_{di}. \tag{2.62}$$

$$= \boldsymbol{c}_i{}^H \boldsymbol{T}_{PDi} \boldsymbol{s}_i x_i + \boldsymbol{c}_i{}^H \left(\boldsymbol{T}_{PDi} \sum_{\substack{k=1 \\ k \neq i}}^{M} \boldsymbol{s}_k x_k + \widetilde{\boldsymbol{n}}_{di}\right). \tag{2.63}$$

Theorem 2: Let $\boldsymbol{Q}_{PDi} \triangleq P_s \sum_{\substack{k=1 \\ k\neq i}}^{\boldsymbol{M}} \boldsymbol{T}_{PDi}\boldsymbol{s}_k\boldsymbol{s}_k^H\boldsymbol{T}_{PDi}^H + \boldsymbol{K}_i$ denote the covariance matrix of the interference-plus-noise component $\boldsymbol{c}_i{}^H\left(\boldsymbol{T}_{PDi}\sum_{\substack{k=1 \\ k\neq i}}^{M} \boldsymbol{s}_k x_k + \widetilde{\boldsymbol{n}}_{di}\right)$ in equation (2.63). Let $\boldsymbol{A}_{PDi}$ denote the Cholesky decomposition matrix of covariance matrix $\boldsymbol{Q}_{PDi}$ as $\boldsymbol{Q}_{PDi} = \boldsymbol{A}_{PDi}\boldsymbol{A}_{PDi}^H$. Let $\boldsymbol{v}_{PDi,max}$ and $\boldsymbol{u}_{PDi,max}$ denote the right and left singular vectors, respectively, corresponding to the maximum singular value $\lambda_{PDi,max}$ of matrix $\boldsymbol{A}_{PDi}^{-1}\boldsymbol{T}_{PDi}$. Then it can be stated that the sequences that maximize the SINR at destination D_i are $\boldsymbol{s}_i^\dagger = \boldsymbol{v}_{PDi,max}$ and $\boldsymbol{c}_i^\dagger = (\boldsymbol{A}_{PDi}^H)^{-1}\boldsymbol{u}_{PDi,max}$, and the corresponding maximum SINR for the downlink relay network can be written as

$$\max_{\boldsymbol{s}_i,\boldsymbol{c}_i} \gamma_{PDi} = P_s\left|\lambda_{PDi,max}\right|^2. \tag{2.64}$$

Proof of Theorem 2:

$$\gamma_{PDi} = \frac{\mathrm{E}\left[\left|\boldsymbol{c}_i^H\boldsymbol{T}_{PDi}\boldsymbol{s}_i x_i\right|^2\right]}{\mathrm{E}\left[\left|\boldsymbol{c}_i^H\boldsymbol{T}_{PDi}\sum_{\substack{k=1 \\ k\neq i}}^{M}\boldsymbol{s}_k x_k + \boldsymbol{c}_i{}^H\widetilde{\boldsymbol{n}}_{di}\right|^2\right]} \tag{2.65}$$

$$= \frac{P_s\left|\boldsymbol{c}_i^H\boldsymbol{T}_{PDi}\boldsymbol{s}_i\right|^2}{\boldsymbol{c}_i^H\boldsymbol{Q}_{PDi}\boldsymbol{c}_i} \tag{2.66}$$

$$= \frac{P_s\left|\boldsymbol{c}_i^H\boldsymbol{A}_{PDi}\boldsymbol{A}_{PDi}^{-1}\boldsymbol{T}_{PDi}\boldsymbol{s}_i\right|^2}{\boldsymbol{c}_i^H\boldsymbol{A}_{PDi}\boldsymbol{A}_{PDi}^H\boldsymbol{c}_i} \tag{2.67}$$

$$= \frac{P_s\left|\tilde{\boldsymbol{c}}_i^H(\mathbf{U}_{PDi}\Sigma_{PDi}\boldsymbol{V}_{PDi}^H)\boldsymbol{s}_i\right|^2}{\|\tilde{\boldsymbol{c}}_i\|^2}. \tag{2.68}$$

If the sequences are designed as $\boldsymbol{s}_i^\dagger = \boldsymbol{v}_{PDi,max}$ and $\boldsymbol{c}_i^\dagger = (\boldsymbol{A}_{PDi}^H)^{-1}\boldsymbol{u}_{PDi,max}$, then γ_{PDi} is maximized as $P_s\left|\lambda_{PDi,max}\right|^2$. ■

2.4 Simulation Results for PC Relay Networks

Monte Carlo simulations are performed to illustrate the bit error rate (BER) performance of the proposed spreading sequence design scheme. Binary phase shift keying (BPSK) modulation is applied to all simulations, and the input signal-to-noise ratio (SNR) is E_b/N_0, where E_b is the bit energy of source transmitted symbol x, and N_0 is the one-sided power spectral density of thermal noise at the relays and the destinations.

For a relay network, the number of iterations needed depends on the number of users, number of relays, and spreading sequence length. Figure 2.7 shows an example of the iteration plots for a single-layer relay network under a frequency-selective fading channel with L = 6 number of taps, where pc211 represents partial connectivity with two sources, one relay, and one destination; and pc241 represents partial connectivity with two sources, four relays, and one destination. We choose $\varepsilon = 0.01$. As can be seen from the simulation results, as the spreading sequence length increases, the number of iterations increases; and as the number of users and relays increases, the number of iterations also increases. Figure 2.8 shows the maximum singular values of each iteration for the two users in the pc211 relay network.

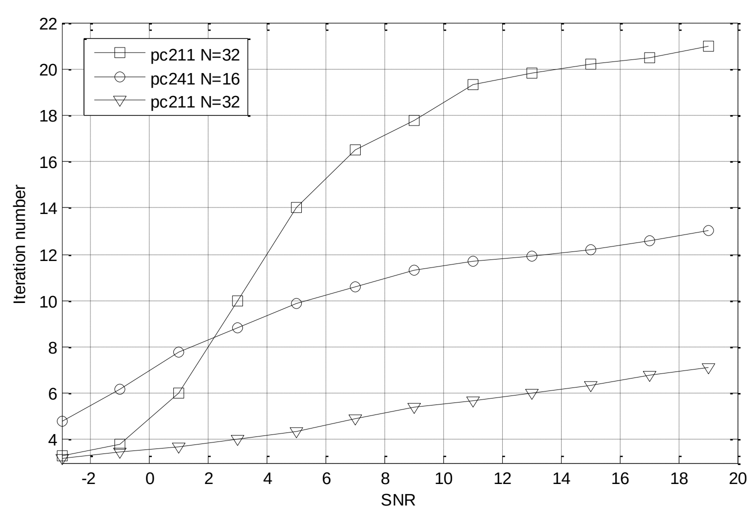

Figure 2.7. Iteration number versus SNR for uplink PC relay networks.

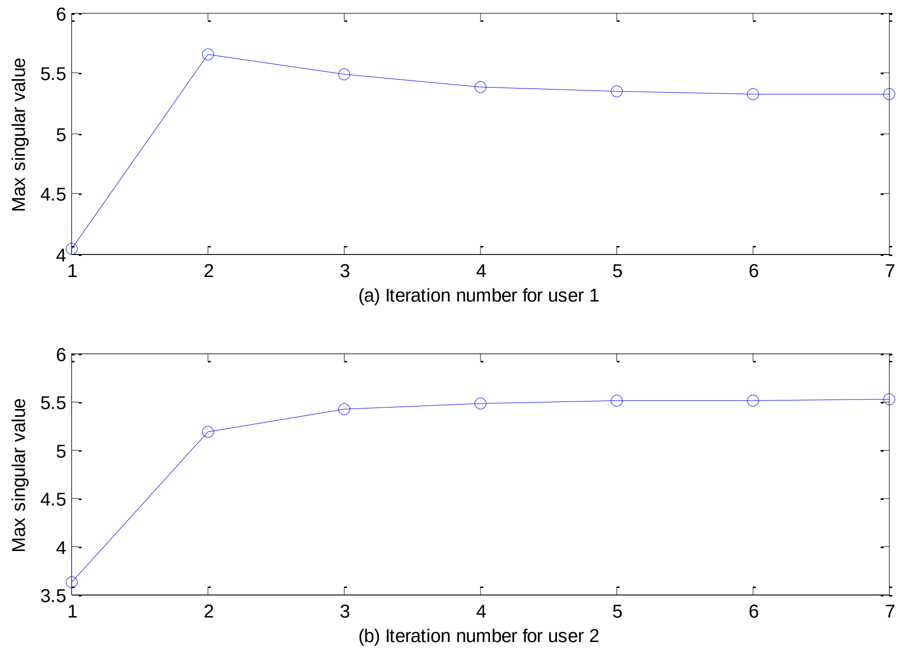

Figure 2.8. Maximum singular values for two users of pc211 versus iteration number.

If there are no relays between the sources and the destinations, then two iterations are sufficient. Figures 2.9 (a) and (b) show the maximum singular value versus the iteration index for two sources and one destination by using the proposed algorithm. Figures 2.9 (c) and (d) show the results using the algorithm in the work of Rajappan and Honig [36, eq. (17)] under the same environments used in Figures 2.9 (a) and (b). In Figure 2.9, no relay is used for fair comparisons because the algorithm in the work of Rajappan and Honig [36, eq. (17)] is for a direct link only, i.e., no relay case. The PN sequence length is chosen as $N = 16$, the number of multipaths $L = 4$, and the iteration stopping criterion $\varepsilon = 0.01$. The channel vectors $\boldsymbol{h}_1$ and $\boldsymbol{h}_2$ from source 1 and source 2 to the destination are randomly generated, as follows:

$$\boldsymbol{h}_1 = [0.3414 - 0.5025i, -0.3126 + 0.2715i, 0.4190 + 0.3748i, -0.1986 - 0.3224i, 0,0,0,0,0,0,0,0,0,0,0,0]^T$$

$$\boldsymbol{h}_2 = [-0.5130 + 0.1285i, 0.2561 - 0.7744i, 0.1648 + 0.1409i, -0.0539 + 0.0716i, 0,0,0,0,0,0,0,0,0,0,0,0]^T.$$

Observe in Figure 2.9 that the proposed algorithm converges within two iterations, whereas the algorithm in the work of Rajappan and Honig [36] often does not converge, as stated in that reference.

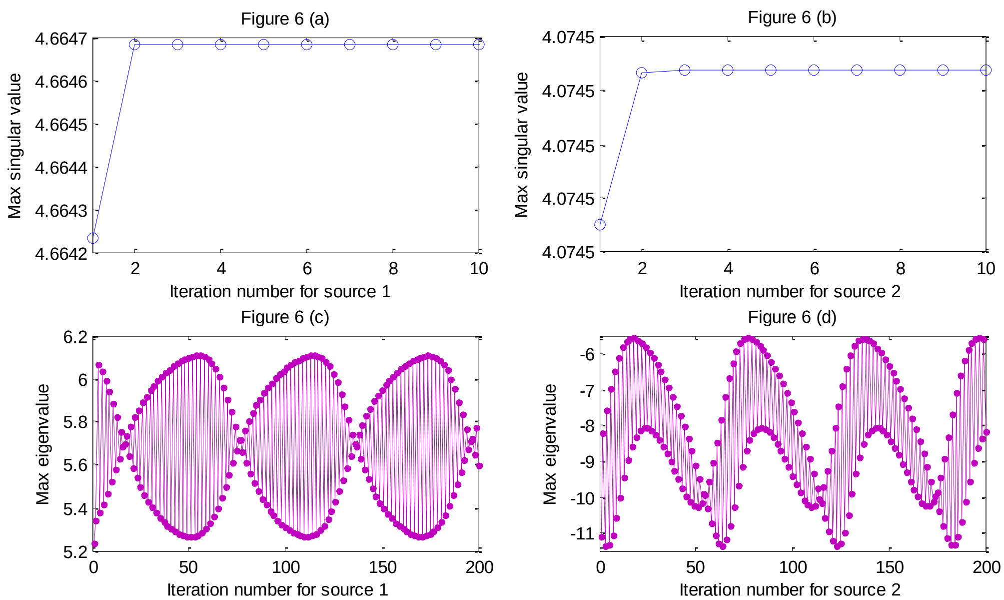

Figure 2.9. (a) and (b): maximum singular value versus iteration index for two sources and one destination by using proposed algorithm; (c) and (d): maximum eigenvalues using algorithm in work of Rajappan and Honig [36, eq. (17)] under same environment.

Figure 2.10 shows corresponding BER comparisons between the proposed algorithm and that in the work of Rajappan and Honig [36]. In the legend, the RH notation is expressed as "RH $i1$," representing i number of sources and one destination case for the network [36]. In the plot, "RH 11," "Proposed 11," and "Proposed 21" show the same performance, implying that the proposed algorithm is effective for a multiple number of sources. Observe that when the number of users increases from one to two for the algorithm in the work of Rajappan and Honig [36], the performance gets 10.5 dB worse at BER = 10^{-3}, whereas the proposed algorithm does not show any degradation. For the single-user case, when the eigenvector corresponding to the maximum eigenvalue for the algorithm in the work of Rajappan and Honig [36] is used, it can be seen that the BER is not decreasing as the SNR increases, which is not plotted in Figure 2.10. Hence, the singular vector is applied for this case and gets the same BER as the algorithm proposed in this dissertation.

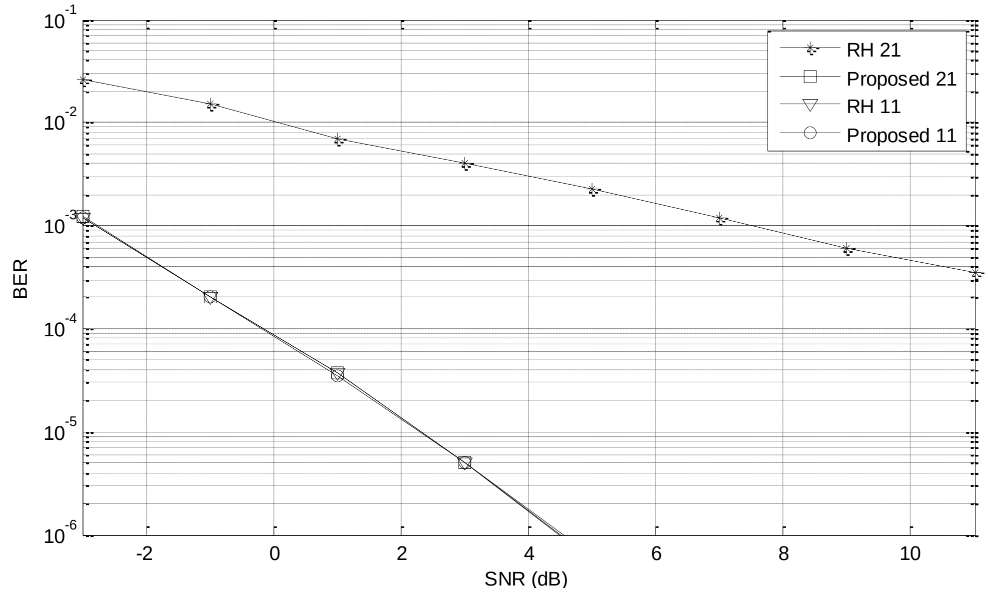

Figure 2.10. BER comparison between proposed algorithm and one in work of Rajappan and Honig [36].

Figure 2.11 shows BER versus input SNR simulation results for a single-layer uplink relay network. Sequence length $N = 16$, frequency-selective fading channel with $L = 6$ number of taps, and the iteration stopping criterion $\varepsilon = 0.05$ are used. In the legend, the pc notation is expressed as "pcij1," representing a partial connectivity relay network with i number of sources, j number of relays, and one destination. Observe that the BER performance improves as the number of relays increases, when the number of sources and the number of destinations are fixed. For example, pc241 is 2 dB better in SNR at BER = 10^{-4} than pc221. This is reasonable because higher spatial diversity gain can be achieved with a greater number of relays. Also, observe that BER performance becomes slightly worse as the number of sources increases, when the number of relays and the number of destinations are fixed. For example, pc12,12,1 is 0.3 dB worse in SNR at BER = 10^{-4} than pc6,12,1. This is also reasonable because a greater number of sources causes more network interference.

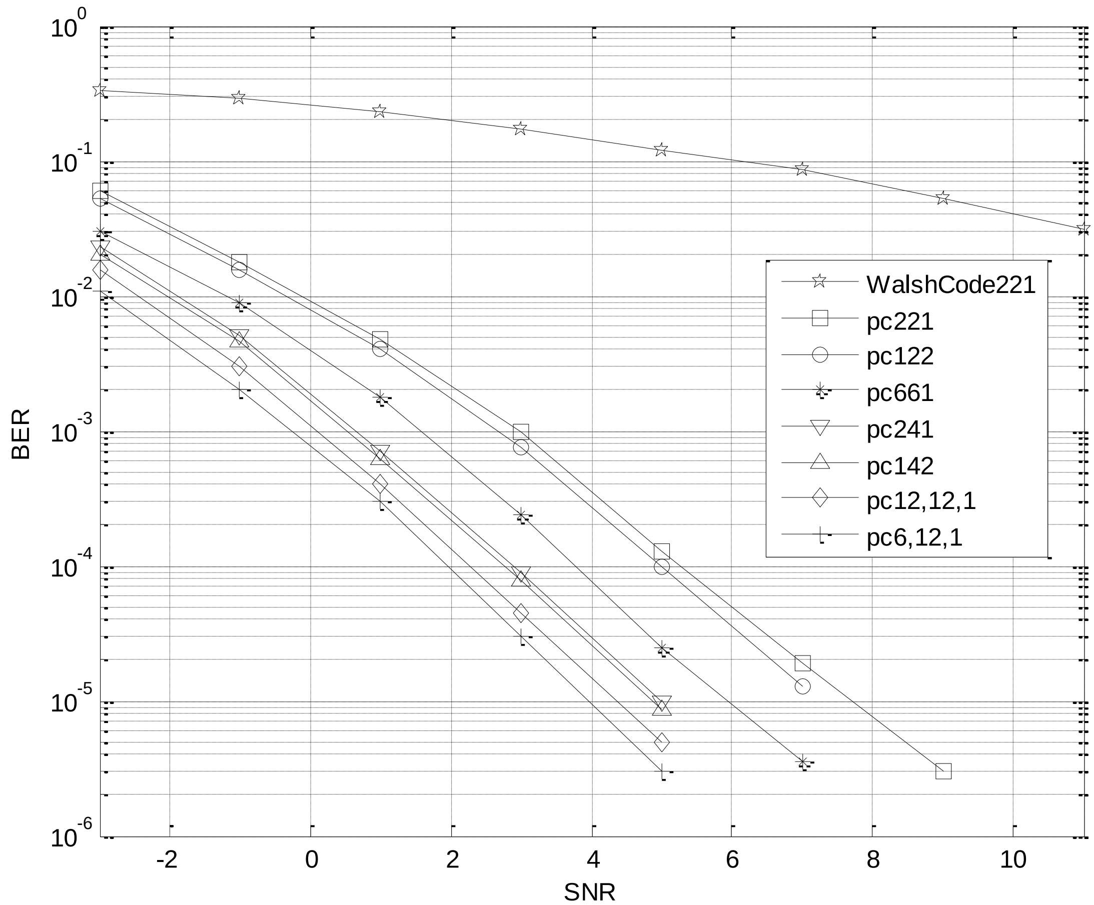

Figure 2.11. BER for uplink PC relay network (N = 16, L = 6).

Another important result can be observed in Figure 2.11. The proposed optimum adaptive PN spreading scheme shows significantly better performance than the conventional non-adaptive Walsh codes for an uplink relay network. For example, pc221 is 13 dB better in SNR at $BER = 3 \times 10^{-2}$ than Walsh code 221. An important lesson here is that using a fixed Walsh code for both PN spreading and despreading sequences is not desirable and not effective in the multipath frequency-selective fading environment because the orthogonality in the Walsh code can be destroyed. However, the proposed adaptive PN spreading scheme can mitigate the effects of the frequency-selective fading. Finally, observe in Figure 2.11 that a downlink single-layer relay network shows a similar performance as the uplink single-layer relay network. For example, the BER difference between the pc241 uplink and the pc142 downlink is within 0.1 dB at $BER = 10^{-4}$, because the interference expressions or effects for uplink and downlink are similar to each other, as in equations (2.26) and (2.65).

Figures 2.12 and 2.13 show the degree to which the network's BER performance will be degraded when channels experience broadband noise jamming. Parameters N = 16, L = 6, and $\varepsilon = 0.05$ are used. Three different cases are considered: (1) jamming between sources and relays (i.e., jamR in the legend), (2) jamming between relays and destinations (i.e., jamD in the legend), and (3) jamming at both places (i.e., jamRD in the legend).

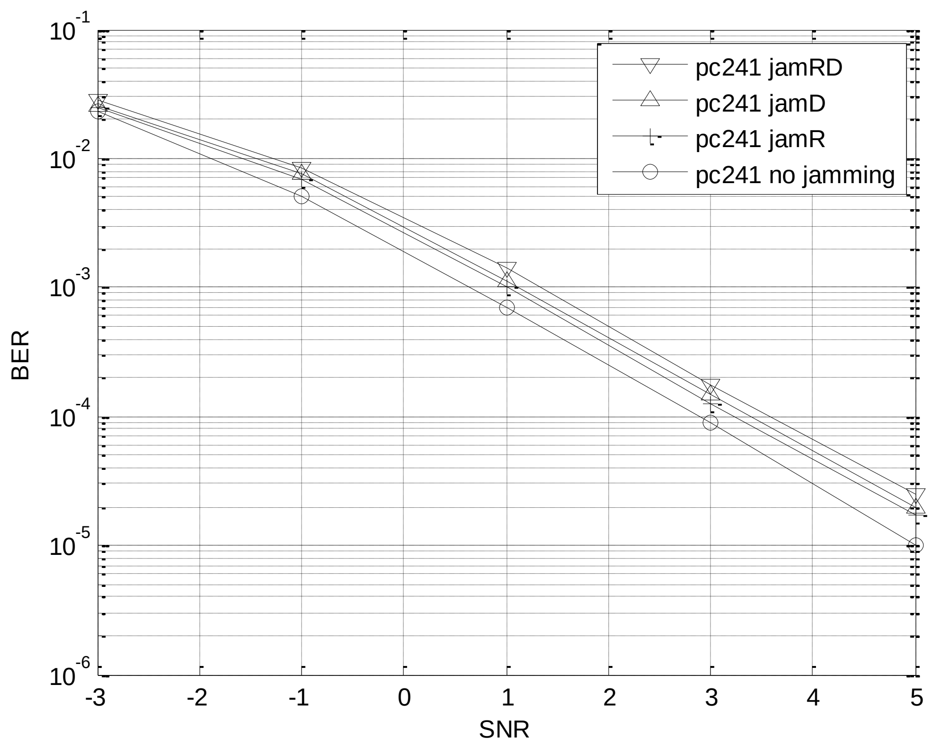

Figure 2.12 BER for uplink PC relay network with jamming signal power 0.3 P_S (N = 16, L = 6).

Observe in Figure 2.12 that a jamming signal can only degrade the BER performance less than 1 dB in SNR at BER = 10^{-4} for the pc241 uplink, even if the jammer uses significant power such as 30% of the desired signal's power P_S. Also, observe in Figure 2.13 that a jamming signal can only degrade the BER performance less than 1.3 dB in SNR at $BER = 10^{-4}$ for the pc142 downlink, even if the jammer uses significant power, such as 30% of the desired signal's power.

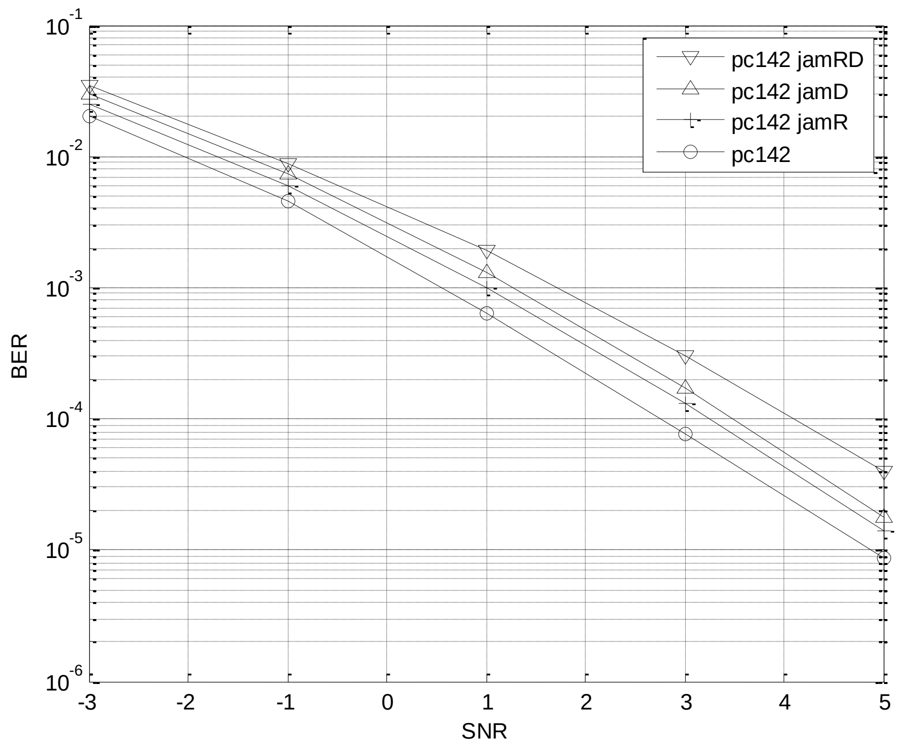

Figure 2.13. BER for downlink PC relay network with jamming signal power 0.3 P_s (N = 16, L = 6).

In practice, imperfect estimates of channel state information matrix $\widehat{\boldsymbol{H}}$ are available instead of perfect CSI $\boldsymbol{H}$. The estimated channel matrices are represented as $\widehat{\boldsymbol{H}} = \boldsymbol{H} + \Delta_{\boldsymbol{H}}$, where $\Delta_{\boldsymbol{H}}$ represents the channel estimation error matrix consisting of independent zero-mean Gaussian random variables with variances $\sigma_{\Delta_{\boldsymbol{H}}}^2$. Figure 2.14 shows BER performance versus input SNR with channel estimation errors power of $\sigma_{\Delta_{\boldsymbol{H}}}^2 = 0.3\ \sigma_{\boldsymbol{H}}^2$. Parameters $N = 16$, $L = 6$, and $\varepsilon = 0.05$ are used. Observe in Figure 2.14 that channel uncertainty can degrade BER performance by 2.1 dB and 2.7 dB in SNR at $BER = 10^{-3}$ for the pc142 downlink and the pc241 uplink, respectively, when channel uncertainty variance is $0.3\ \sigma_{\boldsymbol{H}}^2$. By comparing the results in Figures 2.12 to 2.14, channel uncertainty can cause a worse performance than a broadband jamming signal with the same amount of power. This is because the jamming signal is added as an additional noise, and the covariance matrix of the jamming plus noise is constant, which has less influence on the iteration process in finding the PN sequences than the channel uncertainty in equations (2.26) and (2.65).

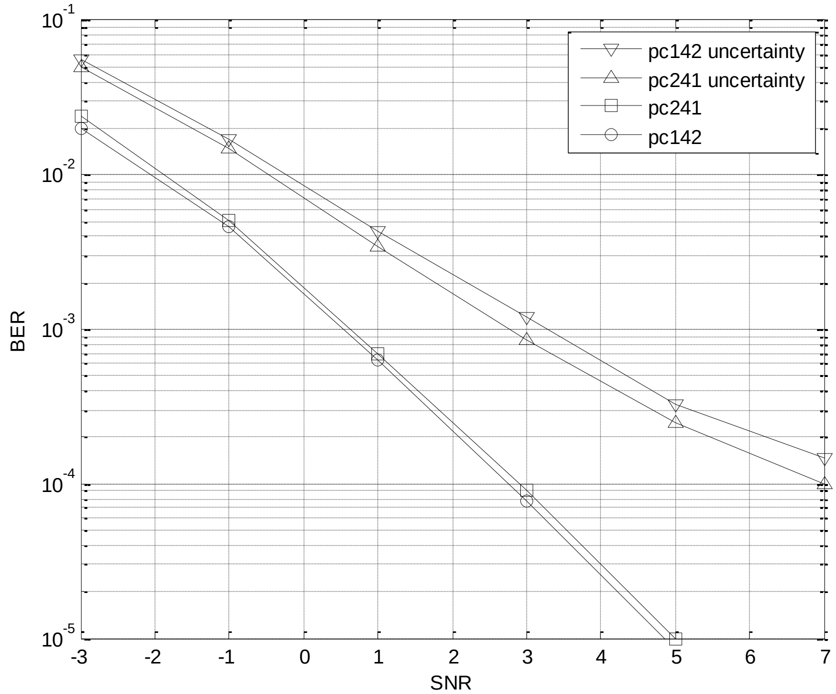

Figure 2.14. BER for PC relay network with channel uncertainty variance 0.3 $\sigma_{\boldsymbol{H}}^2$ (N = 16, L = 6).

Figure 2.15 shows simulation results for sequence length N = 32, frequency-selective fading channel with L = 4 number of taps, and four iterations. Comparing Figures 2.15 and Figure 2.11, it can be seen that the BER decreases as the number of multipath taps increases from L = 4 to L = 6. This is because with a greater number of multipaths, the destination receives more duplicates of the transmitted signal and hence can improve the decoding accuracy.

Figures 2.16, 2.17, and 2.18 show simulation results for N = 32, L= 4, under broadband noise jamming at the destination. Assume that all channels from the relays to the destination are jammed. The jamming signal power shown in these figures is 0.1 P_s, 0.2 P_s, and 0.3 P_s, respectively. As can be seen, as the jamming signal power increases, the BER performance degrades non-negligibly. In other words, both the spatial and the time diversity get lost.

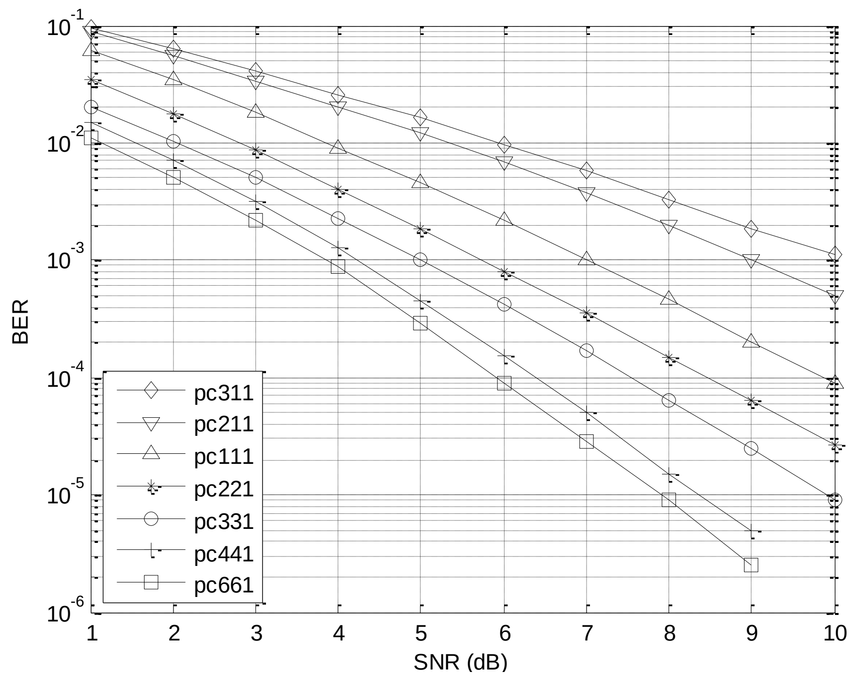

Figure 2.15. BER for uplink PC relay network (N = 32, L = 4).

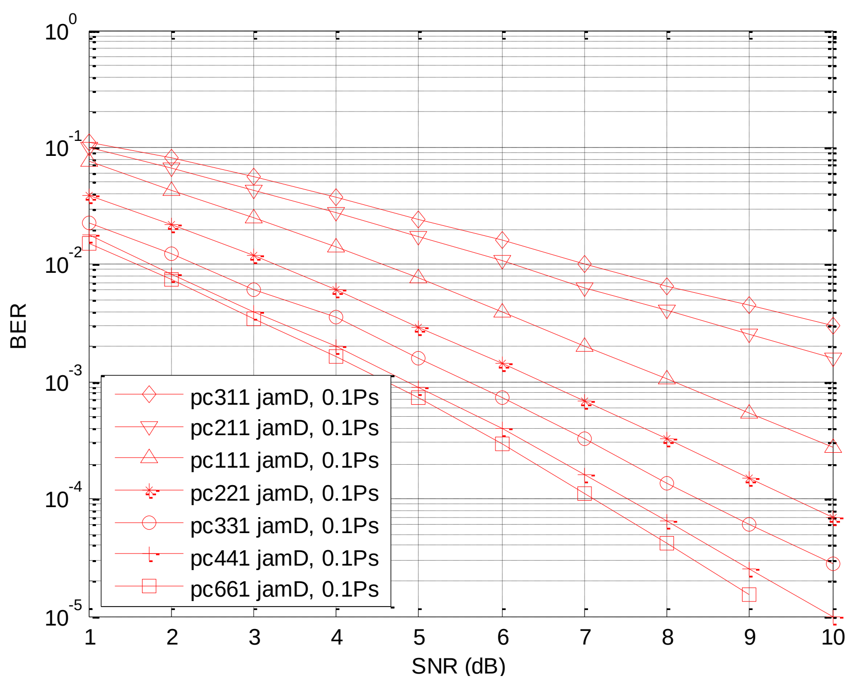

Figure 2.16. BER for uplink PC relay network with jamming signal power 0.1 P_S (N = 32, L = 4).

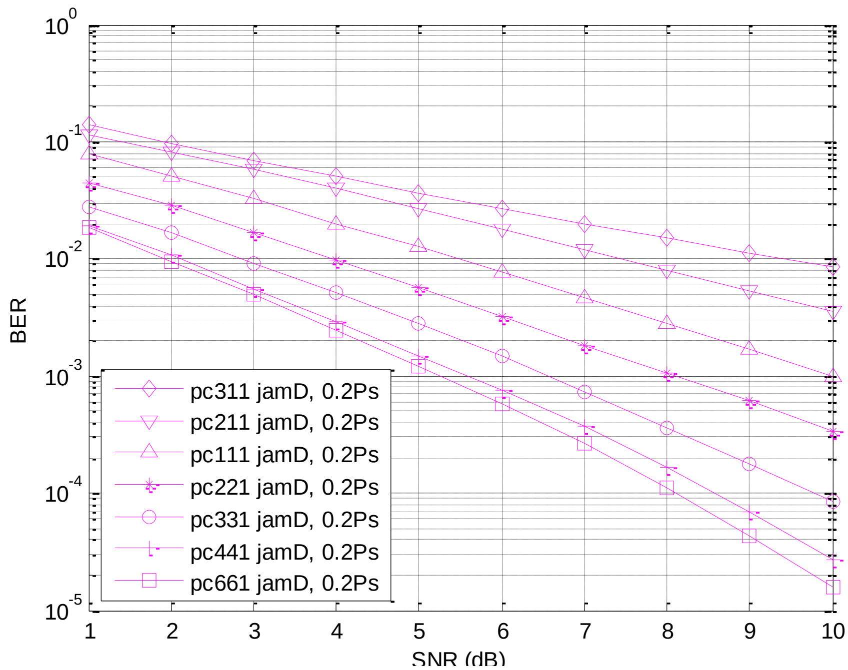

Figure 2.17. BER for uplink PC relay network with jamming signal power 0.2 P_S (N = 32, L = 4).

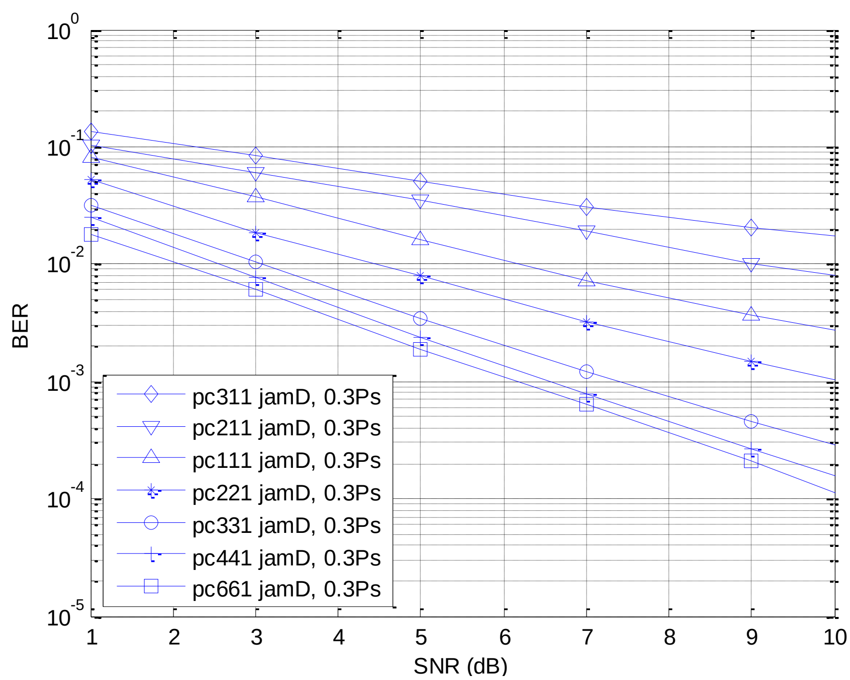

Figure 2.18. BER for uplink PC relay network with jamming signal power 0.3 P_S (N = 32, L = 4).

2.5 Chapter Conclusion

A method of designing spreading sequences based on maximizing the SINR under frequency-selective fading channels was studied in this chapter. The proposed algorithm is applicable to a general partially connected relay network with multiple sources, relays, and destinations. First, it was observed that the proposed algorithm converges much faster than the existing algorithm in the work of Rajappan and Honig [36], which often does not converge. Second, when there are no relays and the number of users increases, performance gets much worse for the existing algorithm in the work of Rajappan and Honig [36], whereas the proposed algorithm shows negligible degradation. Third, the proposed adaptive PN spreading scheme can mitigate the effects of frequency-selective fading well, compared to the fixed non-adaptive sequences, e.g., Walsh code. Fourth, channel uncertainty can degrade BER performance non-negligibly when channel uncertainty is as high as thirty percent of the channel power. Fifth, channel uncertainty can cause a worse performance than a broadband jamming signal with the same amount of power. Finally, the proposed PN sequences are not available to a jammer, in general, but rather to the sources and destinations. In addition, the PN sequences keep changing from one frame to another. Therefore, the proposed DS-CDMA relay network is more secure than the existing systems with fixed PN sequences.

CHAPTER 3

FULLY CONNECTED RELAY NETWORK

3.1 FC Network with One Source, One Relay, and One Destination

If a source, a relay and a destination are located arbitrarily, then the direct link signal strength from the source to the destination is not negligible. In this case, it may be necessary to include the direct link in the performance analysis.

Definition 2 (Fully Connected): A relay network is called a fully connected relay network when the direct link from a source to a destination is not negligible, compared to the link from a source to a relay or from a relay to a destination, as shown in Figure 3.1. First, consider the three-terminal network: a source, a relay, and a destination, each equipped with a single antenna, as shown in Figure 3.2.

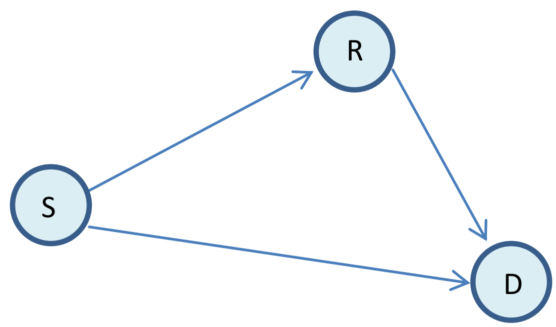

Figure 3.1. Fully connected relay network.

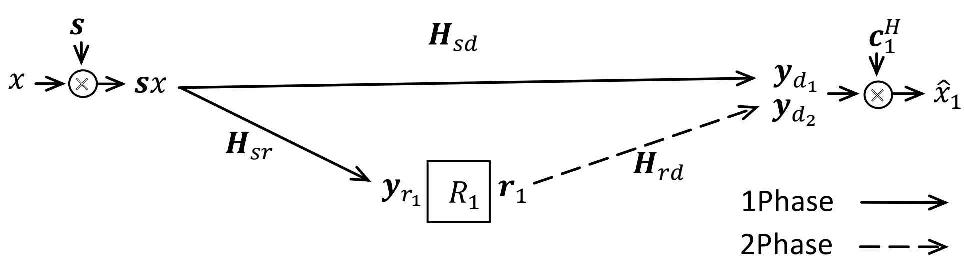

Figure 3.2. FC relay network with one source, one relay, and one destination.

The overall transmission interval is divided into two phases. In phase one, the source transmits to the destination, while the relay remains silent. In phase two, the relay transmits to the destination, while the source remains silent.

In phase one, the source broadcasts its signal to both the relay and the destination. Assume that the source employs a length N spreading sequence $\boldsymbol{s} = [s_1, s_2, \cdots, s_N]^T$ to transmit its information symbol x, with power $E\{|x|^2\} = P_s$. The received signal at the relay can be written as

$$\boldsymbol{y}_r = \boldsymbol{H}_{sr}\boldsymbol{s}x + \boldsymbol{n}_r \tag{3.1}$$

where $\boldsymbol{n}_r$ is the $N \times 1$ zero-mean complex additive Gaussian noise vector with covariance matrix $\boldsymbol{Z}_r = E\{\boldsymbol{n}_r\boldsymbol{n}_r^H\} = \sigma_{nr}^2\boldsymbol{I}_N$. The received signal at the destination during phase one is

$$\boldsymbol{y}_{d1} = \boldsymbol{H}_{sd}\boldsymbol{s}x + \boldsymbol{n}_{d1}. \tag{3.2}$$

In phase two, the relay sends $\boldsymbol{r} = \alpha\boldsymbol{y}_r$ to the destination, where α is a scaling factor that preserves the power constraint P_R at the relay, $\alpha = \sqrt{\frac{P_R}{E\{\|\boldsymbol{y}_r\|^2\}}}$. The received signal at the destination during phase two is

$$\boldsymbol{y}_{d2} = \alpha\boldsymbol{H}_{rd}\boldsymbol{H}_{sr}\boldsymbol{s}x + \alpha\boldsymbol{H}_{rd}\boldsymbol{n}_r + \boldsymbol{n}_{d2} \tag{3.3}$$

Then the overall received signal at the destination can be written as

$$\boldsymbol{y}_d = \begin{bmatrix}\boldsymbol{y}_{d1}\\ \boldsymbol{y}_{d2}\end{bmatrix} = \begin{bmatrix}\boldsymbol{H}_{sd}\boldsymbol{s}x + \boldsymbol{n}_{d1}\\ \alpha\boldsymbol{H}_{rd}\boldsymbol{H}_{sr}\boldsymbol{s}x + \alpha\boldsymbol{H}_{rd}\boldsymbol{n}_r + \boldsymbol{n}_{d2}\end{bmatrix} \tag{3.4}$$

$$= \boldsymbol{H}\boldsymbol{s}x + \boldsymbol{n}_1 \tag{3.5}$$

where $\boldsymbol{H} \triangleq \begin{bmatrix}\boldsymbol{H}_{sd}\\ \alpha\boldsymbol{H}_{rd}\boldsymbol{H}_{sr}\end{bmatrix}$ and $\boldsymbol{n}_1 \triangleq \begin{bmatrix}\boldsymbol{n}_{d1}\\ \alpha\boldsymbol{H}_{rd}\boldsymbol{n}_r + \boldsymbol{n}_{d2}\end{bmatrix}$.

The covariance matrix of noise $\boldsymbol{n}_1$ is

$$\boldsymbol{K}_{F1} = \begin{bmatrix} \boldsymbol{Z}_{d1} & 0 \\ 0 & \alpha^2 \boldsymbol{H}_{rd} \boldsymbol{Z}_r \boldsymbol{H}_{rd}^H + \boldsymbol{Z}_{d2} \end{bmatrix}. \tag{3.6}$$

Define the destination receive filter (despreading sequence) as $\boldsymbol{c}$. Then the destination generates its estimated soft value symbol as

$$\hat{x} = \boldsymbol{c}^H \boldsymbol{y}_d = \boldsymbol{c}^H \boldsymbol{H} \boldsymbol{s} x + \boldsymbol{c}^H \boldsymbol{n}_1. \tag{3.7}$$

Lemma 2: Define $\boldsymbol{B}$ as the Cholesky decomposition matrix of Hermitian matrix $\boldsymbol{K}_F$. Then the SINR maximizing sequences are $\boldsymbol{s}^\dagger = \boldsymbol{v}_{F,max}$ and $\boldsymbol{c}^\dagger = (\boldsymbol{B}^H)^{-1} \boldsymbol{u}_{F,max}$, where $\boldsymbol{v}_{F,max}$ and $\boldsymbol{u}_{F,max}$ are the right and left singular vectors, respectively, corresponding to the maximum singular value $\lambda_{F,max}$ of matrix $\boldsymbol{B}^{-1}\boldsymbol{H}$. And the corresponding maximum SINR is

$\max_{\boldsymbol{s},\boldsymbol{c}} \gamma_F = P_s \left|\lambda_{F,max}\right|^2$.

Proof of Lemma 2: The SINR at the destination is

$$\gamma = \frac{E\left[\left|\boldsymbol{c}^H \boldsymbol{H} \boldsymbol{s} x\right|^2\right]}{E[|\boldsymbol{c}^H \boldsymbol{n}_1|^2]} \tag{3.8}$$

$$= \frac{P_s \left|\boldsymbol{c}^H \boldsymbol{H} \boldsymbol{s}\right|^2}{\boldsymbol{c}^H \boldsymbol{K}_{F1} \boldsymbol{c}} \tag{3.9}$$

$$= \frac{P_s \left|\boldsymbol{c}^H \boldsymbol{B} \boldsymbol{B}^{-1} \boldsymbol{H} \boldsymbol{s}\right|^2}{\boldsymbol{c}^H \boldsymbol{B} \boldsymbol{B}^H \boldsymbol{c}} \tag{3.10}$$

$$= \frac{P_s \left|\tilde{\boldsymbol{c}}^H (\boldsymbol{B}^{-1} \boldsymbol{H}) \boldsymbol{s}\right|^2}{\tilde{\boldsymbol{c}}^H \tilde{\boldsymbol{c}}} \tag{3.11}$$

$$= \frac{P_s \left|\tilde{\boldsymbol{c}}^H \left(\boldsymbol{U}_F \Sigma_F \boldsymbol{V}_F^H\right) \boldsymbol{s}\right|^2}{|\tilde{\boldsymbol{c}}|^2} \tag{3.12}$$

where $\tilde{\boldsymbol{c}} \triangleq \boldsymbol{B}^H \boldsymbol{c}$. Cholesky decomposition is applied to Hermitian matrix $\boldsymbol{K}_{F1}$ in equation (3.9) such that $\boldsymbol{K}_{F1} = \boldsymbol{B}\boldsymbol{B}^H$, and a singular value decomposition is applied to matrix $\boldsymbol{B}^{-1}\boldsymbol{H}$ in equation (3.11). If the sequences are designed as $\boldsymbol{s}^\dagger = \boldsymbol{v}_{F,max}$ and $\boldsymbol{c}^\dagger = (\boldsymbol{B}^H)^{-1}\boldsymbol{u}_{F,max}$, then the SINR is maximized, which is $P_s\left|\lambda_{F,max}\right|^2$. ■

3.2 Uplink FC Relay Network

3.2.1 FC Network with Two Sources, Four Relays, and One Destination

For a relay network with two sources, four relays, and one destination, as shown in Figure 3.3, the destination receives

$$\boldsymbol{y}_d = \begin{bmatrix} \boldsymbol{y}_{d_1} \\ \boldsymbol{y}_{d_2} \end{bmatrix} = \boldsymbol{H}_{FU1}\boldsymbol{s}_1 x_1 + \boldsymbol{H}_{FU2}\boldsymbol{s}_2 x_2 + \boldsymbol{n}_2 \tag{3.13}$$

where

$$\boldsymbol{H}_{FU1} \triangleq \begin{bmatrix} \boldsymbol{H}_{s_1 d} \\ \sum_{j=1}^{4} \alpha_j \boldsymbol{H}_{r_j d} \boldsymbol{H}_{1j} \end{bmatrix} \tag{3.14}$$

$$\boldsymbol{H}_{FU2} \triangleq \begin{bmatrix} \boldsymbol{H}_{s_2 d} \\ \sum_{j=1}^{4} \alpha_j \boldsymbol{H}_{r_j d} \boldsymbol{H}_{2j} \end{bmatrix} \tag{3.15}$$

$$\boldsymbol{n}_2 \triangleq \begin{bmatrix} \boldsymbol{n}_{d_1} \\ \sum_{j=1}^{4} \alpha_j \boldsymbol{H}_{r_j d} \boldsymbol{n}_{r_j} + \boldsymbol{n}_{d_2} \end{bmatrix}. \tag{3.16}$$

The covariance matrix of noise $\boldsymbol{n}_2$ is

$$\boldsymbol{K}_{FU2} = \begin{bmatrix} \boldsymbol{Z}_{d_1} & 0 \\ 0 & \sum_{j=1}^{4} \alpha_j^2 \boldsymbol{H}_{r_j d} \boldsymbol{Z}_{r_j} \boldsymbol{H}_{r_j d}^H + \boldsymbol{Z}_{d_2} \end{bmatrix}. \tag{3.17}$$

The destination processes the received signal with two sets of despreading sequences, $\boldsymbol{c}_1$ for symbols from source one (upper branch) and $\boldsymbol{c}_2$ for symbols from source two (lower branch). The destination destination generates its estimated symbols of source one and source two as

$$\hat{x}_1 = \boldsymbol{c}_1^H \boldsymbol{y}_d = \boldsymbol{c}_1^H \boldsymbol{H}_{FU1}\boldsymbol{s}_1 x_1 + \boldsymbol{c}_1^H \boldsymbol{H}_{FU2}\boldsymbol{s}_2 x_2 + \boldsymbol{c}_1^H \boldsymbol{n}_2 \tag{3.18}$$

$$\hat{x}_2 = \boldsymbol{c}_2^H \boldsymbol{y}_d = \boldsymbol{c}_2^H \boldsymbol{H}_{FU1}\boldsymbol{s}_1 x_1 + \boldsymbol{c}_2^H \boldsymbol{H}_{FU2}\boldsymbol{s}_2 x_2 + \boldsymbol{c}_2^H \boldsymbol{n}_2. \tag{3.19}$$

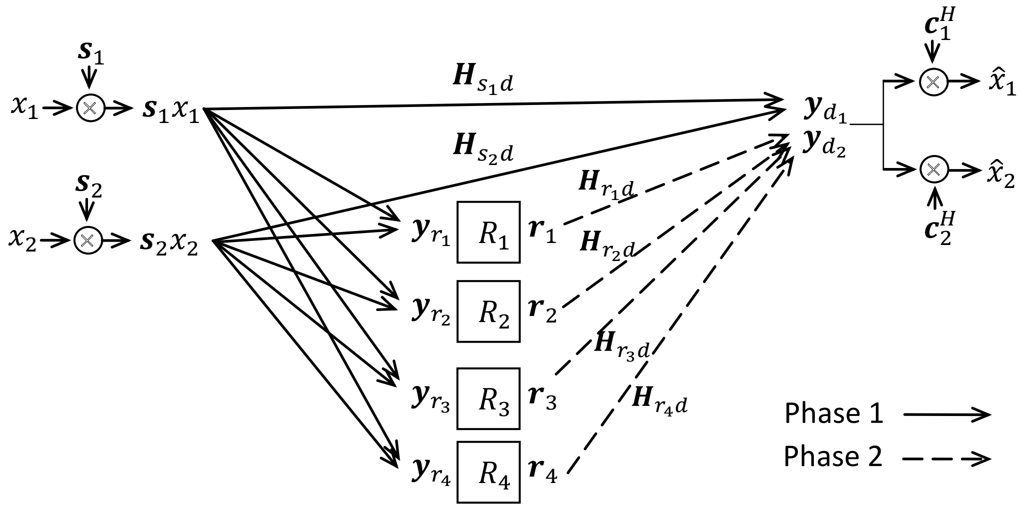

Figure 3.3. Uplink FC network with two sources, four relays, and one destination.

Define $\boldsymbol{Q}_{FU1} \triangleq P_s\boldsymbol{H}_{FU2}\boldsymbol{s}_2\boldsymbol{s}_2^H\boldsymbol{H}_{FU2}^H + \boldsymbol{K}_{FU1}$ as the covariance matrix of the interference-plus-noise components $\boldsymbol{c}_1^H\boldsymbol{H}_{FU2}\boldsymbol{s}_2x_2 + \boldsymbol{c}_1^H\boldsymbol{n}_2$ in equation (3.18) at destination 1. Apply Cholesky decomposition to matrix $\boldsymbol{Q}_{FU1}$ as $\boldsymbol{Q}_{FU1} = \boldsymbol{A}_{FU1}\boldsymbol{A}_{FU1}^H$. Note that $\boldsymbol{Q}_{FU1}$is a function of $\boldsymbol{s}_2$. Then the spreading and despreading sequences that maximize the SINR for the upper branch are $\boldsymbol{s}_1^\dagger = \boldsymbol{v}_{FU1,max}$ and $\boldsymbol{c}_1^\dagger = (\boldsymbol{A}_{FU1}^H)^{-1}\boldsymbol{u}_{FU1,max}$, where $\boldsymbol{v}_{FU1,max}$ and $\boldsymbol{u}_{FU1,max}$ are the right and left singular vectors, respectively, corresponding to the maximum singular value $\lambda_{FU1,max}$ of matrix $\boldsymbol{A}_{FU1}^{-1}\boldsymbol{H}_{FU1}$. The corresponding maximum SINR can be written as

$$\max_{\boldsymbol{s}_1,\boldsymbol{c}_1} \gamma_{FU1} = P_s\left|\lambda_{FU1,max}\right|^2. \tag{3.20}$$

Define $\boldsymbol{Q}_{FU2} \triangleq P_s\boldsymbol{H}_{FU1}\boldsymbol{s}_1\boldsymbol{s}_1^H\boldsymbol{H}_{FU1}^H + \boldsymbol{K}_{FU2}$ as the covariance matrix of the interference-plus-noise components $\boldsymbol{c}_2^H\boldsymbol{H}_{FU1}\boldsymbol{s}_1x_1 + \boldsymbol{c}_2^H\boldsymbol{n}_2$ in equation (3.19) at destination 2. Apply Cholesky decomposition to matrix $\boldsymbol{Q}_{FU2}$ as $\boldsymbol{Q}_{FU2} = \boldsymbol{A}_{FU2}\boldsymbol{A}_{FU2}^H$. Then the spreading and despreading sequences that maximize the SINR for the lower branch are $\boldsymbol{s}_2^\dagger = \boldsymbol{v}_{FU2,max}$ and $\boldsymbol{c}_2^\dagger = (\boldsymbol{A}_{FU2}^H)^{-1}\boldsymbol{u}_{FU2,max}$, where $\boldsymbol{v}_{FU2,max}$ and $\boldsymbol{u}_{FU2,max}$ are the right and left singular vectors, respectively, corresponding to the maximum singular value $\lambda_{F2,max}$ of matrix $\boldsymbol{A}_{FU2}^{-1}\boldsymbol{H}_{FU2}$. The corresponding maximum SINR can be written as

$$\max_{\boldsymbol{s}_2,\boldsymbol{c}_2} \gamma_{FU2} = P_s\left|\lambda_{FU2,max}\right|^2. \quad (3.21)$$

Note that the purpose of $\boldsymbol{Q}_{FU1}$ is to treat the signal from the other sources as a multiple access noise, and to design sequence $\boldsymbol{s}_1^\dagger$ and $\boldsymbol{c}_1^\dagger$ to suppress multiple access interference and noise; vice versa for $\boldsymbol{Q}_{FU2}$.

3.2.2 FC Network with M Sources, K Relays, and One Destination

Figure 3.4 shows a relay network with *M* number of sources, *K* number of relays, and one destination. Here, the sources, relays, and destination can represent the mobiles, relays, and base station, respectively, in an uplink of a cellular system. $\boldsymbol{H}_{ij}$ is defined as the channel matrix from source S_i to relay R_j, $\boldsymbol{H}_{s_id}$ as the channel matrix from source S_i to destination, and $\boldsymbol{H}_{r_jd}$ as the channel matrix from relay R_j to destination, where i denotes the source index ($i = 1,\cdots,M$) and j is the relay index ($j = 1,\cdots,K$). Due to the time-spreading of *N* chips per symbol, i.e., $\boldsymbol{s}_i x_i$, $i = 1,\cdots,M$, an $N \times N$ matrix is needed to describe the channel from a transmitter to a receiver, even if a single antenna is employed at each transmitter.

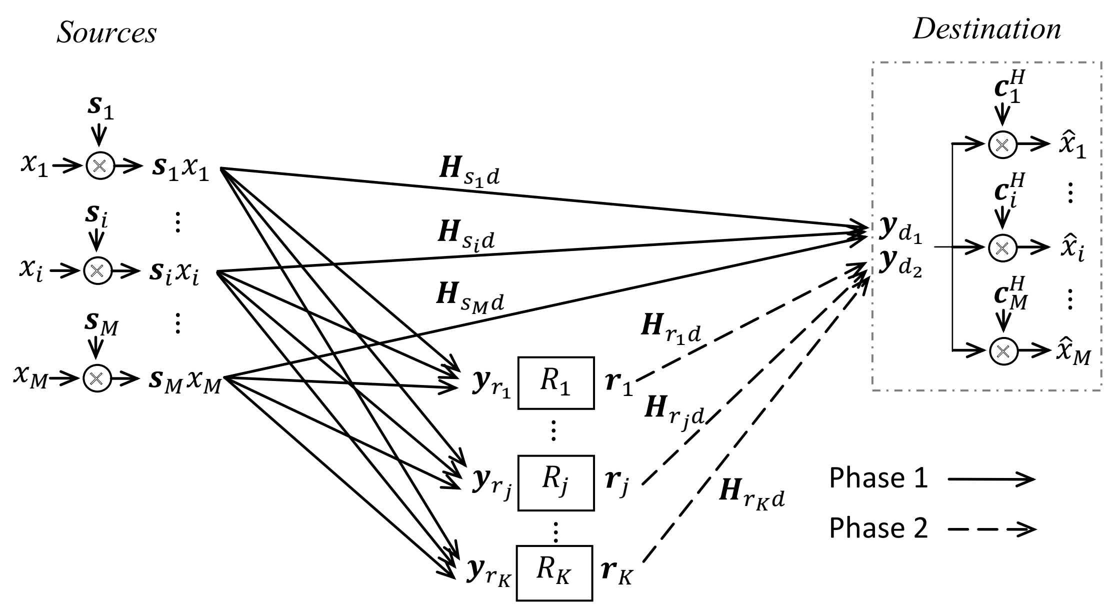

Figure 3.4. Uplink FC network with *M* sources, *K* relays, and one destination.

The overall transmission is divided into two phases. In phase one, the source broadcasts to both the relays and the destination. Source S_i employs a length-N spreading sequence $\boldsymbol{s}_i = [s_{i1}, s_{i2}, \cdots, s_{iN}]^T$ to transmit its information symbol x_i. All sources have the same power $E\{|x_i|^2\} = P_s$.

At the end of phase one, the received signal at relay R_j from the M sources is

$$\boldsymbol{y}_{r_j} = \sum_{i=1}^{M} \boldsymbol{H}_{i,j} \boldsymbol{s}_i x_i + \boldsymbol{n}_{r_j}. \tag{3.22}$$

The received signal at the destination from the M sources is

$$\boldsymbol{y}_{d_1} = \sum_{i=1}^{M} \boldsymbol{H}_{s_i d} \boldsymbol{s}_i x_i + \boldsymbol{n}_{d_1}. \tag{3.23}$$

During phase two, relay R_j forwards the amplified signal $\boldsymbol{r}_j = \alpha_j \boldsymbol{y}_{r_j}$ with power $E\left\{\left|r_j\right|^2\right\} = P_r$ to the destination. At the end of phase two, the received signal at the destination is

$$\boldsymbol{y}_{d_2} = \sum_{i=1}^{M} \sum_{j=1}^{K} \left(\alpha_j \boldsymbol{H}_{r_j d} \boldsymbol{H}_{i,j} \boldsymbol{s}_i x_i\right) + \sum_{j=1}^{K} \alpha_j \boldsymbol{H}_{r_j d} \boldsymbol{n}_{r_j} + \boldsymbol{n}_{d_2} \tag{3.24}$$

$$= \sum_{i=1}^{M} (\boldsymbol{T}_{FUi} \boldsymbol{s}_i x_i) + \widetilde{\boldsymbol{n}}_{d_2} \tag{3.25}$$

where $\boldsymbol{T}_{FUi} \triangleq \sum_{j=1}^{K} \alpha_j \boldsymbol{H}_{r_j d} \boldsymbol{H}_{i,j}$, and $\widetilde{\boldsymbol{n}}_{d_2} \triangleq \sum_{j=1}^{K} \alpha_j \boldsymbol{H}_{r_j d} \boldsymbol{n}_{r_j} + \boldsymbol{n}_{d_2}$.

Then the overall received signal at the destination can be written as

$$\boldsymbol{y}_d = \begin{bmatrix} \boldsymbol{y}_{d_1} \\ \boldsymbol{y}_{d_2} \end{bmatrix} = \sum_{i=1}^{M} (\boldsymbol{H}_{FUi} \boldsymbol{s}_i x_i) + \boldsymbol{n} \tag{3.26}$$

where $\boldsymbol{H}_{FUi} \triangleq \begin{bmatrix} \boldsymbol{H}_{sd_i} \\ \boldsymbol{T}_{FUi} \end{bmatrix}$ and $\boldsymbol{n} \triangleq \begin{bmatrix} \boldsymbol{n}_{d_1} \\ \widetilde{\boldsymbol{n}}_{d_2} \end{bmatrix}$. The covariance matrix of noise $\boldsymbol{n}$ is

$$\boldsymbol{K}_{FU} = \begin{bmatrix} \boldsymbol{Z}_{d_1} & 0 \\ 0 & \sum_{j=1}^{K} \alpha_j^2 \boldsymbol{H}_{r_j d} \boldsymbol{Z}_{r_j} \boldsymbol{H}_{r_j d}^H + \boldsymbol{Z}_{d_2} \end{bmatrix}. \tag{3.27}$$

Then the destination despreads the received signal for source i with despreading sequence $\boldsymbol{c}_i$ as

$$\hat{x}_i = \boldsymbol{c}_i^H \boldsymbol{y}_d \tag{3.28}$$

$$= \boldsymbol{c}_i^H \left[\sum_{k=1}^{M} (\boldsymbol{H}_{FUk} \boldsymbol{s}_k x_k) + \widetilde{\boldsymbol{n}}_d\right] \tag{3.29}$$

$$= \boldsymbol{c}_i^H \boldsymbol{H}_{FUi} \boldsymbol{s}_i x_i + \boldsymbol{c}_i^H \left(\sum_{\substack{k=1 \\ k \neq i}}^{M} (\boldsymbol{H}_{FUk} \boldsymbol{s}_k x_k) + \widetilde{\boldsymbol{n}}_d \right). \tag{3.30}$$

Theorem 3: Define $\boldsymbol{Q}_{FUi} \triangleq \sum_{\substack{k=1 \\ k \neq i}}^{M} (P_s \boldsymbol{H}_{FUk} \boldsymbol{s}_k \boldsymbol{s}_k^H \boldsymbol{H}_{FUk}^H) + \boldsymbol{K}_{FU}$ as the covariance matrix of the interference-plus-noise components $\boldsymbol{c}_i^H \left(\sum_{\substack{k=1 \\ k \neq i}}^{M} (\boldsymbol{H}_{FUk} \boldsymbol{s}_k x_k) + \widetilde{\boldsymbol{n}}_d \right)$ in equation (3.30), excluding the desired signal. Apply Cholesky decomposition to matrix $\boldsymbol{Q}_{FUi}$ as $\boldsymbol{Q}_{FUi} = \boldsymbol{A}_{FUi} \boldsymbol{A}_{FUi}^H$. Then the optimal spreading and despreading sequences that maximize the $SINR_i$ can be found as $\boldsymbol{s}_i^{\dagger} = \boldsymbol{v}_{FUi,max}$ and $\boldsymbol{c}_i^{\dagger} = (\boldsymbol{A}_{FUi}^H)^{-1} \boldsymbol{u}_{FUi,max}$, where $\boldsymbol{v}_{FUi,max}$ and $\boldsymbol{u}_{FUi,max}$ are the right and left singular vectors, respectively, corresponding to the maximum singular value $\lambda_{FUi,max}$ of matrix $\boldsymbol{A}_{FUi}^{-1} \boldsymbol{H}_i$. The corresponding maximum $SINR_i$ can be written as

$$\max_{\boldsymbol{s}_i, \boldsymbol{c}_i} \gamma_{FUi} = P_s \left| \lambda_{FUi,max} \right|^2. \tag{3.31}$$

Proof of Theorem 3: Define γ_{FUi} as the SINR ratio of the desired signal component power to the interference-plus-noise power after despreading for user i in equation (3.30).

$$\gamma_{FUi} = \frac{\mathrm{E}\left[\left| \boldsymbol{c}_i^H \boldsymbol{H}_{FUi} \boldsymbol{s}_i x_i \right|^2 \right]}{\mathrm{E}\left[\left| \boldsymbol{c}_i^H \left(\sum_{\substack{k=1 \\ k \neq i}}^{M} \boldsymbol{H}_{FUk} \boldsymbol{s}_k x_k + \boldsymbol{n} \right) \right|^2 \right]} \tag{3.32}$$

$$= \frac{P_s \left| \boldsymbol{c}_i^H \boldsymbol{H}_{FUi} \boldsymbol{s}_i \right|^2}{\boldsymbol{c}_i^H (\sum_{\substack{k=1 \\ k \neq i}}^{M} P_s \boldsymbol{H}_{FUk} \boldsymbol{s}_k \boldsymbol{s}_k^H \boldsymbol{H}_{FUk}^H + \boldsymbol{K}_{FU}) \boldsymbol{c}_i} \tag{3.33}$$

$$= \frac{P_s \left| \boldsymbol{c}_i^H \boldsymbol{H}_{FUi} \boldsymbol{s}_i \right|^2}{\boldsymbol{c}_i^H \boldsymbol{Q}_{FUi} \boldsymbol{c}_i} \tag{3.34}$$

$$= \frac{P_s \left| \boldsymbol{c}_i^H \boldsymbol{A}_{FUi} \boldsymbol{A}_{FUi}^{-1} \boldsymbol{H}_{FUi} \boldsymbol{s}_i \right|^2}{\boldsymbol{c}_i^H \boldsymbol{A}_{FUi} \boldsymbol{A}_{FUi}^H \boldsymbol{c}_i} \tag{3.35}$$

$$= \frac{P_s \left| \tilde{\boldsymbol{c}}_i^H (\mathbf{U}_{FUi} \Sigma_{FUi} \boldsymbol{V}_{FUi}^H) \boldsymbol{s}_i \right|^2}{|\tilde{\boldsymbol{c}}_i|^2} \tag{3.36}$$

where $\tilde{\boldsymbol{c}}_i \triangleq \boldsymbol{A}_{FUi}^H \boldsymbol{c}_i$, and $\boldsymbol{Q}_{FUi} \triangleq \sum_{\substack{k=1 \\ k \neq i}}^{M} (P_s \boldsymbol{H}_{FUk} \boldsymbol{s}_k \boldsymbol{s}_k^H \boldsymbol{H}_{FUk}^H) + \boldsymbol{K}_{FU}$. Here the definition of $\boldsymbol{Q}_{FUi}$ is to treat all the multiple access signals as interference excluding itself. Cholesky decomposition is applied to $\boldsymbol{Q}_{FUi}$ in equation (3.35) such that $\boldsymbol{Q}_{FUi} = \boldsymbol{A}_{FUi} \boldsymbol{A}_{FUi}^H$, and singular value decomposition is applied to matrix $\boldsymbol{A}_{FUi}^{-1} \boldsymbol{H}_{FUi}$ in equation (3.36). If the sequences are designed as $\boldsymbol{s}_i^{\dagger} = \boldsymbol{v}_{FUi,max}$ and $\boldsymbol{c}_i^{\dagger} = (\boldsymbol{A}_{FUi}^H)^{-1} \boldsymbol{u}_{FUi,max}$, then γ_{FUi} is maximized, which is $P_s |\lambda_{FUi,max}|^2$. ■

3.3 Downlink Fully Connected Relay Network

3.3.1 FC Network with One Source, Two Relays, and Two Destinations

Figure 3.5 shows a downlink relay network with a base station of one combined source, two relays, and two destinations. During phase one, the source transmits the sum of the spread messages ($\boldsymbol{s}_1 x_1 + \boldsymbol{s}_2 x_2$) to the relays and the destinations. During phase two, the relays amplify and forward the signals to the destinations. Let $\boldsymbol{s}_1$ and $\boldsymbol{s}_2$ be the spreading sequences intended for destinations D_1 and D_2, respectively. And let $\boldsymbol{c}_1$ and $\boldsymbol{c}_2$ denote the despreading sequences used at destinations D_1 and D_2, respectively.

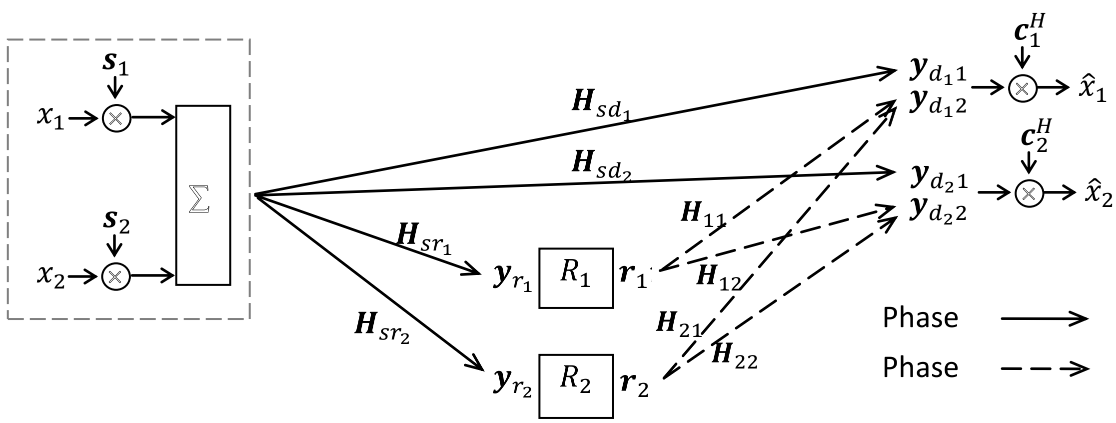

Figure 3.5. Downlink relay network with base station of one combined source, two relays, and two destinations.

During phase one, the received signal at relay R_1 and R_2 can be written as $\boldsymbol{y}_{r_1}$ and $\boldsymbol{y}_{r_2}$, respectively.

$$\boldsymbol{y}_{r_1} = \boldsymbol{H}_{sr_1}(\boldsymbol{s}_1 x_1 + \boldsymbol{s}_2 x_2) + \boldsymbol{n}_{r_1} \tag{3.37}$$

$$\boldsymbol{y}_{r_2} = \boldsymbol{H}_{sr_2}(\boldsymbol{s}_1 x_1 + \boldsymbol{s}_2 x_2) + \boldsymbol{n}_{r_2} \tag{3.38}$$

where $\boldsymbol{n}_{r_1}$ and $\boldsymbol{n}_{r_2}$ are the zero-mean complex additive Gaussian noise vectors at relays one and two, respectively. Each has covariance matrix $\boldsymbol{Z}_{r_1} = E\{\boldsymbol{n}_{r_1}\boldsymbol{n}_{r_1}^H\} = \sigma_{nr_1}^2 \boldsymbol{I}_N$ and $\boldsymbol{Z}_{r_2} = E\{\boldsymbol{n}_{r_2}\boldsymbol{n}_{r_2}^H\} = \sigma_{nr_2}^2 \boldsymbol{I}_N$. The received signals at destinations during phase one can be written as

$$\boldsymbol{y}_{d_1 1} = \boldsymbol{H}_{sd_1}(\boldsymbol{s}_1 x_1 + \boldsymbol{s}_2 x_2) + \boldsymbol{n}_{d_1 1} \tag{3.39}$$

$$\boldsymbol{y}_{d_2 1} = \boldsymbol{H}_{sd_2}(\boldsymbol{s}_1 x_1 + \boldsymbol{s}_2 x_2) + \boldsymbol{n}_{d_2 1}. \tag{3.40}$$

During phase two, relay R_i sends $\boldsymbol{r}_j = \alpha_j \boldsymbol{y}_{r_j}$ to the destination ($j = 1, 2$), where α_j is the scaling factor that preserves power constraint P_R at relay R_j, $\alpha_j = \sqrt{\frac{P_R}{E\{\|\boldsymbol{y}_{rj}\|^2\}}}$.

The received signals at the destinations during phase two can be written as

$$\boldsymbol{y}_{d_1 2} = \boldsymbol{H}_{11}\boldsymbol{r}_1 + \boldsymbol{H}_{21}\boldsymbol{r}_2 + \boldsymbol{n}_{d_1 2} \tag{3.41}$$

$$\boldsymbol{y}_{d_2 2} = \boldsymbol{H}_{12}\boldsymbol{r}_1 + \boldsymbol{H}_{22}\boldsymbol{r}_2 + \boldsymbol{n}_{d_2 2}. \tag{3.42}$$

Denote

$$\boldsymbol{T}_{FD1} \triangleq \alpha_1 \boldsymbol{H}_{11}\boldsymbol{H}_{sr_1} + \alpha_2 \boldsymbol{H}_{21}\boldsymbol{H}_{sr_2} \tag{3.43}$$

$$\boldsymbol{T}_{FD2} \triangleq \alpha_1 \boldsymbol{H}_{12}\boldsymbol{H}_{sr_1} + \alpha_2 \boldsymbol{H}_{22}\boldsymbol{H}_{sr_2} \tag{3.44}$$

$$\widetilde{\boldsymbol{n}}_{d_1 2} \triangleq \alpha_1 \boldsymbol{H}_{11}\boldsymbol{n}_{r_1} + \alpha_2 \boldsymbol{H}_{21}\boldsymbol{n}_{r_2} + \boldsymbol{n}_{d_1 2} \tag{3.45}$$

$$\widetilde{\boldsymbol{n}}_{d_2 2} \triangleq \alpha_1 \boldsymbol{H}_{12}\boldsymbol{n}_{r1} + \alpha_2 \boldsymbol{H}_{22}\boldsymbol{n}_{r_2} + \boldsymbol{n}_{d_2 2}. \tag{3.46}$$

Then the received signals can be rewritten as

$$\boldsymbol{y}_{d_1 2} = \boldsymbol{T}_{FD1}(\boldsymbol{s}_1 x_1 + \boldsymbol{s}_2 x_2) + \widetilde{\boldsymbol{n}}_{d_1 2} \tag{3.47}$$

$$\boldsymbol{y}_{d_2 2} = \boldsymbol{T}_{FD2}(\boldsymbol{s}_1 x_1 + \boldsymbol{s}_2 x_2) + \widetilde{\boldsymbol{n}}_{d_2 2}. \tag{3.48}$$

By denoting $\boldsymbol{H}_{FD1} \triangleq \begin{bmatrix} \boldsymbol{H}_{sd_1} \\ \boldsymbol{T}_{FD1} \end{bmatrix}$, $\boldsymbol{H}_{FD2} \triangleq \begin{bmatrix} \boldsymbol{H}_{sd_2} \\ \boldsymbol{T}_{FD2} \end{bmatrix}$, $\boldsymbol{n}_{d_1} \triangleq \begin{bmatrix} \boldsymbol{n}_{d_1 1} \\ \widetilde{\boldsymbol{n}}_{d_1 2} \end{bmatrix}$, and $\boldsymbol{n}_{d_2} \triangleq \begin{bmatrix} \boldsymbol{n}_{d_2 1} \\ \widetilde{\boldsymbol{n}}_{d_2 2} \end{bmatrix}$, then the overall received signals at the destination D_1 and D_2 can be written as

$$\boldsymbol{y}_{d_1} = \begin{bmatrix} \boldsymbol{y}_{d_1 1} \\ \boldsymbol{y}_{d_1 2} \end{bmatrix} = \boldsymbol{H}_{FD1}(\boldsymbol{s}_1 x_1 + \boldsymbol{s}_2 x_2) + \boldsymbol{n}_{d_1} \tag{3.49}$$

$$\boldsymbol{y}_{d_2} = \begin{bmatrix} \boldsymbol{y}_{d_2 1} \\ \boldsymbol{y}_{d_2 2} \end{bmatrix} = \boldsymbol{H}_{FD2}(\boldsymbol{s}_1 x_1 + \boldsymbol{s}_2 x_2) + \boldsymbol{n}_{d_2}. \tag{3.50}$$

The covariance matrices of noise vector $\boldsymbol{n}_{d_1}$ and $\boldsymbol{n}_{d_2}$ can be written, respectively as

$$\boldsymbol{K}_{FD1} = \begin{bmatrix} \boldsymbol{Z}_{d_1 1} & 0 \\ 0 & \alpha_1^2 \boldsymbol{H}_{11} \boldsymbol{Z}_{r1} \boldsymbol{H}_{11}^H + \alpha_2^2 \boldsymbol{H}_{21} \boldsymbol{Z}_{r2} \boldsymbol{H}_{21}^H + \boldsymbol{Z}_{d_1 2} \end{bmatrix} \tag{3.51}$$

$$\boldsymbol{K}_{FD2} = \begin{bmatrix} \boldsymbol{Z}_{d_2 1} & 0 \\ 0 & \alpha_1^2 \boldsymbol{H}_{12} \boldsymbol{Z}_{r1} \boldsymbol{H}_{12}^H + \alpha_2^2 \boldsymbol{H}_{22} \boldsymbol{Z}_{r2} \boldsymbol{H}_{22}^H + \boldsymbol{Z}_{d_2 2} \end{bmatrix}. \tag{3.52}$$

Then the destinations despread the received signals as

$$\hat{x}_1 = \boldsymbol{c}_1^H \boldsymbol{y}_{d_1} = \boldsymbol{c}_1^H \boldsymbol{H}_{FD1} \boldsymbol{s}_1 x_1 + \boldsymbol{c}_1^H \boldsymbol{H}_{FD1} \boldsymbol{s}_2 x_2 + \boldsymbol{c}_1^H \boldsymbol{n}_{d_1} \tag{3.53}$$

$$\hat{x}_2 = \boldsymbol{c}_2^H \boldsymbol{y}_{d_2} = \boldsymbol{c}_2^H \boldsymbol{H}_{FD2} \boldsymbol{s}_1 x_1 + \boldsymbol{c}_2^H \boldsymbol{H}_{FD2} \boldsymbol{s}_2 x_2 + \boldsymbol{c}_2^H \boldsymbol{n}_{d_2}. \tag{3.54}$$

Let $\boldsymbol{Q}_{FD1}$ and $\boldsymbol{Q}_{FD2}$ denote the covariance matrices of the interference plus noise vectors as

$$\boldsymbol{Q}_{FD1} \triangleq P_S \boldsymbol{H}_{FD1} \boldsymbol{s}_2 \boldsymbol{s}_2^H \boldsymbol{H}_{FD1}^H + \boldsymbol{K}_{FD1} \tag{3.55}$$

$$\boldsymbol{Q}_{FD2} \triangleq P_S \boldsymbol{H}_{FD2} \boldsymbol{s}_1 \boldsymbol{s}_1^H \boldsymbol{H}_{FD2}^H + \boldsymbol{K}_{FD2}. \tag{3.56}$$

Define $\boldsymbol{A}_{FD1}$ and $\boldsymbol{A}_{FD2}$ as the Cholesky decomposition matrices of covariance matrices $\boldsymbol{Q}_{FD1}$ and $\boldsymbol{Q}_{FD2}$, respectively. Moreover, let $\boldsymbol{v}_{FD1,max}$ and $\boldsymbol{u}_{FD1,max}$ denote the right and left singular vectors, respectively, corresponding to the maximum singular value $\lambda_{FD1,max}$ of matrix $\boldsymbol{A}_{FD1}^{-1} \boldsymbol{H}_{FD1}$; and $\boldsymbol{v}_{FD2,max}$ and $\boldsymbol{u}_{FD2,max}$ as the right and left singular vectors, respectively, corresponding to the maximum singular value $\lambda_{FD2,max}$ of matrix $\boldsymbol{A}_{FD2}^{-1} \boldsymbol{H}_{FD2}$. Then the sequences that maximize the SINR at destination $\boldsymbol{D}_1$ are $\boldsymbol{s}_1^\dagger = \boldsymbol{v}_{FD1,max}$ and $\boldsymbol{c}_1^\dagger = (\boldsymbol{A}_{FD1}^H)^{-1} \boldsymbol{u}_{FD1,max}$, and the corresponding sequences that maximize the SINR at destination $\boldsymbol{D}_2$ are $\boldsymbol{s}_2^\dagger = \boldsymbol{v}_{FD2,max}$ and $\boldsymbol{c}_2^\dagger = (\boldsymbol{A}_{FD2}^H)^{-1}\boldsymbol{u}_{FD2,max}$. The corresponding maximum SINR can be written as

$$\max_{\boldsymbol{s}_1,\boldsymbol{c}_1} \gamma_1 = P_s\left|\lambda_{FD1,max}\right|^2 \tag{3.57}$$

$$\max_{\boldsymbol{s}_2,\boldsymbol{c}_2} \gamma_2 = P_s\left|\lambda_{FD2,max}\right|^2. \tag{3.58}$$

3.3.2 FC Network with One Source, K Relays, and M Destinations

A downlink relay network with one combined source, K number of relays, and M number of destinations is shown in Figure 3.6 $\boldsymbol{H}_{sd_i}$ is defined as the channel matrix from the source to destination D_i, $\boldsymbol{H}_{sr_j}$ as the channel matrix from the source to relay R_j, $\boldsymbol{G}_{ji}$ as the channel matrix from relay R_j to destination D_i, where i is the destination index ($i = 1, \cdots, M$), and j as the relay index ($j = 1, \cdots, K$). Figure 3.6 can represent a downlink network consisting of multiple mobiles, multiple relays, and a base station. Here, a BS transmits the M number of spread source signals together.

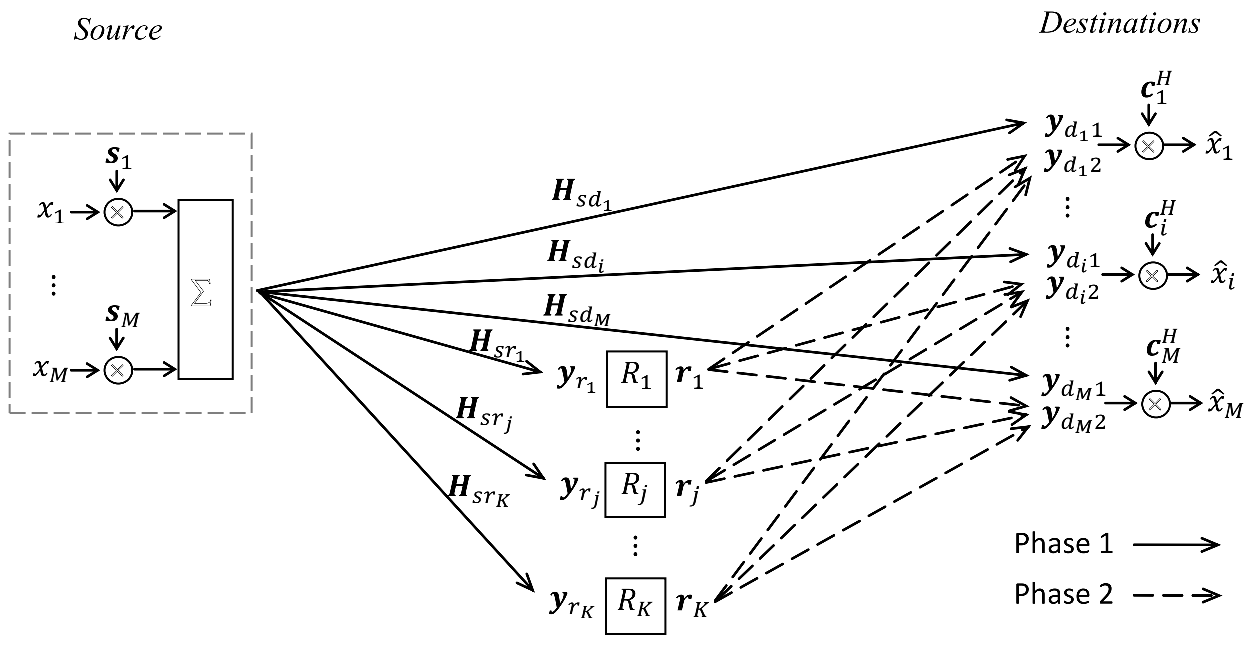

Figure 3.6. Downlink relay network with one combined source, *K* relays, and *M* destinations.

During phase one, source transmits the spread signals to the relays and destinations. The received signal at relay R_j is

$$\boldsymbol{y}_{r_j} = \boldsymbol{H}_{sr_j} \sum_{i=1}^{M} \boldsymbol{s}_i x_i + \boldsymbol{n}_{r_j}. \tag{3.59}$$

The received signal during phase one at destination D_i is

$$\boldsymbol{y}_{d_i 1} = \boldsymbol{H}_{sd_i} \sum_{i=1}^{M} \boldsymbol{s}_i x_i + \boldsymbol{n}_{d_i 1}. \tag{3.60}$$

During phase two, relay R_j forwards $\boldsymbol{r}_j = \alpha_j \boldsymbol{y}_{r_j}$ to destinations, where α_j is the scaling factor that preserves power constraint P_R at relay R_j, $\alpha_j = \sqrt{P_R / E\{\left\|\boldsymbol{y}_{r_j}\right\|^2\}}$. The received signals during phase 2 at destination D_i can be written as

$$\boldsymbol{y}_{d_i 2} = \sum_{j=1}^{K} \boldsymbol{H}_{ji} \boldsymbol{r}_j + \boldsymbol{n}_{d_i 2} \tag{3.61}$$

$$= \left(\sum_{j=1}^{K} \alpha_j \boldsymbol{H}_{ji} \boldsymbol{H}_{sr_j}\right) \sum_{k=1}^{M} \boldsymbol{s}_k x_k + \sum_{j=1}^{K} \alpha_j \boldsymbol{H}_{ji} \boldsymbol{n}_{r_j} + \boldsymbol{n}_{d_i 2}. \tag{3.62}$$

Denote

$$\boldsymbol{T}_{FDi} \triangleq \sum_{j=1}^{K} \alpha_j \boldsymbol{H}_{ji} \boldsymbol{H}_{sr_j} \tag{3.63}$$

$$\widetilde{\boldsymbol{n}}_{d_i 2} \triangleq \sum_{j=1}^{k} \alpha_j \boldsymbol{H}_{ji} \boldsymbol{n}_{r_j} + \boldsymbol{n}_{d_i 2}. \tag{3.64}$$

Then the received signal at destination D_i during phase two can be rewritten as

$$\boldsymbol{y}_{d_i 2} = \boldsymbol{T}_{FDi} \sum_{k=1}^{M} \boldsymbol{s}_k x_k + \widetilde{\boldsymbol{n}}_{d_i 2}. \tag{3.65}$$

By denoting $\boldsymbol{H}_{FDi} \triangleq \begin{bmatrix} \boldsymbol{H}_{sd_i} \\ \boldsymbol{T}_{FDi} \end{bmatrix}$ and $\boldsymbol{n}_{d_i} \triangleq \begin{bmatrix} \boldsymbol{n}_{d_i 1} \\ \widetilde{\boldsymbol{n}}_{d_i 2} \end{bmatrix}$, then the overall received signal at the destination D_i can be written as

$$\boldsymbol{y}_{d_i} = \begin{bmatrix} \boldsymbol{y}_{d_i 1} \\ \boldsymbol{y}_{d_i 2} \end{bmatrix} = \boldsymbol{H}_{FDi} \sum_{k=1}^{M} \boldsymbol{s}_k x_k + \boldsymbol{n}_{d_i}. \tag{3.66}$$

The covariance matrix of the overall noise vector $\boldsymbol{n}_{d_i}$ can be written as

$$\boldsymbol{K}_{FDi} = \begin{bmatrix} \boldsymbol{Z}_{d_i 1} & 0 \\ 0 & \sum_{j=1}^{K} \alpha_j^2 \boldsymbol{H}_{ji} \boldsymbol{Z}_{rj} \boldsymbol{H}_{ji}^H + \boldsymbol{Z}_{d_i 2} \end{bmatrix}. \tag{3.67}$$

Then the destination despreads the received signal for source i with despreading sequence $\boldsymbol{c}_i$ as

$$\hat{x}_i = \boldsymbol{c}_i^H \boldsymbol{y}_d \tag{3.68}$$

$$= \boldsymbol{c}_i^H \left[\boldsymbol{H}_{FDi} \sum_{k=1}^{M} \boldsymbol{s}_k x_k + \boldsymbol{n}_{d_i}\right] \tag{3.69}$$

$$= \boldsymbol{c}_i^H \boldsymbol{H}_{FDi} \boldsymbol{s}_i x_i + \boldsymbol{c}_i^H \left(\boldsymbol{H}_{FDi} \sum_{\substack{k=1 \\ k\neq i}}^{M} \boldsymbol{s}_k x_k + \boldsymbol{n}_{d_i}\right). \tag{3.70}$$

Theorem 4: Define $\boldsymbol{Q}_{FDi} \triangleq P_s \sum_{\substack{k=1 \\ k\neq i}}^{\boldsymbol{M}} \boldsymbol{T}_{FDi} \boldsymbol{s}_k \boldsymbol{s}_k^H \boldsymbol{T}_{FDi}^H + \boldsymbol{K}_{FDi}$ as the covariance matrix of the interference plus noise components $\boldsymbol{c}_i^H \left(\boldsymbol{H}_{FDi} \sum_{\substack{k=1 \\ k\neq i}}^{M} \boldsymbol{s}_k x_k + \boldsymbol{n}_{d_i}\right)$ in equation (3.70), excluding the desired signal. Apply Cholesky decomposition to matrix $\boldsymbol{Q}_{FDi}$ as $\boldsymbol{Q}_{FDi} = \boldsymbol{A}_{FDi} \boldsymbol{A}_{FDi}^H$. Then the optimal spreading and despreading sequences that maximize SINR at destination D_i can be found as $\boldsymbol{s}_i^\dagger = \boldsymbol{v}_{FDi,max}$ and $\boldsymbol{c}_i^\dagger = (\boldsymbol{A}_{FDi}^H)^{-1} \boldsymbol{u}_{FDi,max}$, where $\boldsymbol{v}_{FDi,max}$ and $\boldsymbol{u}_{FDi,max}$ are the right and left singular vectors, respectively, corresponding to the maximum singular value $\lambda_{FDi,max}$ of matrix $\boldsymbol{A}_{FDi}^{-1} \boldsymbol{H}_i$. Then the corresponding maximum SINR can be written as

$$\max_{\boldsymbol{s}_i, \boldsymbol{c}_i} \gamma_{FDi} = P_s \left|\lambda_{FDi,max}\right|^2. \tag{3.71}$$

Proof of Theorem 4: Define γ_{FDi} as the ratio of the desired signal component power to the interference-plus-noise power after despreading for user i.

$$\gamma_{FDi} = \frac{\mathrm{E}\left[\left|\boldsymbol{c}_i^H \boldsymbol{H}_{FDi} \boldsymbol{s}_i x_i\right|^2\right]}{\mathrm{E}\left[\left|\boldsymbol{c}_i^H \boldsymbol{H}_{FDi} \sum_{\substack{k=1 \\ k\neq i}}^{M} \boldsymbol{s}_k x_k + \boldsymbol{c}_i^H \boldsymbol{n}_{d_i}\right|^2\right]} \tag{3.72}$$

$$= \frac{P_S \left|\boldsymbol{c}_i^H \boldsymbol{H}_{FDi} \boldsymbol{s}_i\right|^2}{\boldsymbol{c}_i^H (P_S \sum_{\substack{k=1 \\ k\neq i}}^{M} \boldsymbol{H}_{FDk} \boldsymbol{s}_k \boldsymbol{s}_k^H \boldsymbol{H}_{FDk}^H + \boldsymbol{K}_{FDi}) \boldsymbol{c}_i} \tag{3.73}$$

$$= \frac{P_S \left|\boldsymbol{c}_i^H \boldsymbol{H}_{FDi} \boldsymbol{s}_i\right|^2}{\boldsymbol{c}_i^H \boldsymbol{Q}_{FDi} \boldsymbol{c}_i} \tag{3.74}$$

$$= \frac{P_s \left| \boldsymbol{c}_i^H \boldsymbol{A}_{FDi} \boldsymbol{A}_{FDi}^{-1} \boldsymbol{H}_{FDi} \boldsymbol{s}_i \right|^2}{\boldsymbol{c}_i^H \boldsymbol{A}_{FDi} \boldsymbol{A}_{FDi}^H \boldsymbol{c}_i} \tag{3.75}$$

$$= \frac{P_s \left| \tilde{\boldsymbol{c}}_i^H (\mathbf{U}_{FDi} \Sigma_{FDi} \boldsymbol{V}_{FDi}^H) \boldsymbol{s}_i \right|^2}{|\tilde{\boldsymbol{c}}_i|^2} \tag{3.76}$$

where $\tilde{\boldsymbol{c}}_i \triangleq \boldsymbol{A}_{FDi}^H \boldsymbol{c}_i$ and $\boldsymbol{Q}_{FDi} \triangleq \sum_{\substack{k=1 \\ k \neq i}}^{M} (P_s \boldsymbol{H}_{FDk} \boldsymbol{s}_k \boldsymbol{s}_k^H \boldsymbol{H}_{FDk}^H) + \boldsymbol{K}_{FDi}$. Here the purpose of $\boldsymbol{Q}_{FDi}$ is to treat all multiple access signals as interference excluding itself. Cholesky decomposition is applied to $\boldsymbol{Q}_{FDi}$ in equation (3.74) as $\boldsymbol{Q}_{FDi} = \boldsymbol{A}_{FDi} \boldsymbol{A}_{FDi}^H$, and then the singular value decomposition is applied to matrix $\boldsymbol{A}_{FDi}^{-1} \boldsymbol{H}_{FDi}$ in equation (3.75). If the sequences are designed as $\boldsymbol{s}_i^\dagger = \boldsymbol{v}_{FDi,max}$ and $\boldsymbol{c}_i^\dagger = (\boldsymbol{A}_{FDi}^H)^{-1} \boldsymbol{u}_{FDi,max}$, then γ_{FDi} is maximized, which is $P_s \left| \lambda_{FDi,max} \right|^2$. ■

3.4 Simulation Results for FC Relay Networks

Monte Carlo simulations are performed to illustrate the BER performance of the proposed spreading sequence design scheme. BPSK modulation is applied to all simulations, and the input SNR is E_b/N_0, where E_b is the bit energy of the source transmitted symbol x, and N_0 is the one-sided power spectral density of the thermal noise at the relays and the destinations.

Figure 3.7 shows BER versus the input SNR simulation results for a FC uplink CDMA AF relay network. Sequence length N = 32, frequency-selective fading channel with L = 5 number of taps, and the iteration stopping criterion $\varepsilon = 0.05$ are used. Each multipath has unit gain in average. In the legend, the FC notation is expressed as "FC1 *ij*1," representing an FC relay network with i number of sources, j number of relays, and one destination. Observe that BER performance improves as the number of relays increases when the number of sources and number of destinations are fixed. For example, "FC1 241" is 0.9 dB better in SNR at BER = 10^{-5} than "FC1 221.."This is reasonable because higher spatial diversity gain can be achieved with a greater number of relays. Also observe that BER performance worsens as the number of sources increases when the number of relays and the number of destinations are fixed. For example, "FC1 441" is 0.4 dB worse in SNR at BER = 10^{-5} than "FC1 241." This is also reasonable because a greater number of sources causes more interference in the network.

Also observe in Figure 3.7 that "FC1 12,12,1" and "FC1 241" are crossing each other at around SNR = 1 dB. At an SNR less than 1 dB, "FC1 12,12,1" shows better performance than "FC1 241," and at SNR greater than 1 dB, "FC1 241" shows better performance than "FC1 12,12,1." However, for partially connected relay networks, "PC 12,12,1" always performs better than "PC 241." This is because the direct link in the fully connected relay network is influenced more than the relay links by multiple access interference at a high SINR; hence, the performance of "FC1 12,12,1" can be worse than "FC1 241" because of the higher number of multiple access interfering users.

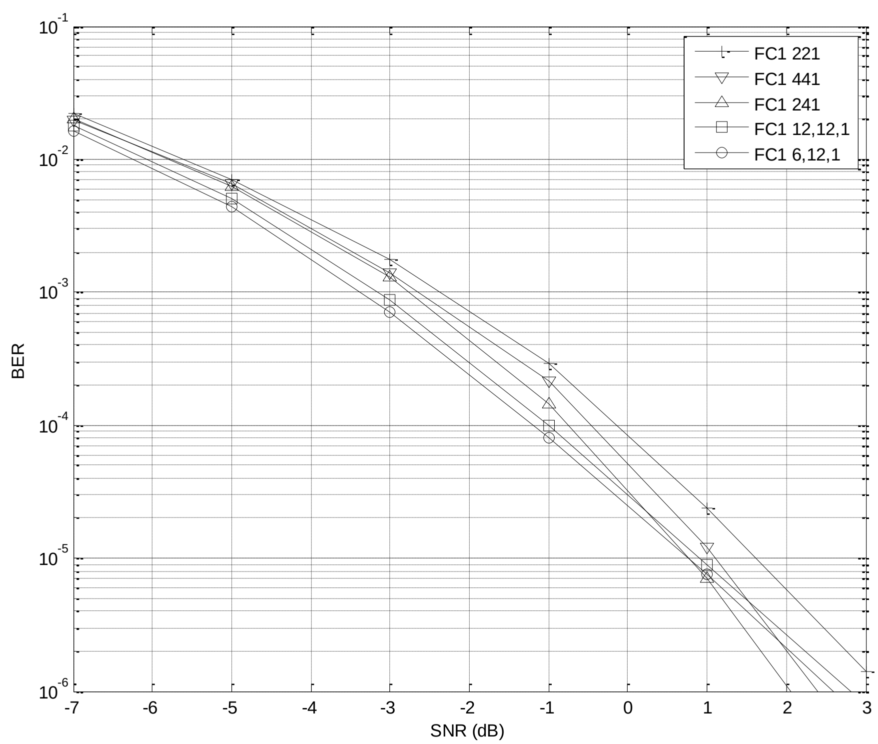

Figure 3.7. BER versus SNB for FC uplink relay networks.

As can be seen in Figure 3.8, a downlink FC relay network shows a similar performance to the uplink FC relay network. This is because the interference expressions for uplink and downlink are similar to each other, as in equations (3.32) and (3.72).

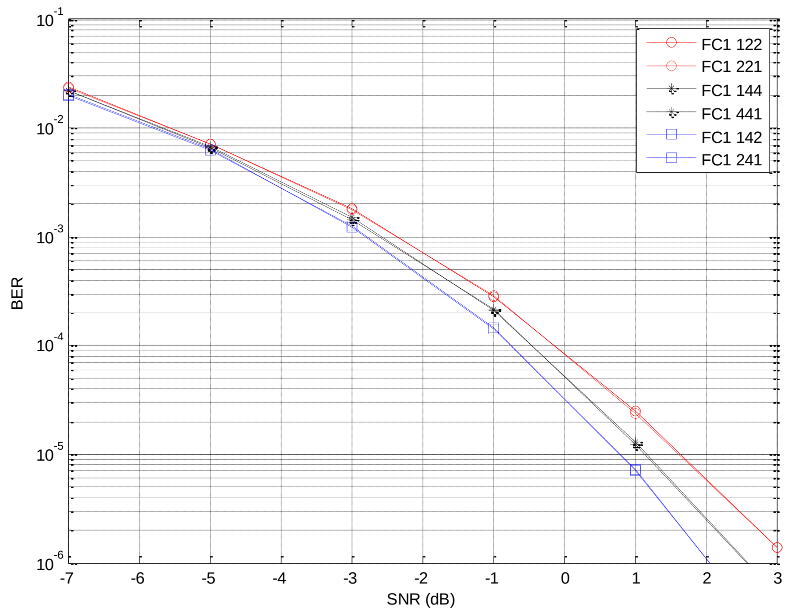

Figure 3.8. BER comparison for uplink and downlink FC relay networks.

Figures 3.9, 3.10, and 3.11 show how much the network's BER performance will be degraded when channels are under broadband noise jamming. Three different cases are considered: (1) jamming between sources and relays (i.e., R in the legend), (2) jamming between relays and destinations (i.e., D in the legend), and (3) jamming at both places (i.e., RD in the legend). Observe in Figures 3.9 and 3.10 that a jamming signal between the sources and relays can only degrade the BER performance less than 1 dB in SNR at BER = 10^{-4} for both uplink and downlink, even if the jamming power is the same as the desired signal's power P_S. This is because the jamming signal at the relays will be included in the iteration process for finding the optimum spreading sequences so that the jamming effects can be suppressed. However, observe in Figures 3.9 and 3.10 that the jamming signals between the relays and destinations can degrade system performance much worse than jamming signals between the sources and relays. For example, consider networks "FC1 241" and "FC1 142" at BER = 10^{-4}. The jamming signals between the relays and the destinations can degrade the BER performance by 4 dB for the uplink and 6 dB for the downlink. This is because the jamming signals at the destinations are not included in the sequence finding iteration process.

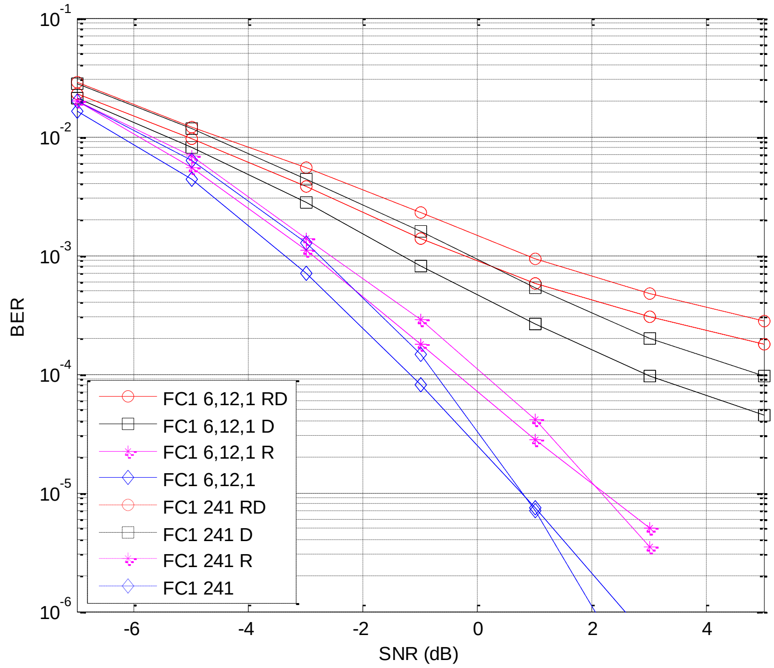

Figure 3.9. BER comparison for uplink relay networks with jamming signal power P_s.

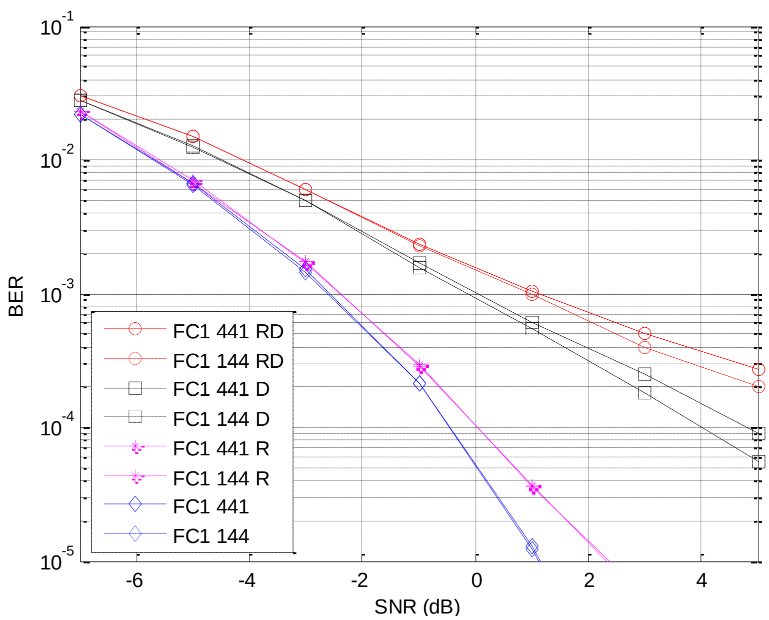

Figure 3.10. BER comparison for FC1 441 and FC1 144 with jamming signal power P_s.

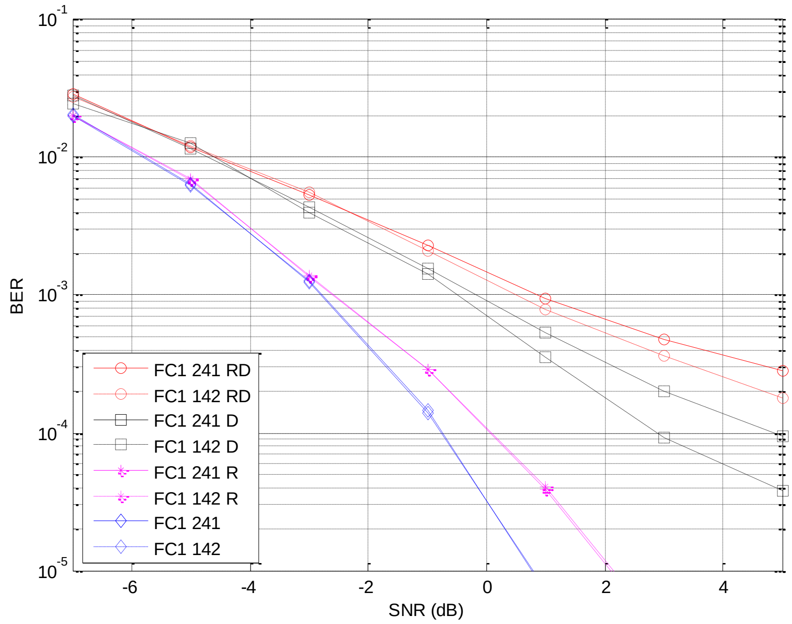

Figure 3.11 BER comparison for FC1 241 and FC1 142 with jamming signal power P_s.

In practice, imperfect estimates of the channel state information matrix $\widehat{\boldsymbol{H}}$ are available instead of the perfect CSI $\boldsymbol{H}$. The estimated channel matrices are represented as $\widehat{\boldsymbol{H}} = \boldsymbol{H} + \Delta_{\boldsymbol{H}}$, where $\Delta_{\boldsymbol{H}}$ is the channel estimation error matrix consisting of independent zero-mean Gaussian random variables with variances $\sigma_{\Delta_{\boldsymbol{H}}}^2$. Figure 3.12 shows the BER performance versus the input SNR with channel estimation error power of $\sigma_{\Delta_{\boldsymbol{H}}}^2 = 0.3\,\sigma_{\boldsymbol{H}}^2$. Observe in Figures 3.12 and 3.13 that channel uncertainty can degrade BER performance by around 2 dB in SNR at BER = 10^{-4} when channel uncertainty variance is $0.3\,\sigma_{\boldsymbol{H}}^2$. For example, the BER performance is degraded by 1.9 dB for both the "FC1 441" downlink and "FC1 144" uplink.

Figure 3.14 shows the BER performance comparison between the partially connected relay network "PC 241" and fully connected relay network "FC1 241." Observe in Figure 3.14 that "FC1 241" shows a 4 dB better performance in SNR at BER = 10^{-4} than "PC 241." This is because the FC relay network has a direct link from the sources to the destinations. The direct link signal strength is the same as that of the link between the relays and destinations. On the other hand, the partially connected relay network has no direct link.

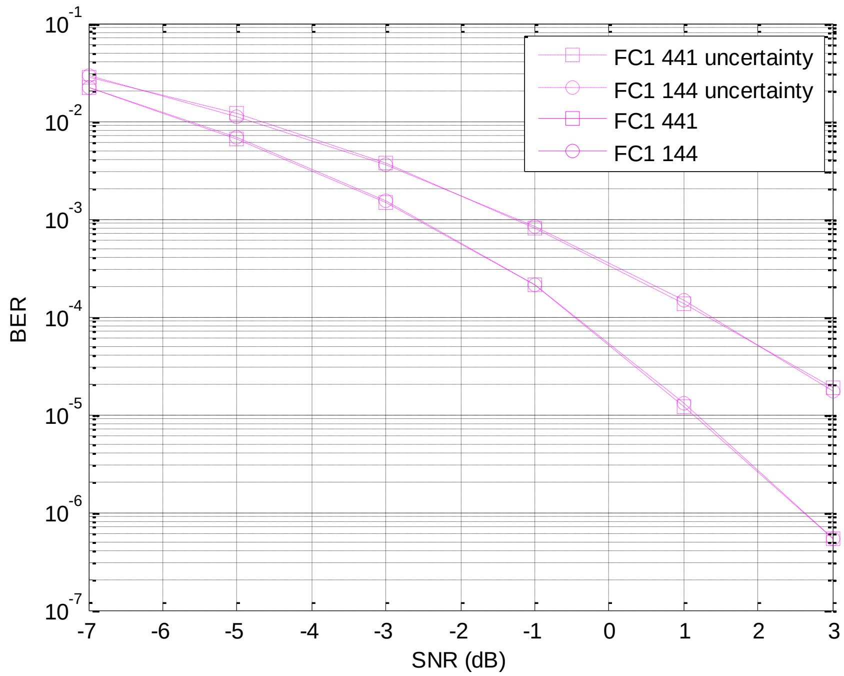

Figure 3.12. BER comparison for "FC1 441" and "FC1 144" with channel uncertainty variance 0.3 $\sigma_{\boldsymbol{H}}^2$.

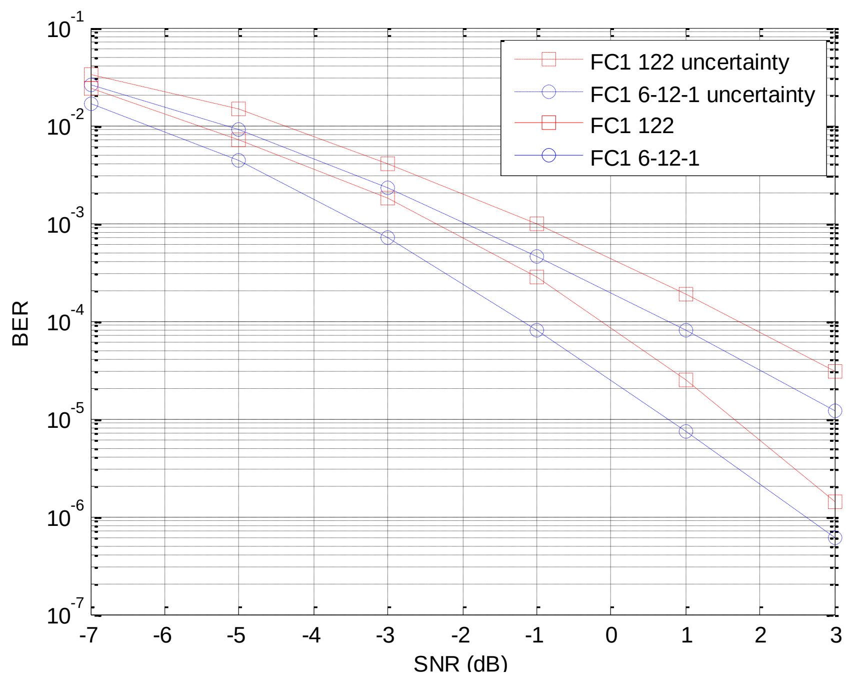

Figure 3.13. BER for PC relay network with channel uncertainty variance 0.3 $\sigma_{\boldsymbol{H}}^2$.

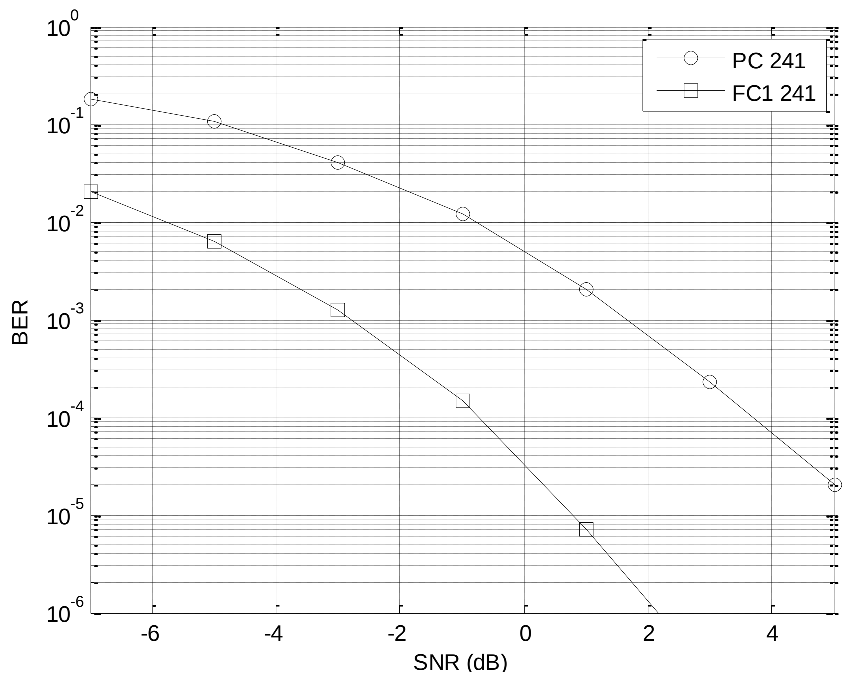

Figure 3.14 BER comparison between PC and FC relay network.

3.5 Chapter Conclusion

A method of designing spreading sequences based on maximizing the SINR was studied in this chapter for the fully connected CDMA AF relay networks under frequency-selective fading. Optimum secure, unique, and nonbinary spreading and despreading pseudo noise sequences were found by employing the Cholesky and singular value decompositions with channel state information. The proposed algorithm can also be applicable to a general relay network with an arbitrary geometry of multiple sources, relays, and destinations. The proposed algorithm can converge much faster and show better performance than the existing algorithms. The proposed adaptive PN spreading scheme can efficiently mitigate the effects of the frequency-selective fading, compared to the fixed non-adaptive sequences, for example, Walsh code, maximum length sequence, Gold sequence, etc. It was also observed that a fully connected relay network shows better BER performance than a partially connected relay network due to the availability of the direct link. However, as the SNR increases, the BER for a high number of users is not decreasing as fast as that for a low number of users due to the presence of significant multiple-access interference in the direct link.

Channel uncertainty can degrade BER performance non-negligibly and cause a worse performance than the broadband jamming signal with the same amount of power.

CHAPTER 4

MULTIHOP PC RELAY NETWORK

4.1 PC Relay Network with Three Hops

The proposed method can be extended to the case of a multihop relay network. Figure 4.1 is an example of a three-hop PC uplink relay network with two sources, two layers of relays, and one destination. The sources transmit to the destination through the help of two layers of relays. If the first layer of relays is far away from the destination, then the signals transmitted from the first layer will be too weak at the destination to analyze. In this case, the destination only receives and estimates the signals transmitted from the second layer. If relays are located arbitrarily and the first layer is located closer to the destination, then the signal strength is not negligible. In this case, the link from the first layer to the destination may be included in the performance analysis.

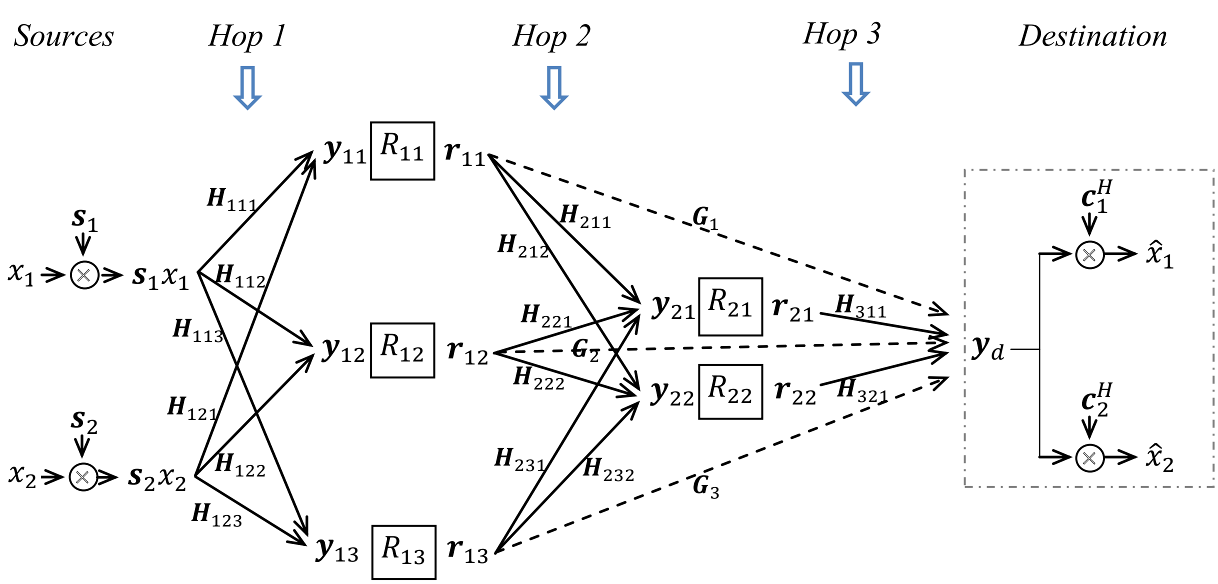

Figure 4.1. Uplink PC relay network with three hops.

Case 1. Here, the destination receives signals from both layers of relays. The received signals at the first layer of relays can be written as

$$\boldsymbol{y}_{11} = \boldsymbol{H}_{111}\boldsymbol{s}_1 x_1 + \boldsymbol{H}_{121}\boldsymbol{s}_2 x_2 + \boldsymbol{n}_{11} \tag{4.1}$$

$$\boldsymbol{y}_{12} = \boldsymbol{H}_{112}\boldsymbol{s}_1 x_1 + \boldsymbol{H}_{122}\boldsymbol{s}_2 x_2 + \boldsymbol{n}_{12} \tag{4.2}$$

$$\boldsymbol{y}_{13} = \boldsymbol{H}_{113}\boldsymbol{s}_1 x_1 + \boldsymbol{H}_{123}\boldsymbol{s}_2 x_2 + \boldsymbol{n}_{13} \tag{4.3}$$

The relays at the first layer then amplify and forward $\boldsymbol{r}_{1,j_1} = \alpha_{1,j_1}\boldsymbol{y}_{1,j_1}$ $(j_1 = 1, 2, 3)$ to the second layer of relays. The received signals at the second layer of relays can be written as

$$\boldsymbol{y}_{21} = \widetilde{\boldsymbol{H}}_{211}\boldsymbol{s}_1 x_1 + \widetilde{\boldsymbol{H}}_{221}\boldsymbol{s}_2 x_2 + \widetilde{\boldsymbol{n}}_{21} \tag{4.4}$$

$$\boldsymbol{y}_{22} = \widetilde{\boldsymbol{H}}_{212}\boldsymbol{s}_1 x_1 + \widetilde{\boldsymbol{H}}_{222}\boldsymbol{s}_2 x_2 + \widetilde{\boldsymbol{n}}_{22} \tag{4.5}$$

where

$$\widetilde{\boldsymbol{H}}_{211} = \alpha_{11}\boldsymbol{H}_{211}\boldsymbol{H}_{111} + \alpha_{12}\boldsymbol{H}_{221}\boldsymbol{H}_{112} + \alpha_{13}\boldsymbol{H}_{231}\boldsymbol{H}_{113} \tag{4.6}$$

$$\widetilde{\boldsymbol{H}}_{221} = \alpha_{11}\boldsymbol{H}_{211}\boldsymbol{H}_{121} + \alpha_{12}\boldsymbol{H}_{221}\boldsymbol{H}_{122} + \alpha_{13}\boldsymbol{H}_{231}\boldsymbol{H}_{123} \tag{4.7}$$

$$\widetilde{\boldsymbol{H}}_{212} = \alpha_{11}\boldsymbol{H}_{212}\boldsymbol{H}_{111} + \alpha_{12}\boldsymbol{H}_{222}\boldsymbol{H}_{112} + \alpha_{13}\boldsymbol{H}_{232}\boldsymbol{H}_{113} \tag{4.8}$$

$$\widetilde{\boldsymbol{H}}_{222} = \alpha_{11}\boldsymbol{H}_{212}\boldsymbol{H}_{121} + \alpha_{12}\boldsymbol{H}_{222}\boldsymbol{H}_{122} + \alpha_{13}\boldsymbol{H}_{232}\boldsymbol{H}_{123} \tag{4.9}$$

$$\widetilde{\boldsymbol{n}}_{21} = \alpha_{11}\boldsymbol{H}_{211}\boldsymbol{n}_{11} + \alpha_{12}\boldsymbol{H}_{221}\boldsymbol{n}_{12} + \alpha_{13}\boldsymbol{H}_{231}\boldsymbol{n}_{13} + \boldsymbol{n}_{21} \tag{4.10}$$

$$\widetilde{\boldsymbol{n}}_{22} = \alpha_{11}\boldsymbol{H}_{212}\boldsymbol{n}_{11} + \alpha_{12}\boldsymbol{H}_{222}\boldsymbol{n}_{12} + \alpha_{13}\boldsymbol{H}_{232}\boldsymbol{n}_{13} + \boldsymbol{n}_{22}. \tag{4.11}$$

The relays at the second layer then amplify and forward $\boldsymbol{r}_{2,j_2} = \alpha_{2,j_2}\boldsymbol{y}_{2,j_2}$ $(j_2 = 1, 2)$ to the destination. The received signals at the destination can be written as

$$\boldsymbol{y}_3 = \widetilde{\boldsymbol{H}}_{311}\boldsymbol{s}_1 x_1 + \widetilde{\boldsymbol{H}}_{321}\boldsymbol{s}_2 x_2 + \widetilde{\boldsymbol{n}}_3 \tag{4.12}$$

where

$$\widetilde{\boldsymbol{H}}_{311} = \alpha_{11}\boldsymbol{G}_1\boldsymbol{H}_{111} + \alpha_{12}\boldsymbol{G}_2\boldsymbol{H}_{112} + \alpha_{13}\boldsymbol{G}_3\boldsymbol{H}_{113} + \alpha_{21}\boldsymbol{H}_{311}\widetilde{\boldsymbol{H}}_{211} + \alpha_{22}\boldsymbol{H}_{321}\widetilde{\boldsymbol{H}}_{212} \tag{4.13}$$

$$\widetilde{\boldsymbol{H}}_{321} = \alpha_{11}\boldsymbol{G}_1\boldsymbol{H}_{121} + \alpha_{12}\boldsymbol{G}_2\boldsymbol{H}_{122} + \alpha_{13}\boldsymbol{G}_3\boldsymbol{H}_{123} + \alpha_{21}\boldsymbol{H}_{311}\widetilde{\boldsymbol{H}}_{221} + \alpha_{22}\boldsymbol{H}_{321}\widetilde{\boldsymbol{H}}_{222} \tag{4.14}$$

$$\widetilde{\boldsymbol{n}}_3 = \alpha_{11}\boldsymbol{G}_1\boldsymbol{n}_{11} + \alpha_{12}\boldsymbol{G}_2\boldsymbol{n}_{12} + \alpha_{13}\boldsymbol{G}_3\boldsymbol{n}_{13} + \alpha_{21}\boldsymbol{H}_{311}\widetilde{\boldsymbol{n}}_{21} + \alpha_{22}\boldsymbol{H}_{321}\widetilde{\boldsymbol{n}}_{22} + \boldsymbol{n}_3 \tag{4.15}$$

The covariance matrix of the noise component $\tilde{\boldsymbol{n}}_3$ is denoted as

$$\begin{aligned}\boldsymbol{K}_3 &\triangleq E[\tilde{\boldsymbol{n}}_3\tilde{\boldsymbol{n}}_3^H] \\ &= \alpha_{11}^2\boldsymbol{G}_1\boldsymbol{Z}_{11}\boldsymbol{G}_1^H + \alpha_{12}^2\boldsymbol{G}_2\boldsymbol{Z}_{12}\boldsymbol{G}_2^H + \alpha_{13}^2\boldsymbol{G}_3\boldsymbol{Z}_{13}\boldsymbol{G}_3^H + \\ &\quad \alpha_{21}^2\boldsymbol{H}_{311}\boldsymbol{K}_{21}\boldsymbol{H}_{311}^H + \alpha_{22}^2\boldsymbol{H}_{321}\boldsymbol{K}_{22}\boldsymbol{H}_{321}^H + \boldsymbol{Z}_3 \qquad (4.16)\end{aligned}$$

where

$$\begin{aligned}\boldsymbol{K}_{21} &\triangleq E[\tilde{\boldsymbol{n}}_{21}\tilde{\boldsymbol{n}}_{21}^H] \\ &= \alpha_{11}^2\boldsymbol{H}_{211}\boldsymbol{Z}_{11}\boldsymbol{H}_{211}^H + \alpha_{12}^2\boldsymbol{H}_{221}\boldsymbol{Z}_{12}\boldsymbol{H}_{221}^H + \alpha_{13}^2\boldsymbol{H}_{231}\boldsymbol{Z}_{13}\boldsymbol{H}_{231}^H + \boldsymbol{Z}_{21} \qquad (4.17)\end{aligned}$$

$$\begin{aligned}\boldsymbol{K}_{22} &\triangleq E[\tilde{\boldsymbol{n}}_{22}\tilde{\boldsymbol{n}}_{22}^H] \\ &= \alpha_{11}^2\boldsymbol{H}_{212}\boldsymbol{Z}_{11}\boldsymbol{H}_{212}^H + \alpha_{12}^2\boldsymbol{H}_{222}\boldsymbol{Z}_{12}\boldsymbol{H}_{222}^H + \alpha_{13}^2\boldsymbol{H}_{232}\boldsymbol{Z}_{13}\boldsymbol{H}_{232}^H + \boldsymbol{Z}_{22} \qquad (4.18)\end{aligned}$$

$$\boldsymbol{Z}_3 \triangleq E[\boldsymbol{n}_3\boldsymbol{n}_3^H],\ \boldsymbol{Z}_{1,j_1} \triangleq E\left[\boldsymbol{n}_{1,j_1}\boldsymbol{n}_{1,j_1}^H\right],\ \boldsymbol{Z}_{2,j_2} \triangleq E\left[\boldsymbol{n}_{2,j_2}\boldsymbol{n}_{2,j_2}^H\right],\ j_1 = 1,2,3,\ j_2 = 1,2.$$

The destination despreads the received signal as

$$\begin{aligned}\hat{x}_1 &= \boldsymbol{c}_1^H\boldsymbol{y}_3 \\ &= \boldsymbol{c}_1^H\tilde{\boldsymbol{H}}_{311}\boldsymbol{s}_1x_1 + \boldsymbol{c}_1^H(\tilde{\boldsymbol{H}}_{321}\boldsymbol{s}_2x_2 + \tilde{\boldsymbol{n}}_3) \qquad (4.19)\end{aligned}$$

$$\begin{aligned}\hat{x}_2 &= \boldsymbol{c}_2^H\boldsymbol{y}_3 \\ &= \boldsymbol{c}_2^H\tilde{\boldsymbol{H}}_{321}\boldsymbol{s}_2x_2 + \boldsymbol{c}_2^H(\tilde{\boldsymbol{H}}_{311}\boldsymbol{s}_1x_1 + \tilde{\boldsymbol{n}}_3) \qquad .(4.20)\end{aligned}$$

The SINR for the upper branch can be written as

$$\tilde{\gamma}_1 = \frac{E\left[\left|\boldsymbol{c}_1^H\tilde{\boldsymbol{H}}_{311}\boldsymbol{s}_1x_1\right|^2\right]}{E\left[\left|\boldsymbol{c}_1^H(\tilde{\boldsymbol{H}}_{321}\boldsymbol{s}_2x_2+\tilde{\boldsymbol{n}}_3)\right|^2\right]} \qquad (4.21)$$

$$= \frac{P_S\left|\boldsymbol{c}_1^H\tilde{\boldsymbol{H}}_{311}\boldsymbol{s}_1\right|^2}{\boldsymbol{c}_1^H(P_S\tilde{\boldsymbol{H}}_{321}\boldsymbol{s}_2\boldsymbol{s}_2^H\tilde{\boldsymbol{H}}_{321}^H+\boldsymbol{K}_3)\boldsymbol{c}_1} \qquad (4.22)$$

$$= \frac{P_S\left|\boldsymbol{c}_1^H\tilde{\boldsymbol{H}}_{311}\boldsymbol{s}_1\right|^2}{\boldsymbol{c}_1^H\tilde{\boldsymbol{Q}}_1\boldsymbol{c}_1} \qquad (4.23)$$

$$= \frac{P_S\left|\boldsymbol{c}_1^H\tilde{\boldsymbol{A}}_1(\tilde{\boldsymbol{A}}_1^{-1}\tilde{\boldsymbol{H}}_{311})\boldsymbol{s}_1\right|^2}{\boldsymbol{c}_1^H\tilde{\boldsymbol{A}}_1\tilde{\boldsymbol{A}}_1^H\boldsymbol{c}_1} \qquad (4.24)$$

$$= \frac{P_S\left|\tilde{\boldsymbol{c}}_1^H(\widetilde{\boldsymbol{U}}_1\widetilde{\Sigma}_1\widetilde{\boldsymbol{V}}_1^H)\boldsymbol{s}_1\right|^2}{|\tilde{\boldsymbol{c}}_1|^2}. \tag{4.25}$$

Let $\widetilde{\boldsymbol{v}}_{1,max}$ and $\widetilde{\boldsymbol{u}}_{1,max}$ denote the right and left singular vectors, respectively corresponding to the maximum singular value $\tilde{\lambda}_{1,max}$ of matrix $\widetilde{\boldsymbol{A}}_1^{-1}\widetilde{\boldsymbol{H}}_{311}$. If the sequences are designed as $\boldsymbol{s}_1^\dagger = \widetilde{\boldsymbol{v}}_{1,max}$ and $\boldsymbol{c}_1^\dagger = \left(\widetilde{\boldsymbol{A}}_1^H\right)^{-1}\widetilde{\boldsymbol{u}}_{1,max}$, then $\tilde{\gamma}_1$ would be maximized, which can be written as $P_s\left|\tilde{\lambda}_{1,max}\right|^2$.

The SINR for the lower branch can be written as

$$\tilde{\gamma}_2 = \frac{E\left[\left|\boldsymbol{c}_2^H\widetilde{\boldsymbol{H}}_{32}\boldsymbol{s}_2x_2\right|^2\right]}{E\left[\left|\boldsymbol{c}_2^H(\widetilde{\boldsymbol{H}}_{311}\boldsymbol{s}_1x_1+\widetilde{\boldsymbol{n}}_3)\right|^2\right]} \tag{4.26}$$

$$= \frac{P_S\left|\boldsymbol{c}_2^H\widetilde{\boldsymbol{H}}_{321}\boldsymbol{s}_2\right|^2}{\boldsymbol{c}_2^H(P_S\widetilde{\boldsymbol{H}}_{311}\boldsymbol{s}_1\boldsymbol{s}_1^H\widetilde{\boldsymbol{H}}_{311}^H+\boldsymbol{K}_3)\boldsymbol{c}_2} \tag{4.27}$$

$$= \frac{P_S\left|\boldsymbol{c}_2^H\widetilde{\boldsymbol{H}}_{321}\boldsymbol{s}_2\right|^2}{\boldsymbol{c}_2^H\widetilde{\boldsymbol{Q}}_2\boldsymbol{c}_2} \tag{4.28}$$

$$= \frac{P_S\left|\boldsymbol{c}_2^H\widetilde{\boldsymbol{A}}_2(\widetilde{\boldsymbol{A}}_2^{-1}\widetilde{\boldsymbol{H}}_{321})\boldsymbol{s}_2\right|^2}{\boldsymbol{c}_2^H\widetilde{\boldsymbol{A}}_2\widetilde{\boldsymbol{A}}_2^H\boldsymbol{c}_2} \tag{4.29}$$

$$= \frac{P_S\left|\tilde{\boldsymbol{c}}_2^H(\widetilde{\boldsymbol{U}}_2\widetilde{\Sigma}_2\widetilde{\boldsymbol{V}}_2^H)\boldsymbol{s}_2\right|^2}{|\tilde{\boldsymbol{c}}_2|^2} \tag{4.30}$$

Let $\widetilde{\boldsymbol{v}}_{2,max}$ and $\widetilde{\boldsymbol{u}}_{2,max}$ denote the right and left singular vectors, respectively corresponding to the maximum singular value $\tilde{\lambda}_{2,max}$ of matrix $\widetilde{\boldsymbol{A}}_2^{-1}\widetilde{\boldsymbol{H}}_{321}$. If we design the sequences as $\boldsymbol{s}_2^\dagger = \widetilde{\boldsymbol{v}}_{2,max}$ and $\boldsymbol{c}_2^\dagger = \left(\widetilde{\boldsymbol{A}}_2^H\right)^{-1}\widetilde{\boldsymbol{u}}_{2,max}$, then $\tilde{\gamma}_2$ would be maximized, which can be written as $P_s\left|\tilde{\lambda}_{2,max}\right|^2$.

Case 2. The destination receives signals only from the second layer of relays. In this case, the destination does not receive from the first layer of relays. The signals' transmission process are similar to case 1, except that all terms, including $\boldsymbol{G}_i$ are removed in equations (4.13)–(4.16), $i = 1, 2, 3$.

4.2 PC Relay Network with R hops

The proposed method can be extended to the case of multihops with multiple sources, multiple layers of relays, and one destination. Figure 4.2 shows a network of M sources, R hops, and one destination. Let r denote the hop index. At the r^{th} hop, K_r denotes the number of relays, j_r the index of relays, and α_{r,j_r} the amplifying coefficient for relay j_r ($r = 1, \cdots, R-1$). Here, the subindices r, i, and j of the channel matrix $\boldsymbol{H}_{rij}$ denote, respectively, the hop, the transmitter, and the receiver relay index, where each hop can have a different number of relays, K_r.

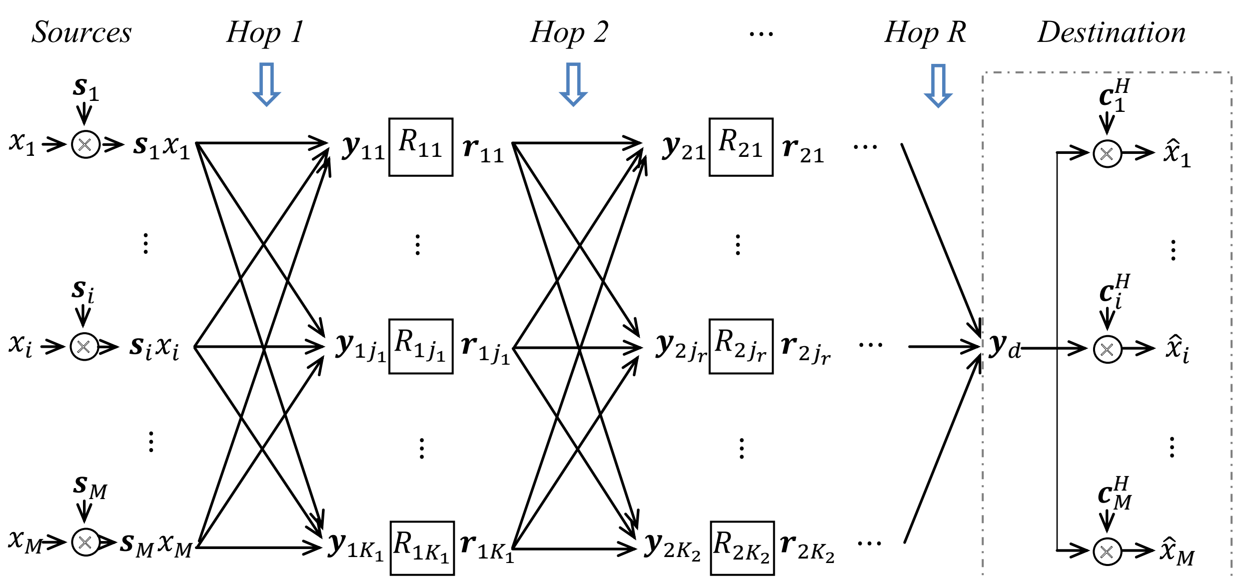

Figure 4.2. PC relay network with R hops.

For the first hop, the received signal at relay j_1($j_1 = 1,2, \cdots, K_1$) can be written as

$$\boldsymbol{y}_{1,j_1} = \sum_{i=1}^{M} \boldsymbol{H}_{1,i,j_1} \boldsymbol{s}_i x_i + \boldsymbol{n}_{1,j_1}. \tag{4.31}$$

Then the $j_1{}^{th}$ AF relay in hop 1 forwards the signal $\boldsymbol{r}_{1,j_1} = \alpha_{1,j_1} \boldsymbol{y}_{1,j_1}$. For the second hop, the received signal at relay j_2($j_2 = 1,2, \cdots K_2$) can be written as

$$\boldsymbol{y}_{2,j_2} = \sum_{j_1=1}^{K_1} \boldsymbol{H}_{2,j_1,j_2} \boldsymbol{r}_{1,j_1} + \boldsymbol{n}_{2,j_2} \tag{4.32}$$

$$= \sum_{i=1}^{M} \left(\sum_{j_1=1}^{K_1} \alpha_{1,j_1} \boldsymbol{H}_{2,j_1,j_2} \boldsymbol{H}_{1,i,j_1} \right) s_i x_i + \left(\sum_{j_1=1}^{K_1} \alpha_{1,j_1} \boldsymbol{H}_{2,j_1,j_2} \boldsymbol{n}_{1,j_1} + \boldsymbol{n}_{2,j_2} \right) \tag{4.33}$$

$$= \sum_{i=1}^{M} \widetilde{\boldsymbol{H}}_{2,i,j_2} \boldsymbol{s}_i x_i + \widetilde{\boldsymbol{n}}_{2,j_2} \tag{4.34}$$

where $\widetilde{\boldsymbol{H}}_{2,i,j_2} \triangleq \sum_{j_1=1}^{K_1} \alpha_{1,j_1} \boldsymbol{H}_{2,j_1,j_2} \boldsymbol{H}_{1,i,j_1}$, and $\widetilde{\boldsymbol{n}}_{2,j_2} \triangleq \sum_{j_1=1}^{K_1} \alpha_{1,j_1} \boldsymbol{H}_{2,j_1,j_2} \boldsymbol{n}_{1,j_1} + \boldsymbol{n}_{2,j_2}$.

Similarly, for the r^{th} hop, the received signal at relay $j_r(j_r = 1,2,\cdots K_r)$ can be written as

$$\boldsymbol{y}_{r,j_r} = \sum_{i=1}^{M} \widetilde{\boldsymbol{H}}_{r,i,j_r} \boldsymbol{s}_i x_i + \widetilde{\boldsymbol{n}}_{r,j_r} \tag{4.35}$$

where

$$\widetilde{\boldsymbol{H}}_{r,i,j_r} \triangleq \sum_{j_{r-1}=1}^{K_{r-1}} \alpha_{r-1,j_{r-1}} \boldsymbol{H}_{r,j_{r-1},j_r} \widetilde{\boldsymbol{H}}_{r-1,i,j_{r-1}} \tag{4.36}$$

$$\widetilde{\boldsymbol{n}}_{r,j_r} \triangleq \sum_{j_{r-1}=1}^{K_{r-1}} \alpha_{r-1,j_{r-1}} \boldsymbol{H}_{r,j_{r-1},j_r} \widetilde{\boldsymbol{n}}_{r-1,j_{r-1}} + \boldsymbol{n}_{r,j_r}. \tag{4.37}$$

At the destination, which is the R^{th} hop, the received signal can be written as

$$y_{R,1} = \sum_{i=1}^{M} \widetilde{\boldsymbol{H}}_{R,i,1} \boldsymbol{s}_i x_i + \widetilde{\boldsymbol{n}}_{R,1} \tag{4.38}$$

where

$$\widetilde{\boldsymbol{H}}_{R,i,1} \triangleq \sum_{j_{R-1}=1}^{K_{R-1}} \alpha_{R-1,j_{R-1}} \boldsymbol{H}_{R,j_{R-1},1} \widetilde{\boldsymbol{H}}_{R-1,i,j_{R-1}} \tag{4.39}$$

$$\widetilde{\boldsymbol{n}}_{R,1} \triangleq \sum_{j_{R-1}=1}^{K_{R-1}} \alpha_{R-1,j_{R-1}} \boldsymbol{H}_{R,j_{R-1},1} \widetilde{\boldsymbol{n}}_{R-1,j_{R-1}} + \boldsymbol{n}_{R,1}. \tag{4.40}$$

The covariance matrix of the noise component $\widetilde{\boldsymbol{n}}_{R,1}$ is denoted as

$$\boldsymbol{K}_{R1} \triangleq E\left[\widetilde{\boldsymbol{n}}_{R,1} \widetilde{\boldsymbol{n}}_{R,1}^H\right] \tag{4.41}$$

$$= \sum_{j_{R-1}=1}^{K_{R-1}} \alpha_{R-1,j_{R-1}}^2 \boldsymbol{H}_{R,j_{R-1},1} \boldsymbol{K}_{R-1,j_{R-1}} \boldsymbol{H}_{R,j_{R-1},1}^H + \boldsymbol{Z}_{R,1} \tag{4.42}$$

where $\boldsymbol{K}_{r,j_r} \triangleq E\left[\widetilde{\boldsymbol{n}}_{r,j_r} \widetilde{\boldsymbol{n}}_{r,j_r}^H\right] = \sum_{j_{r-1}=1}^{K_{r-1}} \alpha_{r-1,j_{r-1}}^2 \boldsymbol{H}_{r,j_{r-1},j_r} \boldsymbol{K}_{r-1,j_{r-1}} \boldsymbol{H}_{r,j_{r-1},j_r}^H + \boldsymbol{Z}_{r,j_r}$.

The destination despreads the received signal for source i as

$$\hat{x}_i = \boldsymbol{c}_i^H \boldsymbol{y}_{R,1} \tag{4.43}$$

$$= \boldsymbol{c}_i^H \widetilde{\boldsymbol{H}}_{R,i,1} \boldsymbol{s}_i x_i + \boldsymbol{c}_i^H \left(\sum_{\substack{k=1 \\ k \neq i}}^{M} \widetilde{\boldsymbol{H}}_{R,k,1} \, \boldsymbol{s}_k x_k + \widetilde{\boldsymbol{n}}_{R,1} \right). \tag{4.44}$$

Theorem 5: Let $\widetilde{\boldsymbol{Q}}_i \triangleq \sum_{\substack{k=1 \\ k \neq i}}^{M} (P_s \widetilde{\boldsymbol{H}}_{R,k,1} \boldsymbol{s}_k \boldsymbol{s}_k^H \widetilde{\boldsymbol{H}}_{R,k,1}^H) + \boldsymbol{K}_{R,1}$ represent the covariance matrix of the interference-plus-noise component $\boldsymbol{c}_i^H \left(\sum_{\substack{k=1 \\ k \neq i}}^{M} \widetilde{\boldsymbol{H}}_{R,k,1} \, \boldsymbol{s}_k x_k + \widetilde{\boldsymbol{n}}_{R,1} \right)$ in equation (4.44) at the destination after despreading. Define $\widetilde{\boldsymbol{A}}_i$ as the Cholesky decomposition matrix of covariance matrix $\widetilde{\boldsymbol{Q}}_i$ as $\widetilde{\boldsymbol{Q}}_i = \widetilde{\boldsymbol{A}}_i \widetilde{\boldsymbol{A}}_i^H$. Then the sequences that maximize SINR can be found as $\boldsymbol{s}_i^\dagger = \widetilde{\boldsymbol{v}}_{i,max}$ and $\boldsymbol{c}_i^\dagger = \left(\widetilde{\boldsymbol{A}}_i^H\right)^{-1} \widetilde{\boldsymbol{u}}_{imax}$, where $\widetilde{\boldsymbol{v}}_{i,max}$ and $\widetilde{\boldsymbol{u}}_{i,max}$ are the right and left singular vectors, respectively corresponding to the maximum singular value $\tilde{\lambda}_{i,max}$ of matrix $\widetilde{\boldsymbol{A}}_i^{-1} \widetilde{\boldsymbol{H}}_{R,i,1}$. Then the corresponding maximum SINR can be written as

$$\max_{\boldsymbol{s}_i, \boldsymbol{c}_i} \tilde{\gamma}_i = P_s \left| \tilde{\lambda}_{i,max} \right|^2. \tag{4.45}$$

Proof of Theorem 5: The SINR for source S_i at destination can be written as

$$\tilde{\gamma}_i = \frac{E\left[\left| \boldsymbol{c}_i^H \widetilde{\boldsymbol{H}}_{R,i,1} \boldsymbol{s}_i x_i \right|^2 \right]}{E\left[\left| \boldsymbol{c}_i^H \left(\sum_{\substack{k=1 \\ k \neq i}}^{M} \widetilde{\boldsymbol{H}}_{R,k,1} \boldsymbol{s}_k x_k + \widetilde{\boldsymbol{n}}_{R,1} \right) \right|^2 \right]} \tag{4.46}$$

$$= \frac{P_s \left| \boldsymbol{c}_i^H \widetilde{\boldsymbol{H}}_{R,i,1} \boldsymbol{s}_i \right|^2}{\boldsymbol{c}_i^H \left[\sum_{\substack{k=1 \\ k \neq i}}^{M} P_s \widetilde{\boldsymbol{H}}_{R,k,1} \boldsymbol{s}_k \boldsymbol{s}_k^H \widetilde{\boldsymbol{H}}_{R,k,1}^H + \boldsymbol{K}_{R,1} \right] \boldsymbol{c}_i} \tag{4.47}$$

Define the covariance matrix of the interference-plus-noise component as $\widetilde{\boldsymbol{Q}}_i \triangleq \sum_{\substack{k=1 \\ k \neq i}}^{M} P_s \widetilde{\boldsymbol{H}}_{R,k,1} \, \boldsymbol{s}_k \boldsymbol{s}_k^H \widetilde{\boldsymbol{H}}_{R,k,1}^H + \boldsymbol{K}_{R,1}$. Then the SINR can be rewritten as

$$\tilde{\gamma}_i = \frac{P_s \left| \boldsymbol{c}_i^H \widetilde{\boldsymbol{H}}_{R,i,1} \boldsymbol{s}_i \right|^2}{\boldsymbol{c}_i^H \widetilde{\boldsymbol{Q}}_i \boldsymbol{c}_i} \tag{4.48}$$

$$= \frac{P_s \left| \boldsymbol{c}_i^H \widetilde{\boldsymbol{A}}_i (\widetilde{\boldsymbol{A}}_i^{-1} \widetilde{\boldsymbol{H}}_{R,i,1}) \boldsymbol{s}_i \right|^2}{\boldsymbol{c}_i^H \widetilde{\boldsymbol{A}}_i \widetilde{\boldsymbol{A}}_i^H \boldsymbol{c}_i} \tag{4.49}$$

$$= \frac{P_s \left| \tilde{\boldsymbol{c}}_i^H (\widetilde{\boldsymbol{U}}_i \widetilde{\Sigma}_i \widetilde{\boldsymbol{V}}_i^H) \boldsymbol{s}_i \right|^2}{|\tilde{\boldsymbol{c}}_i|^2} \tag{4.50}$$

where $\tilde{\boldsymbol{c}}_i \triangleq \widetilde{\boldsymbol{A}}_i^H \boldsymbol{c}_i$. Let $\tilde{\boldsymbol{v}}_i$ and $\tilde{\boldsymbol{u}}_i$ denote the right and left singular vectors of $\widetilde{\boldsymbol{A}}_i^{-1} \widetilde{\boldsymbol{H}}_{R,i,1}$, respectively. If the sequences are designed as $\boldsymbol{s}_i^\dagger = \tilde{\boldsymbol{v}}_{i,max}$ and $\boldsymbol{c}_i^\dagger = \left(\widetilde{\boldsymbol{A}}_i^H\right)^{-1} \tilde{\boldsymbol{u}}_{i,max}$, then $\tilde{\gamma}_i$ would be maximized, which can be written as $P_s \left|\tilde{\lambda}_{i,max}\right|^2$. ■

4.3 Simulation Results for Multihop Relay Network

Figure 4.3 shows the performance of several uplink multihop relay networks. Observe that the performance gets worse as the number of hops increases. This is expected because this dissertation does not include the effects of path loss. Hence, more AWGN is added in the overall relay network as the number of hops increases because noise is accumulated after each hop. For example, the pc2221 uplink is 3 dB worse in SNR at $BER = 10^{-3}$ than the pc221 uplink, because pc2221 uses one more hop.

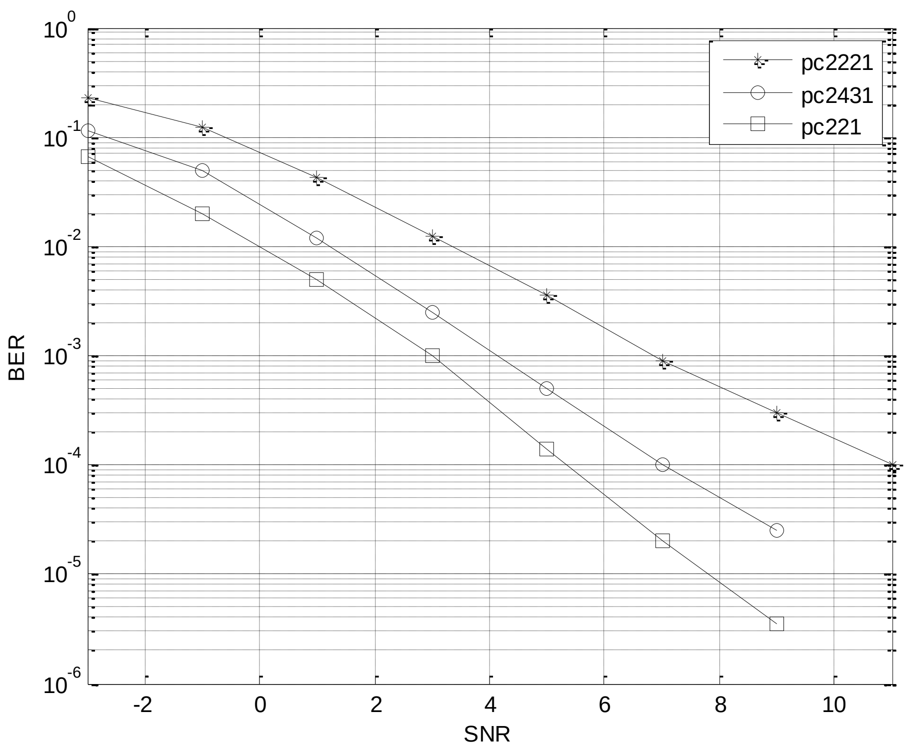

Figure 4.3. BER versus SNR for multihop relay network.

Also observe in Figure 4.3 that with the same number of hops, performance can be improved by increasing the number of relays. For example, both pc2431 and pc2221 use two hops, but pc2431 is 3 dB better in SNR at $BER = 10^{-3}$ than pc2221.

CHAPTER 5

CONCLUSIONS

A method of designing spreading sequences based on maximizing the signal-to-interference-plus-noise ratio was studied in this dissertation for both partially and fully connected code division multiple access amplify-and-forward relay networks under frequency-selective fading. This dissertation considered both uplink and downlink CDMA relay networks. Each node was assumed to have a single-antenna element instead of multiple-antenna elements, although the findings in this dissertation can be extended for a multiple-input multiple-output (MIMO) relay network. The channel matrix representation in this dissertation was already a MIMO type, due to the spreading data symbols into a large number of time chips. Without loss of generality, the proposed method can be effective with higher complexity, and the same or similar conclusions from this dissertation can be valid for the MIMO relay network. The scheme presented in this dissertation is applicable to a general partially or fully connected AF CDMA relay system model with multiple sources, relays, and destinations.

This dissertation employed a signal-to-interference-plus-noise ratio criterion to find the optimum pseudo noise sequences, assuming that channel state information is known at a central station such as a cloud radio access network, which can compute and forward the optimum PN spreading and despreading sequences to the sources and destinations, respectively. This dissertation also assumed that nodes in the AF CDMA relay network are synchronized through the CRAN. Finally, this dissertation presented the sensitivity of the proposed schemes to imperfect CSI and wideband jamming. Simulation results verified that the proposed method shows much faster convergence in finding optimum PN sequences than existing schemes under the same environment.

LIST OF REFERENCES

LIST OF REFERENCES

[1] J. N. Laneman, D. N. C. Tse, and G. W. Wornell, "Cooperative diversity in wireless networks: Efficient protocols and outage behavior," *IEEE Transactions on Information Theory*, vol. 50, no. 12, pp. 3062–3080, Dec. 2004.

[2] J. Joung and A. H. Sayed, "Design of half-and full-duplex relay systems based on the MMSE formulation," *Proceedings of IEEE SSP*, Wales, UK, Aug. 2009.

[3] W. Guan and H. Luo, "Joint MMSE transceiver design in non-regenerative MIMO relay systems," *IEEE Communications Letters*, vol. 12, no. 7, pp. 517–519, July 2008.

[4] R. Mo and Y. Chew, "MMSE-based joint source and relay precoding design for amplify-and-forward MIMO relay networks," *IEEE Transactions on Wireless Communications*, vol. 8, no. 9, pp. 4668–4676, Sept. 2009.

[5] X. Tang and Y. Hua, "Optimal design of non-regenerative MIMO wireless relays," *IEEE Transactions on Wireless Communications*, vol. 6, no. 4, pp. 1398–1407, April 2007.

[6] C. Song, K. Lee, and I. Lee, "Performance analysis of MMSE-based amplify-and-forward spatial multiplexing MIMO relaying systems," *IEEE Transactions on Wireless Communications*, vol. 59, no. 12, pp. 3452–3462, Dec. 2011.

[7] B. Wang, J. Zhang, and A. Høsst-Madsen, "On the capacity of MIMO relay channels," *IEEE Transactions on Information Theory*, vol. 51, no. 1, pp. 29–43, Jan. 2005.

[8] R. Krishna, Z. Xiong, and S. Lambotharan, "A cooperative MMSE relay strategy for wireless sensor networks," *IEEE Signal Processing Letters*, vol. 15, pp. 549–552, 2008.

[9] A. S. Behbahani and A. M. Eltawil, "Multiuser sum MSE minimization relay strategy," *Proceedings of ICC 2011*, Kyoto, Japan, June 2011.

[10] A. S. Behbahani, R. Merched, and A. M. Eltawil, "Optimizations of MIMO relay networks," *IEEE Transactions on Signal Processing*, vol. 55, no. 7, pp. 3336–3348, July 2007.

[11] S. Berger and A. Wittneben, "Cooperative distributed multiuser MMSE relaying in wireless ad-hoc networks," Asilomar Conference, Pacific Grove, CA, Nov. 2005.

[12] B. Rankov and A. Wittneben, "Spectral efficient protocols for half-duplex fading relay channels," *IEEE Journal on Selected Areas in Communications*, vol. 25, no. 2, pp. 379–389, Feb. 2007.

[13] T. Wang, A. Cano, G. B. Giannakis, J. N. Laneman, "High-performance cooperative demodulation with decode-and-forward relays," *IEEE Transactions on Communications*, vol. 55, no. 7, pp. 1427–1438, July 2007.

[14] T. Wang and G. B. Giannakis, "Complex field network coding for multiuser cooperative communications," *IEEE Transactions on Communications*, vol. 26, no. 3, pp. 561–571, April 2008.

[15] T. Wang, G. B. Giannakis, and R. Wang, "Smart regenerative relays for link-adaptive cooperative communications," *IEEE Transactions on Communications*, vol. 56, no. 11, pp. 1950–1960, Nov. 2008.

[16] J. N. Laneman, D. N. C. Tse, and G. W. Wornell, "Cooperative diversity in wireless networks: Efficient protocols and outage behavior," *IEEE Transactions on Information Theory*, vol. 50, no. 12, pp. 3062–3080, Dec. 2004.

[17] A. S. Avestimehr, S. N. Diggavi, and D. N. C. Tse, "Wireless network information flow: A deterministic approach," *IEEE Transactions on Information Theory*, vol. 57, no. 4, pp. 1872–1905, April 2011.

[18] G. Kramer, M. Gastpar, and P. Gupta, "Cooperative strategies and capacity theorems for relay networks," *IEEE Transactions on Information Theory*, vol. 51, no. 9, pp. 3037–3063, Sept. 2005.

[19] H. Minn, X. Fu, and V. K. Bhargava, "Optimal periodic training signal for frequency offset estimation in frequency-selective fading channels," *IEEE Transactions on Communication*, vol. 54, no. 6, pp. 1081–1096, June 2006.

[20] J. Chen, M. Li, and Y. Kuo, "Adaptive OFDM synchronization algorithm in frequency selective fading channels," *IEEE Transactions on Consumer Electronics*, vol. 55, no. 4, pp. 1841–1846, Jan. 2010.

[21] J. Hu and T. M. Duman, "Cooperation over frequency-selective fading relay channels," *IEEE Transactions on Wireless Communications*, vol. 7, no. 12, pp. 5072–5081, Dec. 2008.

[22] T. Ma, Y. Shi, and Y. Wang, "A low complexity MMSE for OFDM systems over frequency-selective fading channels," *IEEE Transactions on Communications*, vol. 16, no. 3, pp. 304–306, Mar. 2012.

[23] M. Huemer, C. Hofbauer, and J. B. Huber, "Non-systematic complex number RS coded OFDM by unique word prefix," *IEEE Transactions on Signal Processing*, vol. 60, no. 1, pp. 285–299, Jan. 2012.

[24] N. Fernando, Y. Hong, and E. Viterbo, “Flip-OFDM for unipolar communication systems,” *IEEE Transactions on Commun*ications, vol. 60, no. 12, pp. 3726–3733, Dec. 2012.

[25] T. E. Abrudan, A. Haghparast, and V. Koivunen, “Time synchronization and ranging in OFDM systems using time-reversal,” *IEEE Transactions on Instrumentation and Measurement*, vol. 62, no. 12, pp. 3276–3290, Dec. 2013.

[26] M. Huemer, C. Hofbauer, A. Onic, and J. B. Huber, “On the exploitation of the redundant energy in UW-OFDM: LMMSE versus sphere detection,” *Signal Processing Letters*, vol. 19, no. 6, pp. 340–343, June 2012.

[27] G. Zhang, M. D. Leenheer, and B. Mukherjee, “Optical traffic grooming in OFDM-based elastic optical networks [Invited],” *IEEE/OSA Jounal of Optical Communications and Networking*, vol. 4, no. 11, pp. B17–B25, Nov. 2012.

[28] E. Alsusa and C. Masouros, “On the selection of the redundant carrier positions in UW-OFDM,” *IEEE Transactions on Signal Processing*, vol. 61, no. 5, pp. 1112–1120, Mar. 2013.

[29] J. F. Hunzinger, J. Hou, and S. Cui, “Relays in HSPA+: Power Control and Mobility,” Qualcomm, 2013.

[30] Z. Shi, M. Zhao, H. Wang, and M. C. Reed, “On the uplink capacity and coverage of relay-assisted UMTS cellular network with multiuser detection,” in IEEE Wireless Communications and Networking Conference (WCNC), 2012, pp. 2979–2983.

[31] D. Torrieri, *Principles of Spread-Spectrum Communication Systems*, New York: Springer, 2005.

[32] P. Viswanath, V. Anantharam, and D. N. C. Tse, “Optimal sequences, power control and capacity of spread-spectrum systems with multiuser linear receivers,” *IEEE Transactions on Information Theory*, vol. 45, no. 6, pp. 1968–1983, Sept. 1999.

[33] J.-T. Chen, C. Papadias, and G. J. Foschini, “Spacetime dynamic signature assignment for the reverse link of DS-CDMA systems,” *IEEE Transactions on Commun*ications, vol. 52, no. 1, pp. 120–129, Jan. 2004.

[34] E. Alsusa and C. Masouros, “Adaptive code allocation for interference management on the downlink of DS-CDMA systems,” *IEEE Transactions on Commun*ications, vol. 7, pp. 2420–2424, July 2008.

[35] P. Viswanath and V. Anantharam, "Optimal sequences and sum capacity of synchronous CDMA systems," *IEEE Transactions on Information Theory*, vol. 45, no. 6, pp. 1984–1991, Sept. 1999.

[36] G. Rajappan and M. L. Honig, "Spreading code adaptation for DS-CDMA with multipath," *Military Communications Conference Proceedings*, pp. 1164–1168, Oct. 2000.

[37] S. Serbetli and A. Yener, "MIMO-CDMA systems: Signature and beamformer design with various levels of feedback," *IEEE Transactions on Signal Processing*, vol. 54, no. 7, pp. 2758–2772, July 2006.

[38] B. Li and E. Ayanoglu, "Full-diversity precoding design of bit-interleaved coded multiple beamforming with orthogonal frequency division multiplexing," *IEEE Transactions on Communication*, vol. 61, no. 6, pp. 2432–2445, June 2013.

[39] J. Chen, M. Li, and Y. Kuo, "Adaptive OFDM synchronization algorithm in frequency selective fading channels," *IEEE Transactions on Consumer Electronics*, vol. 55, no. 4, pp. 1841–1846, Jan. 2010.

[40] T. Ma, Y. Shi, and Y. Wang, "A low complexity MMSE for OFDM systems over frequency-selective fading channels," *IEEE Transactions on Communications*, vol. 16, no. 3, pp. 304–306, Mar. 2012.

[41] S. K. Mohammed and E. G. Larsson, "Constant-envelope multi-user precoding for frequency-selective massive MIMO systems," *IEEE Wireless Communications Letters*, vol. 2, no. 5, pp. 547–550, Nov. 2013.

[42] W. Fang, L. L. Yang, and L. Hanzo, "Performance of DS-CDMA downlink using transmitter preprocessing and relay diversity over Nakagami-m fading channels," *IEEE Transactions on Wireless Communications*, vol. 8, no. 2, pp. 678–682, Feb. 2009.

[43] D. Gregoratti and X. Mestre, "Random DS/CDMA for the amplify and forward relay channel," *IEEE Transactions on Wireless Communications*, vol. 8, no. 2, pp. 1017–1027, Feb. 2009.

[44] A. J. Viterbi, *CDMA Principles of Spread Spectrum Communication*, Addison-Wesley, 1995.

[45] G. H. Golub and C. F. Van Loan, *Matrix Computations*, 3rd ed., Baltimore: Johns Hopkins, 1996.

[46] B. J. Peiris, K. R. Narayanan, and S. L. Miller, "A spectral domain approach to design spreading sequences for DS-CDMA systems in frequency selective fading channels," *IEEE Transactions on Wireless Communications*, vol. 5, no. 9, pp. 2386–2395, Dec. 2006.

[47] I. S. Gradshteyn and I. M. Ryzhik, *Table of Integrals, Series, and Products*, 7th ed., San Diego, CA: Academic, 1979.

[48] K. V. Mardia, J. T. Kent, and J. M. Bibby, *Multivariative Analysis*, San Diego, CA: Academic Press, 2007.

[49] S. Yu, L.-C. Tranchevent, B. D. Moor, and Y. Moreau, *Kernel-Based Data Fusion for Machine Learning*, Berlin, Heidelberg: Springer-Verlag, 2011.

[50] Titus K. Y. Lo, "Maximum ratio transmission," *IEEE Transactions on Communications*, vol. 47, no. 10, pp. 1458–1461, Oct. 1999.

[51] Arti M. K., Ranjan K. Mallik, and Robert Schober, "Beamforming and Combining in two-way AF MIMO relay networks," *IEEE Communications Letters*, vol. 17, no. 7, pp. 1400–1403, July 2013.

LIST OF AUTHOR PUBLICATIONS

LIST OF AUTHOR PUBLICATIONS

Journal Paper

[1] K. Lee, J. Yang, H. M. Kwon, H. Park, and Y. H. Lee, “Closed form of optimum cooperative distributed relay amplifying matrix,” *IEEE Transactions on Wireless Communications*. Jan. 2014.

Conference Papers

[1] J. Yang, K. Lee, S. Feng, and H. M. Kwon, “Spreading sequence design for partial connectivity relay network,” *Proceedings of IEEE VTC,* Seoul, Korea, May 2014.

[2] K. Lee, J. Yang, H. M. Kwon, E. M. Sawan, and H. Park, “Two-way AF wireless relay networks under channel uncertainty,” ,” *Proceedings of IEEE VTC,* Seoul, Korea, May 2014.

[3] K. Lee, J. Yang, H. M. Kwon, E. M. Sawan, and H. Park, “Maximum SNR relaying strategies for AF SIMO wireless relay networks,” ,” *Proceedings of IEEE VTC,* Seoul, Korea, May 2014.

[4] Y. T. Sagar, J. Yang, H. M. Kwon, and W. Nam, “Achievable Rate of a Two-Way Relay Channel with Structured Code under Rayleigh Fading,” *Proceedings of ICNC*, Honolulu, Hawaii, Feb. 2014.

[5] K. Lee, H. M. Kwon, J. Yang, E. M. Sawan, and H. Park, “Channel uncertainty for AF wireless distributed relay networks under power constraint,” *Proceedings of IEEE WCNC*, Istanbul, Turkey, April 2014.

[6] K. Lee, H. M. Kwon, J. Yang, E. M. Sawan, and H. Park, “Two-way MMSE strategies for AF distributed relay networks under power constraint,” *Proceedings of IEEE WCNC*, Istanbul, Turkey, April 2014.

[7] J. Yang, Y. Sagar, K. Lee, and H. M. Kwon, “On sequence design for full connectivity relay network,” *Proceedings of IEEE MILCOM*, San Diego, CA, Nov. 2013.

[8] K. Lee, H. M. Kwon, J. Yang, E. M. Sawan, and H. Park, “Two-Way AF MIMO Beamforming Relay Strategies under Transmit Power Constraint*,” Proceedings of IEEE MILCOM*, San Diego, CA, Nov. 2013.

[9] J. Yang, H. M. Kwon, K. Lee, and Y. Sagar, “On sequence design for relay networks with multipath,” *Proceedings of IEEE VTC,* Las Vegas, NV, Sept. 2013.

LIST OF AUTHOR PUBLICATIONS (continued)

[10] K. Lee, H. M. Kwon, J. Yang, E. M. Sawan, H. Park, and Y. H. Lee, "Power allocation for AF relaying network under channel phase misalignment," *Proceedings of IEEE VTC,* Las Vegas, NV, Sept. 2013.

[11] K. Lee, H. M. Kwon, J. Yang, E. M. Sawan, H. Park, and Y. H. Lee, "Distributed AF mobile relay networks in adverse wireless communication environments," *Proceedings of IEEE VTC,* Las Vegas, NV, Sept. 2013.

[12] K. Lee, H. M. Kwon, J. Yang, E. M. Sawan, H. Park, and Y. H. Lee, "MMSE Relaying Strategy for Two-Way Amp-lify-and-Forward Wireless Networks," *Proceedings of IEEE VTC,* Las Vegas, NV, Sept. 2013.

[13] K. Lee, H. M. Kwon, J. Yang, E. M. Sawan, H. Park, and Y. H. Lee, "MMSE Relaying Strategies under Jamming, Channel Uncertainty, Node Geometry, and Power Constraint," *Proceedings of IEEE VTC,* Las Vegas, NV, Sept. 2013.

[14] K. Lee, H. M. Kwon, H. Kim, J. Yang, H. Park, and Y. H. Lee, "A Cooperative AF Wireless Relay Network under Three Wireless Communication Conditions with Relay Power Constraint," *Proceedings of IEEE ICC,* Budapest, Hungary, June 2013, pp: 1614-1618.

[15] Y. Sagar, J. Yang, and H. M. Kwon, "Capacity of a modulo-sum arbitrary SISO relay network," *Proceedings of IEEE VTC*, Yokohama, Japan, May 2012, pp:1-5.

[16] Y. Sagar, J. Yang, and H. M. Kwon, "Channel capacities of parallel and serial modulo sum relay networks," *Proceedings of IEEE ISIT*, Saint-Petersburg, Russia , Aug. 2011, pp: 269-273.

[17] J. Yang, L. Paarmann, H. M. Kwon, and W. Xiong, "Biological-vision inspired DSA systems for UAVs," *Proceedings of BIO-SIGNALS*, Porto, Portugal, Jan. 2009, pp: 502-505.